TYROSINE KINASE INHIBITORS AS

ADJUNCTS TO CHEMOTHERAPY

IN BLADDER CANCER

Thesis submitted for the degree of Doctor of
Medicine at the University of Leicester

by

Lynsey A. McHugh

Department of Cancer Studies and Molecular
Medicine
University of Leicester

April 2007

UMI Number: U223124

UMI
Dissertation Publishing

ProQuest

ACKNOWLEDGEMENTS

guidance with the statistical analyses. I also owe thanks to BUPA and the British Urology Foundation for their generous financial support.

As is usual in such endeavours, my family and friends are owed a huge thank you for their unquestioning support. However I really have to expand on this by saying to Mum, Dad, Scott, Keith, Rachael, Susie, James and Mark – you know what you've done and it's no exaggeration to say that I truly would not have got through this without all of you.

Finally, this thesis is dedicated to Mike. Without you I wouldn't have completed the first 18 months, and for you I have seen it through to the end.

CONTENTS

CHAPTER 1

INTRODUCTION

1.1 Bladder cancer – general background

1.1.1 Incidence

Bladder cancer is the fifth most common cancer in the UK, with nearly 10,200 new cases diagnosed each year, and a male to female ratio of 2.5:1 (figure 1.1). Presentation is uncommon before the age of 50 years [1 - 4]. It accounts for one in every 20 new cases of cancer each year in the UK, and was responsible for around 4,900 deaths in the UK in 2003, making it the eighth most common cause of death due to cancer [5 – 7].

1.1.2 Types of bladder cancer

There are three main types of bladder cancer, with transitional cell carcinoma (TCC) being by far the most common, accounting for approximately 90% of all bladder tumours. Squamous cell carcinoma and adenocarcinoma represent approximately 5% and 2% of bladder cancers respectively [8].

2
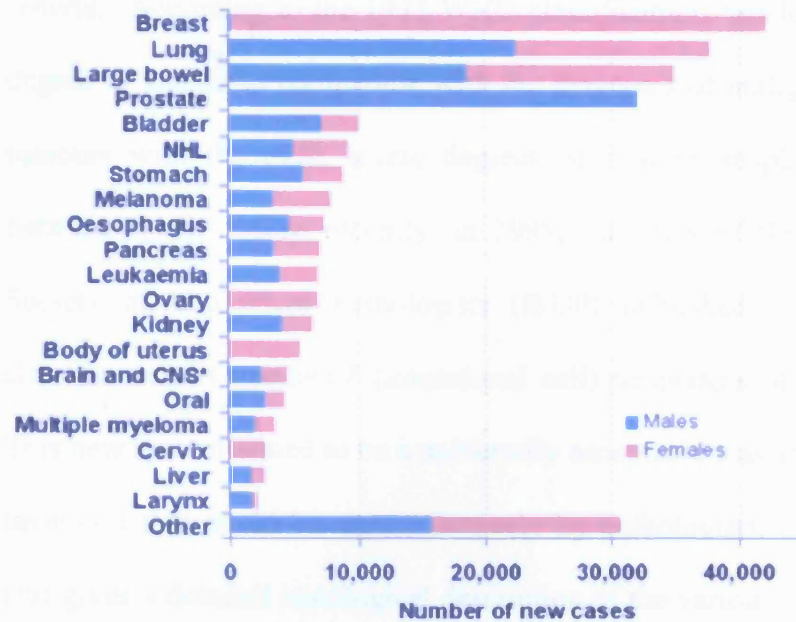
Figure 1.1

The 20 most common cancers in the UK, 2002 (Cancer Research UK).

1.1.3 Stage and grade of bladder cancer

Pathological staging and grading is used to formulate a treatment plan for bladder cancer. The tumour node metastasis (TNM) system of classification, approved by the Union International Contre le Cancer (UICC) is widely used for pathological staging [9] (table 1.1, figure 1.2). Of all new tumours, approximately 20% are muscle-invasive, 75% are pTa/pT1 (superficial tumours), and 5% are *in situ* types (Tis). Of the superficial tumours, up to 20% will progress to become muscle-invasive. The grading of TCC bladder is more complex. The 1973 World Health Organisation (WHO) grading classification, where tumours are labelled as grades 1, 2 and 3, has been the most widely used system [10]. However, the definitions of the different grades are vague and lack information for pathologists regarding specific histological

3

criteria. According to the 1973 WHO classification, 'grade 1 tumours have the least degree of anaplasia compatible with the diagnosis of malignancy, grade 3 applies to tumours with the most severe degrees of cellular anaplasia, and grade 2 lies in between' [10]. More recently, in 1998, members of the WHO and International Society of Urological Pathologists (ISUP) published the WHO/ISUP consensus classification of urothelial (transitional cell) neoplasms of the urinary bladder [11]. This new system aimed to be a universally acceptable classification system for bladder neoplasia that could be used effectively by pathologists, urologists and oncologists, and gives a detailed histological description of the various grades, employing specific cytological and architectural criteria. The system covers not only neoplastic conditions, but also the nomenclature of preneoplastic lesions. A further WHO classification was introduced in 1999 (WHO 1999), which was almost identical to the WHO/ISUP classification, the main difference being that the WHO 1999 scheme subdivided the low- and high-grade spectrum into three grades (grades I, II and III) [12]. Table 1.2 summarises the WHO 1973 and WHO/ISUP grading systems and their relationship to each other [13]. Despite the proposed benefits of the WHO/ISUP and WHO 1999 systems, most pathologists in the United Kingdom still use the original 1973 WHO grading system because of the lack of reproducibility of other two systems [14].

Primary tumour	Depth of invasion
Ta	Non-invasive papillary
Tis	In situ: 'flat tumour'
T1	Subepithelial connective tissues

T2
    T2a
    T2b
	Muscularis propria
	    Inner half
	    Outer half

T3
    T3a
    T3b
	Beyond muscularis propria
	    Microscopically
	    Extravesical mass

T4
    T4a
    T4b
	Other adjacent structures
	    Prostate, vagina, uterus
	    Pelvic wall, abdominal wall

Regional lymph nodes	**Number/size**
N1	Single = 2 cm
N2	Single > 2-5 cm, multiple = 5 cm
N3	> 5 cm
Distant Metastases	**Presence/absence**
M1	Distant metastases

Table 1.1

The 1997 UICC TNM staging classification for bladder cancer [9].
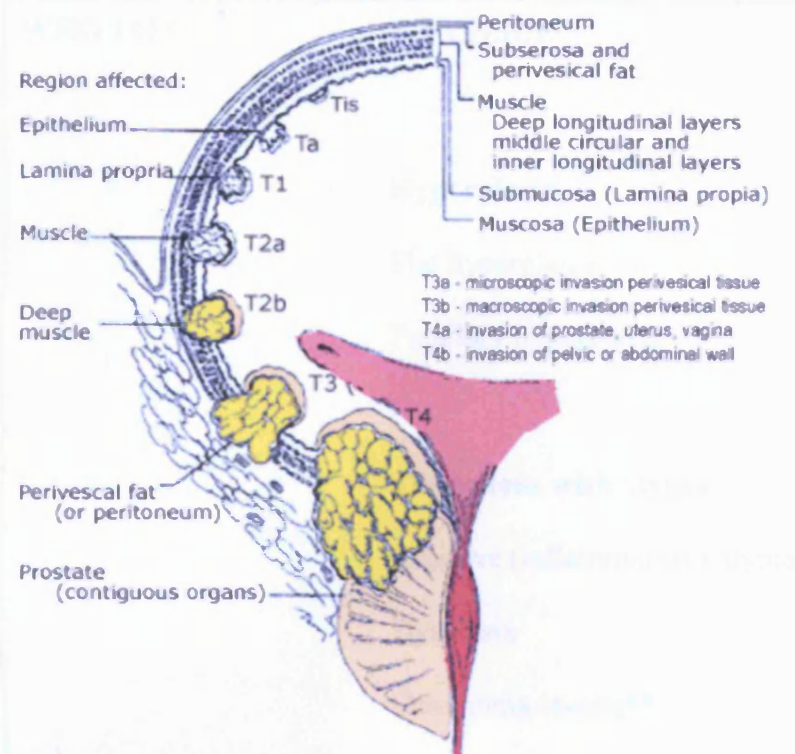
Figure 1.2

Diagrammatic representation of the tumour staging system of bladder cancer.

WHO 1973	WHO/ISUP

Hyperplasia

Flat hyperplasia

Papillary hyperplasia

Flat lesions with atypia

Reactive (inflammatory) atypia

Dysplasia

Carcinoma-in-situ**

Papillary Neoplasms

Papilloma ⟶ Papilloma

Grade 1 ⟶ Papillary neoplasm of low malignant potential (PUNLMP)

Grade 2 ⟶ Papillary carcinoma, low-grade

Grade 3 ⟶ Papillary carcinoma, high-grade

**May include cases formerly known as "severe dysplasia"

Table 1.2

Summary of the 1973 WHO and 1998 WHO/ISUP grading systems for TCC bladder, and their relationship to each other (modified from Epstein [13]).

1.1.4 Risk factors for TCC of the bladder

There are a number of known risk factors for bladder cancer. Tobacco smoke is the most important exogenous risk factor for bladder cancer. Smokers are two to three times more likely to develop TCC than non-smokers [15], and 50% of all bladder tumours can be directly attributed to cigarette smoking [16]. The exact mechanism of bladder carcinogenesis in smokers remains unknown, though more than 60 carcinogens are present in tobacco smoke. A number of industrial chemicals such as aromatic amines, aniline dyes, coal soot and numerous aldehydes have been implicated in bladder carcinogenesis [17, 18], with occupations such as autoworkers, painters, leather workers, metalworkers, machinists and dry cleaners being at increased risk. Occupational exposures are estimated to account for 20% of bladder cancer cases in the United States, with latency periods between exposure and clinical presentation as long as 30-50 years [19, 20]. Several compounds found naturally in the environment and secondary to industrial waste have been associated with carcinoma of the bladder, such as arsenic and nitrates, though studies have failed to reach a consensus on their importance [21 - 24].

1.1.5 Prognostic factors in superficial bladder cancer

Several prognostic factors have been identified for superficial bladder cancer, which are easy to assess [25 - 30]. In descending order of importance, factors predicting disease recurrence are: numbers of tumours present at diagnosis, recurrence rate in the previous period or recurrence at three months, size of the tumour (the greater the size,

8

the higher the chance of recurrence), and the grade of tumour. The first two of these, numbers of tumours at diagnosis and recurrence at three months, are particularly used as an objective method of dividing patients up according to risk of recurrence [27]. For predicting progression to muscle-invasive disease, histological grade, the presence of Tis, and stage, are of utmost importance. Tis of the bladder is defined as a flat, high-grade non-invasive TCC [31]. The untreated natural history of Tis indicates a greater than 50% five year progression rate and an even higher recurrence rate [32], making the importance of its diagnosis and treatment obvious. Based on prognostic factors, superficial bladder cancer can be divided into three risk groups (table 1.3).

Risk group	Prognostic factors
Low-risk tumours	Single, Ta, G1, <3cm diameter
High-risk tumours	T1, G3, multifocal or highly recurrent, Tis
Intermediate-risk tumours	All other tumours, Ta-T1, G1-G2, multifocal, >3cm diameter

Table 1.3

Risk factors for predicting recurrence and progression of superficial bladder tumours, based on prognostic factors [33].

1.2 <u>Management of bladder cancer</u>

1.2.1 Presentation

Early symptom recognition is a key to improving prognosis [34, 35]. Haematuria is the most common finding in bladder cancer, though the degree of bleeding does not correlate with severity of disease, and may be microscopic or macroscopic. Therefore, any degree of haematuria requires investigation, even if another potential cause for haematuria (such as urinary tract calculus, urinary tract infection [UTI]) has been identified. Bladder cancer may also present with symptoms of voiding irritability. Patients may complain of urgency, dysuria or increased frequency of micturition. These symptoms strongly suggest a UTI, though if they are persistent in the absence of a positive urine culture, with or without haematuria, the patient should be investigated for the presence of bladder cancer, including Tis.

1.2.2 Diagnosis

The presence of these symptoms should lead to investigation for bladder cancer. The European Association of Urology (EAU) guidelines on bladder cancer recommend a pathway of investigation [33] (Table 1.4), which starts with a physical examination, including digital rectal and pelvic examination, and then moves on to imaging, urinalysis and urine cytology, and diagnostic cystoscopy. Once a bladder cancer has been identified, transurethral resection (TUR) of the bladder tumour should be

performed. If the tumour is found to be muscle-invasive, and radical treatment is being considered, staging investigations should be organised.

Mandatory investigations

• Physical examination (including digital rectal and pelvic examination)
 	
• Renal and bladder ultrasonography and/or intravenous pyelography (IVP)
 	
• Cystoscopy with description of the tumour: size, site, appearance (a diagram of the bladder should be included)
 	
    • Urinalysis
 	
    • Urine cytology
 	
    • TUR with:
      - biopsy of the underlying tissue
 	
      - random biopsies in the presence of positive cytology, large or non-papillary tumour
 	
      - biopsies of the prostatic urethra in cases of Tis or suspicion of it

When the bladder tumour is muscle-invasive and radical treatment is indicated, the following tests are mandatory
• Chest X-ray • IVP and/or abdominal/pelvic computed tomography (CT) scan • Liver ultrasonography • Bone scan if symptoms are present or alkaline phosphatase level is elevated

Table 1.4

EAU recommendations for diagnosis of suspected bladder tumours [33].

1.2.3 Treatment

1.2.3.1 Superficial bladder cancer

Treatment of Ta and T1 tumours is directed towards prevention of recurrence and progression, and takes into account the prognostic factors of the tumour. As previously mentioned, the risk of progression to muscle-invasive disease is low in the majority of superficial tumours, but reaches up to 50% in G3 T1 tumours [36], which represent approximately 10% of all superficial lesions. A single intravesical chemotherapeutic installation (epirubicin or mitomycin C) immediately after initial TUR is recommended in all papillary tumours to reduce tumour recurrence [37, 38], and this should be all the treatment necessary for single G1 Ta-T1 tumours, < 3cm. For recurrent tumours there is varying evidence for courses of intravesical chemotherapy. If after such treatment, there are still multiple recurrences of tumours, a change to intravesical bacillus Calmette-Guerin (BCG) immunotherapy is advocated because of its proven results in these circumstances [39]. In fact, for all tumours with high risk of progression (T1, G3, multifocal or highly recurrent, CIS [Table 1.3]), maintenance intravesical BCG therapy should be used [40 - 43]. In patients with G3T1 tumours, re-resection should be undertaken two to six weeks after the initial resection, as previous reports have shown that even if detrusor muscle is free of tumour at initial resection, up to 28% of T1 tumours may be up-staged to muscle-invasive at re-resection [44]. The induction course of intravesical BCG is six weekly instillations, followed by three further weekly instillations three months later. T1, G3 or muscle-invasive disease after nine instillations constitutes failure, and

patients should be offered radical cystectomy or radiotherapy. If there is no failure after nine instillations, maintenance BCG should be continued for 27 instillations over three years, if possible. Such a program increased median recurrence-free survival from 35.7 months with no maintenance BCG (six instillations only), to 76.8 months with maintenance therapy (p<0.0001) [40]. Two European Organisation for Research and Treatment of Cancer (EORTC) meta-analyses have further assessed the role of maintenance intravesical BCG therapy, in high-risk tumours [41] and Tis alone [42]. Both showed that maintenance therapy is superior to either intravesical chemotherapy, or only an initial six week course of BCG. This is backed-up by a further report which suggests that intravesical BCG maintenance therapy should be for at least 12 months, and that giving just six instillations is ineffective [43].

1.2.3.2 Organ-confined muscle-invasive bladder cancer

The two main treatment options for organ-confined muscle-invasive TCC of the bladder are radical cystectomy (with urinary diversion or bladder substitution), or radical radiotherapy. However, both these treatments are associated with five year survival rates of only around 40% [45, 46]. This is partly explained by a subgroup of patients undergoing these treatments who are harbouring sub-clinical metastases. Therefore, it is important that radical cystectomy should by accompanied by pelvic lymphadenectomy, particularly if there is no clinical evidence of nodal involvement, as in some patients lymphadenectomy in the presence of low volume lymph node metastases will result in prolonged long term

survival [47]. The role of systemic chemotherapy in the management of patients undergoing radical therapy for organ-confined muscle-invasive bladder cancer is uncertain, and will be discussed later.

1.2.3.3 Metastatic bladder cancer

The treatment of choice for metastatic disease is systemic chemotherapy.

1.3 Current role of systemic chemotherapy in the management of bladder cancer

1.3.1 Metastatic bladder cancer

Until recently, the MVAC regimen (a combination of methotrexate, vinblastine, adriamycin [doxorubicin] and cisplatin) had been considered the 'gold standard' chemotherapy treatment in metastatic TCC of the bladder [48]. Using this regimen, approximately 40 to 60% of patients achieve an objective response, a third achieve a complete response, but the median survival is only one year [49, 50]. Randomized trials have confirmed the superiority of the MVAC regimen over cisplatin alone [49], or over a combination of cyclophosphamide, doxorubicin and cisplatin, in terms of objective response rates and overall survival [50]. Furthermore, combination chemotherapy containing cisplatin is superior to the same combination without

cisplatin (e.g. CMV [cisplatin, methotrexate and vinblastine] is superior to MV) [51].

In a phase III trial which randomised 255 patients to either single-agent cisplatin or

MVAC, only 3.7% of patients treated with MVAC were alive and continuously

disease-free at six years, but this was still superior to survival with single-agent

cisplatin (p = 0.00015) [52].

Attempts have been made to improve the efficacy of the MVAC regimen. A phase III

trial randomised a high-dose MVAC (HD-MVAC) regimen against standard MVAC.

Results showed that although progression-free survival time was significantly better

with HD-MVAC (P = 0.037), with a median progression-free survival time of 9.1

months on the HD-MVAC arm versus 8.2 months on the MVAC arm, there was no

difference in overall survival between the two regimens [53].

As well as demonstrating poor overall survival rates, M-VAC is toxic and has a

treatment-related mortality of about 4% [49, 54].

In view of this, many now consider the GC (gemcitabine and cisplatin) regimen to be

the standard treatment in metastatic bladder cancer following a recent phase III trial

[54]. In this trial, 405 patients with locally-advanced or metastatic TCC of the bladder

and no prior systemic chemotherapy were randomised to GC or MVAC. Overall

survival was similar in both arms, but GC had a better safety-profile, and tolerability

[54]. Certainly, the GC regimen is now employed at many institutions as first-line

therapy, although the financial cost is higher, and EAU guidelines still cite MVAC as

the gold standard treatment, saying that the GC data is not sufficiently statistically

powered to reveal equivalence to MVAC in terms of survival [33]. Phase II trials

incorporating the taxane, paclitaxel, in combination with cisplatin [55], or carboplatin [56], have also shown activity reminiscent of those described for MVAC chemotherapy, but with more favourable toxicity profiles.

Further trials are currently evaluating the potential benefits of adding other active drugs to the GC combination. Phase II trials of triplet combination chemotherapy including paclitaxel and/or gemcitabine, have shown promise with median survivals of two to eight months higher than those described in phase III trials of MVAC [57 - 59]. These promising results have led to a large randomised phase III trial, comparing GC with GTC (gemcitabine, paclitaxel and cisplatin), so that the impact of paclitaxel on survival can be assessed further [60].

Gemcitabine and paclitaxel given in combination every two weeks has shown promise as a second-line treatment in patients who fail to respond to MVAC chemotherapy; the complete response rate was 28% and median survival was 14.4 months [61]. This provides further evidence for the efficacy of paclitaxel in the treatment of advanced bladder cancer.

It is important to note that patient factors play a role in survival following systemic chemotherapy. Patients with visceral metastases do less well than those with surgically inoperable disease without visceral metastases. In one study of MVAC, patients with visceral metastases had a median survival of 11.1 months, compared to 22.3 months in those without visceral metastases [62]. Similar results are seen with GC, where a study of 121 patients showed that the only independent prognostic factor

was the presence of visceral metastases, and patients without visceral metastases had a 24% chance of four year survival [63].

Unfortunately, although precise data are difficult to obtain, a significant proportion of patients with metastatic bladder cancer are not eligible to receive cisplatin-based chemotherapy [64]. Commonly encountered reasons for this unsuitability include renal compromise, impaired cardiac status, inadequate bone marrow reserve, poor performance status and a variety of co-morbid conditions, which are often associated with ageing.

1.3.2 Organ-confined muscle-invasive bladder cancer

1.3.2.1 Neoadjuvant chemotherapy

Most trials of chemotherapy given before radical cystectomy or radiotherapy have failed to significantly improve survival, but many of these studies had sample sizes which were too small for important changes in survival to be detected. In a large EORTC/MRC (Medical Research Council) phase III trial, 976 patients were randomised to three cycles of CMV or no chemotherapy, prior to cystectomy or radical radiotherapy (neoadjuvant chemotherapy) [65]. When first published, there was no significant difference in overall survival, however presented data after seven years of follow-up shows a 6% survival advantage in favour of neoadjuvant chemotherapy (p=0.048). A systematic review and meta-analysis from 11 randomised trials has shown that neoadjuvant platinum-based

combination chemotherapy is associated with a 5% absolute benefit in overall survival at five years (Hazards ratio [HR]=0.86, 95% confidence interval [CI] 0.77-0.95, p=0.003, figure 1.3), and a 9% absolute improvement in disease-free survival at five years (HR=0.78, 95% CI 0.71-0.86, p<0.0001) [66]. However, it should be noted that the EORTC/MRC trial discussed above contributed half the patients who underwent combination chemotherapy.

Survival (y-axis, 0.0 to 1.0)
Years (x-axis, 0 to 10)

	Events	Total
NeoCT	686	1220
Control	744	1213

Patients at risk

	0	1	2	3	4	5	6	7	8	9	10
NeoCT	1220	972	770	659	585	510	403	284	201	140	92
Control	1213	922	705	608	527	448	338	241	171	116	77
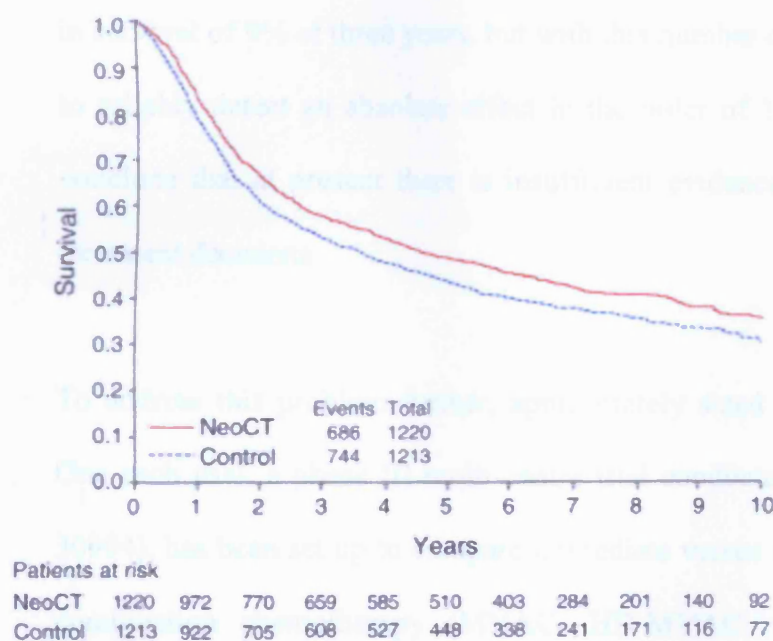
Figure 1.3

Kaplan-Meier curve for overall survival in neoadjuvant platinum-based combination chemotherapy trials (from the advanced bladder cancer [ABC] meta-analysis of adjuvant chemotherapy in muscle-invasive bladder cancer [66]).

1.3.2.2 Adjuvant chemotherapy

There is currently insufficient evidence to support adjuvant chemotherapy following radical cystectomy [67], due to the small numbers of trials investigating the effectiveness of adjuvant chemotherapy in this setting. A recent meta-analysis of 491 patients from six trials has showed a 25% relative decrease in the risk of death with adjuvant chemotherapy compared with control (HR 0.75, 95% CI 0.60 − 0.96, p=0.019) (figure 1.4) [68]. This is equivalent to an absolute improvement in survival of 9% at three years, but with this number of patients it is only possible to reliably detect an absolute effect in the order of 15%. The authors therefore conclude that at present there is insufficient evidence on which to reliably base treatment decisions.

To address this problem further, appropriately sized randomised trials are vital. One such trial, a phase III multi-centre trial conducted by the EORTC (protocol 30994), has been set up to compare immediate versus deferred (at time of relapse) combination chemotherapy (MVAC, HD-MVAC, or GC) following radical cystectomy in high risk patients with pT3-pT4 or node positive disease [69]. Those receiving immediate chemotherapy have four cycles, whereas those getting deferred chemotherapy get six cycles. However, such a protocol may only be applicable to a small number of patients.

The potential advantages and disadvantages of adjuvant versus neoadjuvant chemotherapy are discussed in table 1.5 [70].
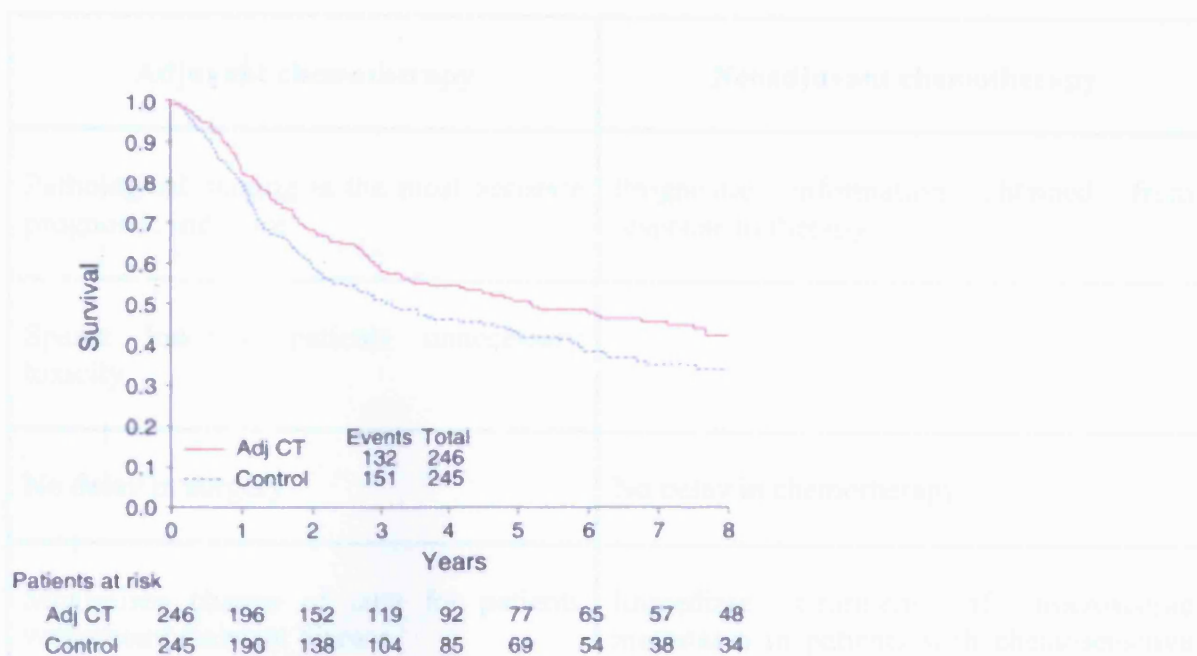
Figure 1.4

Kaplan-Meier curve for survival (all trials) showing results from the ABC meta-analysis of adjuvant chemotherapy in muscle-invasive bladder cancer [68].

Adjuvant chemotherapy	Neoadjuvant chemotherapy
Pathological staging is the most accurate prognostic indicator	Prognostic information obtained from response to therapy
Spares low-risk patients unnecessary toxicity	
No delay in surgery	No delay in chemotherapy
Maximises chance of cure for patients with chemoresistant disease	Immediate treatment of microscopic metastases in patients with chemosensitive disease
Bladder preservation with MVAC alone a possibility in only 1 in 3 patients	Potential for bladder preservation in complete responders
Lower toxicity of newer combination chemotherapy likely to improve tolerance and compliance with postoperative therapy	Greater tolerability and compliance by patients

Table 1.5

The advantages and disadvantages of adjuvant versus neoadjuvant chemotherapy [70].

1.3.2.3 Concomitant chemotherapy

In other solid tumour systems, cisplatin has been used concomitant with radiotherapy to prolong survival. One such tumour system is cervical cancer, in which a systematic review and meta-analysis of 19 reported trials concluded that such concomitant therapy improves overall and progression free survival, and also reduces local and distant recurrence in selected patients with cervical cancer [71]. There has been only one randomised trial of concomitant chemotherapy with radiotherapy in bladder cancer. This trial showed that the rate of local disease recurrence in the pelvis was significantly reduced by concurrent cisplatin (p=0.38), and a 15% improvement in overall survival after three years. However, only 99 patients were recruited, and this improvement in survival was not statistically significant [72]. A more recent report of long-term results of concomitant cisplatin/5-fluorouracil (5FU) and radiotherapy showed no survival benefit, but concluded that such therapy may be beneficial for those unfit to undergo cystectomy [73].

1.4 Future directions of systemic chemotherapy in the management of bladder cancer

In view of the continuing modest survival rates despite advances in chemotherapeutic regimens, there has been much interest in developing novel therapies for the treatment of TCC of the bladder, including sensitisers for current modalities. Such potential therapies may also enable dose reduction of chemotherapy and facilitate reducing the number of cytotoxic agents in a regimen, thus reducing the toxicity profile and making treatment available to more patients. Recent developments in the understanding of the differing phenotypes of bladder cancers have allowed progress in identifying genetic changes and altered patterns of gene expression, which accompany the development of bladder tumours. Particular interest has focused on defects in pathways controlling the G1/S (GAP-1/synthesis) cell cycle checkpoint, involving the tumour suppressor genes p53 and pRb (p-retinoblastoma) [74], and on aberrant expression of growth-factor receptors, such as the epidermal growth factor receptor. Much research currently centres on modifying the activity of the epidermal growth factor receptor (EGFR/ErbB1), a transmembrane protein that has been shown to be an independent predictor of survival in bladder cancer [75]. In particular, small molecule tyrosine kinase inhibitors (TKIs) and monoclonal antibodies (MAbs) to this receptor and other members of its family have been studied as both primary chemotherapeutic agents and as adjuncts to chemotherapy.

1.5 ErbB family of receptors

1.5.1 The ErbB family of receptor tyrosine kinases

The ErbB family of receptor tyrosine kinases, which is frequently dysregulated in human epithelial malignancies, lies at the head of a complex signal transduction cascade that modulates a number of cellular functions, including cell proliferation, survival, adhesion, migration and differentiation [76]. The ErbB family is comprised of four members/homologous receptors: the epidermal growth factor receptor (EGFR/ErbB1), ErbB2, ErbB3, and ErbB4 [76]. These transmembrane receptors are composed of an extracellular ligand-binding domain, a transmembrane lipophilic segment, and an intracellular tyrosine kinase domain with a regulatory COOH-terminal segment. Without ligand-receptor interaction, ErbB receptors are inactive and present in monomeric form. On binding of a number of different ligands, including epidermal growth factor (EGF), transforming growth factor (TGF)-α and heregulin (HRG), to the extracellular domain of ErbB receptors, the formation of receptor homodimers or heterodimers occurs [76] (figure 1.5). This stimulates autophosphorylation of the tyrosine kinase domains, triggering the cascade of multiple intracellular signalling pathways. Of particular note, ErbB3 lacks intrinsic tyrosine kinase activity, due to substitutions in critical residues in its catalytic domain, and thus can signal only in the context of a receptor heterodimer [77]. In addition, ErbB2 is devoid of an activating ligand, and can only function in the context of a heterodimer with a ligand-bound receptor [78]. Generally, ligand-induced signalling must be

initiated by high affinity binding of EGF-like ligands to ErbB1 and ErbB4, or HRG binding to ErbB3 or ErbB4 [79].

There is a hierarchy of interactions between receptors that may reflect differences in affinities of the various hormone-receptor-receptor complexes. For example, EGF stimulated ErbB1 binds with higher affinity to ErbB2 than to ErbB3 or ErbB4. Similarly, HRG stimulated ErbB3 or ErbB4 form stronger heterodimers with ErbB2 than with ErbB1. This suggests that ErbB2 is the preferred target for heterodimerisation for other ErbB family receptors [80]. Furthermore, there is evidence to suggest that ErbB2 and ErbB3 form the most potent heterodimer in terms of cell growth and transformation, in spite of their apparent disabilities [81].
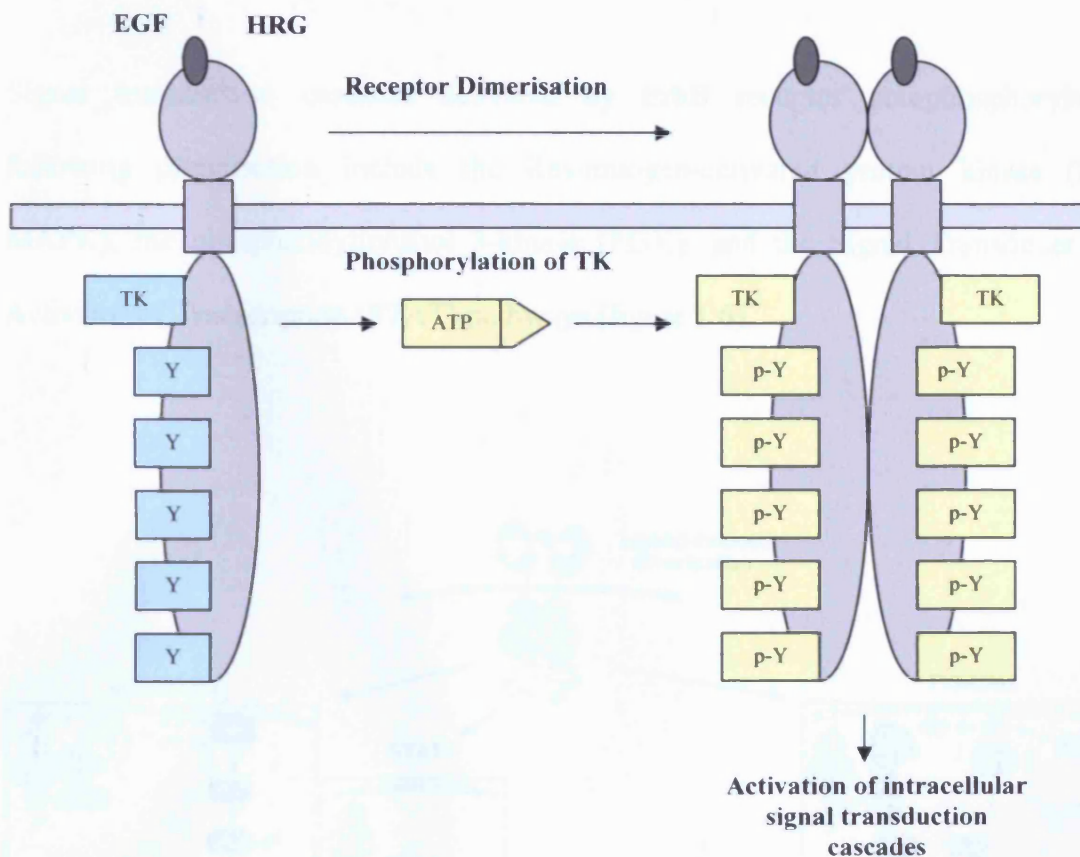
Figure 1.5

Diagrammatic representation of ligand-induced dimerisation of ErbB receptors, which results in phosphorylation of the tyrosine residues (Y) of the tyrosine kinase (TK) in the intracellular component of the receptor via the ATP (adenosine triphosphate) binding site. This leads to activation of downstream signalling, cell cycle progression, and increased cell proliferation and survival.

1.5.2 ErbB receptor-mediated signalling pathways

Signal transduction cascades activated by ErbB receptor autophosphorylation following dimerisation include the Ras-mitogen-activated protein kinase (Ras-MAPK), the phosphatidylinositol 3-kinase (PI3K), and the Signal Transducer and Activator of Transcription (STAT) pathways (figure 1.6).
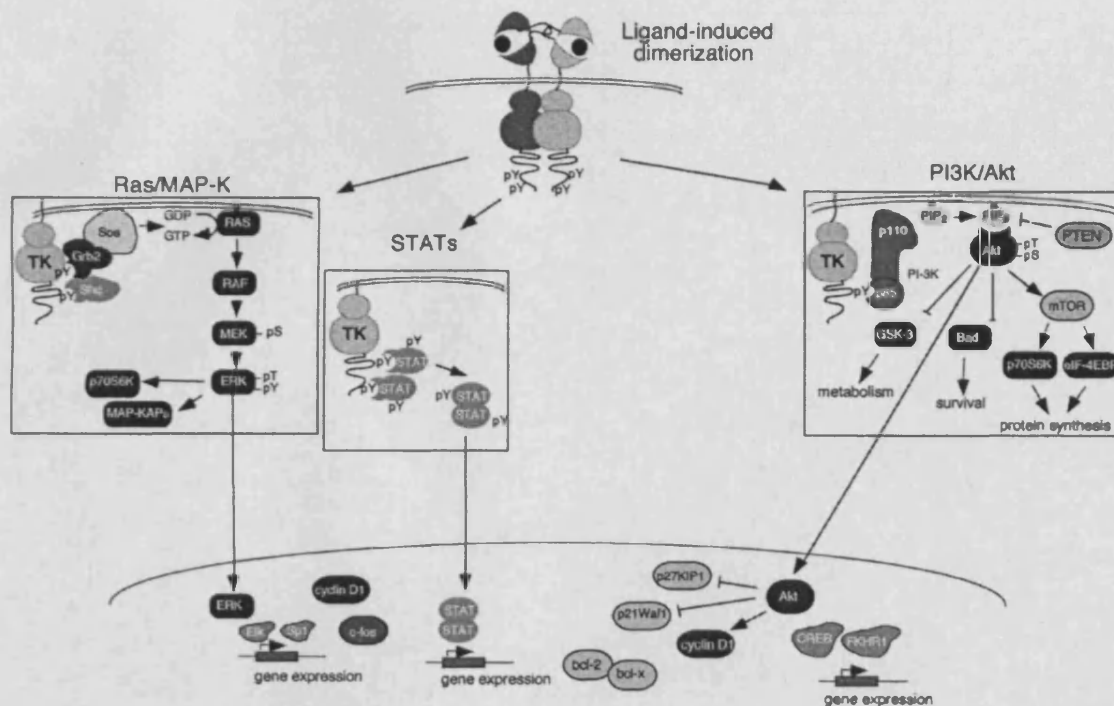
Figure 1.6

ErbB receptor induced signalling pathways [82]. Ligand binding induces receptor homodimerisation or heterodimerisation, which results in the activation of tyrosine kinase activity. This activates a variety of signalling pathways including the Ras-MAPK, PI3K-AKT and STAT pathways. Collectively these pathways culminate in cellular proliferation, migration and survival.

1.5.2.1 MAPK activation

All ErbB ligands and receptors couple to activate the Ras-MAPK pathway, either directly or indirectly. Ras genes code for GTPases that act as molecular switches, cycling between an inactive guanine diphosphate (GDP)-bound state and an active guanine triphosphate (GTP)-bound state [83]. The ErbB receptors stimulate the exchange of GDP for GTP on the small G protein Ras [84]. Among other effectors, the active GTP-Ras binds and activates Raf kinase, initiating a kinase cascade, which leads to phosphorylation of MAPK. Activated MAPK then phosphorylates multiple cytoplasmic and cytoskeletal proteins, and also undergoes rapid translocation into the nucleus where it phosphorylates and activates a variety of transcription factor targets [82].

1.5.2.2 PI3K/AKT activation

PI3K mediates many proliferation and cell survival signals [82]. ErbB receptors stimulate activation of PI3K also via GTP-Ras binding. The protein serine-threonine kinase AKT is a key effector of PI3K, and has many cytoplasmic and nuclear targets. Phosphorylated AKT promotes cell survival by blocking interactions of pro-apoptotic molecules, and promotes cell cycle progression through down regulation of the cyclin dependent kinase (cdk) inhibitor p27 [82]. The effects of the PI3K/AKT pathway are reflected by the tumour suppressive effects of PTEN (phosphatase and tensin homologue deleted on chromosome ten), a lipid phosphatase that de-phosphorylates the 3' position of PI3K products.

PTEN acts to negatively regulate the PI3K/AKT pathway, and is frequently mutationally inactivated in human cancers [85].

1.5.2.3 STAT activation

Seven mammalian STAT proteins have been identified. Over 40 different polypeptides can mediate STAT activation, including receptor tyrosine kinases, such as ErbB1 [86]. This leads to formation of active STAT dimers, which accumulate in the nucleus, recognise specific DNA (deoxyribonucleic acid) elements in the promoters of genes and activate transcription. STATs thus play an important role in controlling cell-cycle progression and apoptosis [86]. It has been shown that human cancer cells have often lost normal control of these signalling systems, especially STAT1, STAT3 and STAT5 [87].

1.5.3 Effect of ErbB signalling on cell cycle

Thus the activation of the ErbB receptors results in stimulation of a large network of signalling pathways that eventually subvert cell cycle checkpoints and pro-apoptotic molecules, leading to dysregulated cell cycle progression and enhanced tumour cell survival. The stages of the cell cycle are G1 (GAP-1), S (Synthesis, when DNA replication occurs), G2 (GAP-2), and M (mitosis) (figure 1.7). Regulation of the cell cycle is complex, but cdks and cyclins are major control switches for the cell cycle, causing the cell cycle to progress from G1 to S, or G2 to M. p27 is a protein that aids

to regulate their action, by binding to cyclin and cdks, thereby blocking entry into S phase. Activation of the ErbB signalling pathways, and in particular the MAPK and AKT pathways, is thought to lead to decreased levels of the cyclin-dependent kinase inhibitor p27, and consequently increased levels of cyclin D1 and various cdks. This in turn causes cell cycle progression from late G_1 into S, via phosphorylation of Rb, which acts to regulate this point in the cell cycle, and thus increased cell proliferation [88].
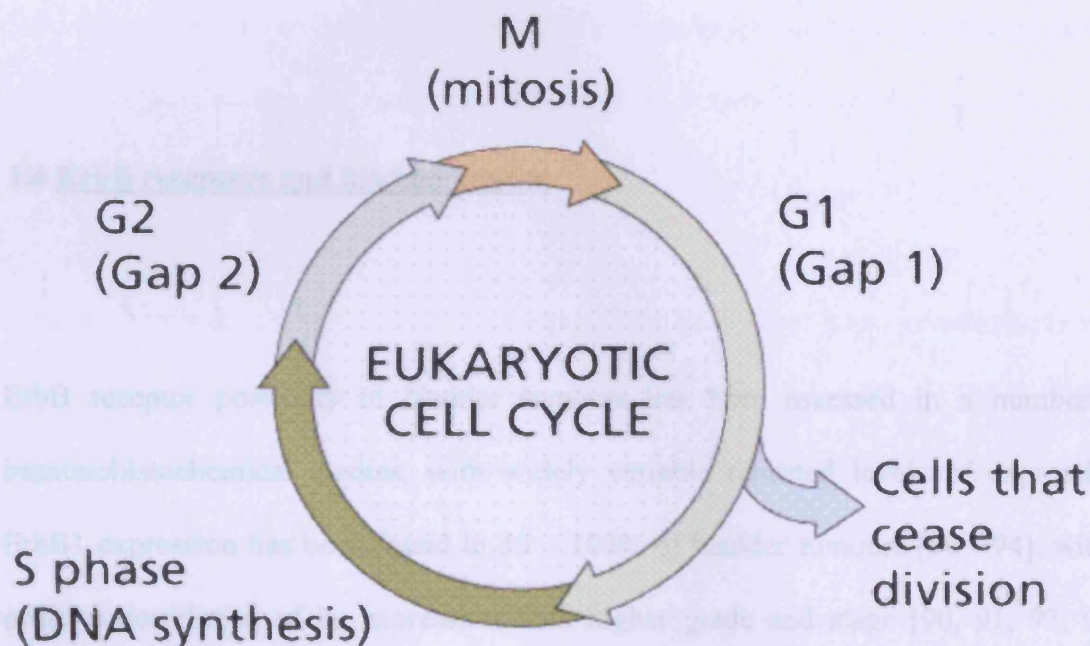
Figure 1.7

Diagrammatic representation of the stages of the cell cycle.

1.5.4 Degradation of ErbB receptors

Upon ligand binding and activation, ErbB receptors undergo internalisation via endocytosis. The contents of the resultant endosomes are then either degraded or recycled to the cell surface, depending upon the activating ligand [89]. For example, in the case of ErbB1 activation, EGF directs the receptor to degradation, whereas TGFα results in recycling.

1.6 ErbB receptors and bladder cancer

ErbB receptor positivity in bladder tumours has been assessed in a number of immunohistochemical studies, with widely variable reported levels of expression. ErbB1 expression has been found in 35 – 100% of bladder tumours [90 - 94], with a positive correlation of its expression with higher grade and stage [90, 91, 93, 95], higher rates of recurrence and progression [91 - 93], and also a worse prognosis and decreased survival [91, 93]. ErbB2 expression has been reported in 2 – 74% of bladder tumours [94, 96 - 101], but the correlations of this with prognostic factors have been contradictory. Several studies have correlated ErbB2 positivity with higher grade and tumour progression [94, 97 - 100] and others have reported independent prediction of earlier death with ErbB2 expression [94, 98, 99]. In contrast, another prospective study found that ErbB2 overexpression in the context of paclitaxel-based chemotherapy decreased the risk of death significantly [101]. Fewer studies have

investigated ErbB3 and ErbB4 expression in bladder cancer. ErbB3 expression has been shown in 20 – 56% of tumours [95, 96, 102], and ErbB4 in 11 – 30% [95, 96]. In one study, ErbB3 expression was correlated with increased size and number of tumours, as well as higher grade and recurrence rate [94]. A further study showed that the predominant subtype of HRG ligand expressed in a tumour type determined whether ErbB3 positivity correlated with a good or bad prognosis [103]. High HRG1β expression correlated to poor survival, but co-expression of HRG4 with ErbB3 and ErbB4 was associated with improved survival [103]. There is little more information about the significance of ErbB4 expression in bladder cancer, though there seems to be no apparent relationship between ErbB4 expression and clinicopathological factors [94].

Various combinations of receptor co-expression have also been investigated, with some pairs being associated with decreased survival. ErbB1-ErbB3 and ErbB3-ErbB4 expression were more common in high grade and more invasive tumours in one study [95]. A second study showed co-expression of ErbB1-ErbB2, ErbB2-ErbB3 and ErbB1-ErbB2-ErbB3 in 34%, 27% and 22% of cases respectively, with ErbB1-ErbB2 and ErbB2-ErbB3 co-expressions being independently correlated with poor long-term survival [94]. This data suggests that expressing multiple ErbB receptors plays an important role in the tumorigenesis of bladder cancer, and that ErbB2 may serve as a critical component of ErbB interactions, especially with ErbB1 and/or ErbB3, whose preferred partner for heterodimerisation is ErbB2, as described earlier.

Signalling pathways downstream of the ErbB receptors have also been studied with respect to their involvement in the tumorigenesis of bladder cancer. The role of

STATs in bladder cancer has been investigated in a couple of studies. Activated STAT3 was suggested to have a crucial role for exhibition of malignant characteristics in one bladder cancer cell line [104], whilst another study showed that methylation of the STAT1 gene is associated with tumour recurrence in non-muscle invasive bladder cancer [105]. Other pathways investigated are those involving PI3K/AKT and MAPK. In one study, the pharmacological and biochemical inhibition of the PI3K/AKT pathway drastically reduced the invasive capacity of bladder cancer cell lines [106]. It has also been shown that the tumour suppressor gene *PTEN*, which inhibits the PI3K pathway, is mutated or homozygously deleted in 23 - 32% of muscle-invasive bladder tumours [107, 108]. In contrast, studies have not found a similar role for MAPK in bladder cancer. It has been found that levels of MAPK in cell lines do not correlate with invasive ability [106], and that typical TCC cell lines do not appear to depend upon MAPK pathways for continuous proliferation [109]. This data suggests that the PI3K/AKT pathway is the more important signalling pathway in bladder cancer cell lines.

1.7 Inhibition of ErbB receptors

There are several approaches to inhibition of ErbB receptors and their signalling pathways, which are currently under preclinical and clinical investigation [110]. These include the use of small molecule tyrosine kinase inhibitors (TKIs), monoclonal antibodies (MAbs), immunotoxin conjugates and antisense oligonucleotides. To date, the most studied methods of inhibition are small molecule TKIs and MAbs.

1.7.1 Immunotoxin conjugates

Monoclonal antibodies can be used alone, or as conjugates for the delivery of toxins, radioisotopes, or drugs [110]. Conjugates with MAbs to ErbB1 and ErbB2 have been studied, though there is little clinical data in this field. However, there have been concerns about hepatotoxicity in some early studies [111].

1.7.2 Antisense oligonucleotides

Overexpression of some oncogenes can affect the prognosis of malignancies, and the suppression of these overexpressed genes has been an area of therapeutic interest. Antisense oligonucleotides are a class of drugs used to specifically inhibit target genes on mRNA (messenger ribonucleic acid) [112]. During gene transcription, DNA becomes partially uncoiled, into "sense" and "antisense" complementary strands. The "antisense" strand generates mRNA (in the "sense" orientation), which is then

34

translated into protein products in the cytoplasm. Translation of the mRNA can be prevented by complementary base-pair binding of "antisense" oligonucleotides [113]. Thus it is possible to inhibit the expression of virtually any gene product without directly affecting other cellular components, and possibly with minimal side-effects, though little clinical data is available.

1.7.3 Monoclonal antibodies

Cetumixab (IMC-C225, ImClone, New York, USA), an anti-ErbB1 MAb, has been shown *in vitro* and *in vivo* (using an orthotopic tumour model) to inhibit bladder cancer cell growth [114]. Cetumixab acts by blocking the extracellular ligand-binding component of ErbB1 thus preventing endogenous ligand binding. Of interest, the combination of cetumixab with paclitaxel has a synergistic growth inhibitory effect in mice with metastatic human bladder carcinoma [115]. However, unlike TKIs, cetumixab is administered intravenously, and therefore would be a more invasive clinical treatment.

A MAb against ErbB2, trastuzumab (Herceptin, Genentech, CA, USA), has been widely studied in breast cancer. Trastuzumab binds the extracellular domain of the ErbB2 receptor, and induces an antibody-dependent cellular cytotoxicity against tumour cell lines [116]. Trastuzumab has a proven clinical benefit in women with metastatic breast cancer with ErbB2 overexpression. A phase III trial in such women showed a more prolonged time to disease progression, and longer survival, in patients treated with trastuzumab and chemotherapy, compared to those treated with

chemotherapy alone [117]. There is no data on efficacy of trastuzumab in the treatment of metastatic bladder cancer at the present time.

Toxicity to MAb's is still mainly in the form of serious allergic reactions, although advances to reduce the amounts of foreign protein they contain have reduced the incidence of hypersensitivity reactions in patients [110]. The MAb's discussed here were both derived from mouse (murine) antibodies, and then manipulated in order to reduce their immunogenicity. Cetumixab is a chimeric MAb, which is formed by replacing the constant regions of a murine MAb with the human constant region of an immunoglobulin [110]. While this reduces the amounts of foreign protein, incorporating the antigen-interacting protein sequence region of murine MAb into a human immunoglobulin framework can decrease this even further, forming a humanised MAb, such as Trastuzumab [110].

1.7.4 Small molecule tyrosine kinase inhibitors

Small molecule TKIs are synthetic, quinazoline-derived low molecular weight molecules. They interact with the intracellular domain of the ErbB receptors, and inhibit ligand-induced receptor autophosphorylation by competing for the intracellular ATP (adenosine triphosphate) binding site [118]. Gefitinib (ZD1839, AstraZeneca USA), the most widely studied, demonstrates remarkable selectivity for ErbB1 compared with other receptor tyrosine kinases. Erlotinib (OSI-774, OSI Pharmaceuticals, NY, USA) is also selective for ErbB1. In contrast, lapatinib (GW572016, GlaxoSmithKline, USA) is a dual tyrosine kinase inhibitor of ErbB1 and

ErbB2. Canertinib (CI-1033, Pfizer, MA, USA) is a pan-ErbB TKI, which is active against all four members of the ErbB receptor tyrosine kinase family. Canertinib is an irreversible inhibitor, whereas gefitinib, erlotinib and lapatinib are all reversible inhibitors. Gefitinib, erlotinib and lapatinib are currently under clinical investigation in phase III trials, and canertinib is being studied in phase II trials.

1.8 Preclinical and clinical activity of TKIs

1.8.1 TKIs as primary chemotherapeutic agents

1.8.1.1 Preclinical data

Early work with TKIs assessed their potential as primary chemotherapeutic agents. They have been shown to be capable of inhibiting the growth of bladder cancer cells *in vitro* [119], as well as inhibiting other cancer cell lines (e.g. ovarian, colon, and breast cancer) [120]. They also have the ability to inhibit signalling pathways downstream of ErbB receptors, including the MAPK, AKT and STAT pathways [121]. *In vivo* work assessing the inhibitory effect of small molecule TKIs, using subcutaneous inoculation of human tumour cell lines (lung, vulval and prostate cancer) in athymic nude mice, has confirmed earlier *in vitro* results [122].

1.8.1.2 Clinical data

Gefitinib has been well tolerated in phase I testing, involving patients with a range of ErbB1-expressing malignancies (including breast, prostate, colorectal, and head and neck cancers) [123]. Phase I data for erlotinib also shows it to be well tolerated in advanced solid malignancies [124]. Canertinib showed dose limiting toxicity of diarrhoea, rash and anorexia in patients with solid tumours refractory to standard therapy in a phase I trial, but was shown to be safe at the maximum tolerated dose [125].

Both gefitinib and erlotinib have received United States. Food and Drug Administration (US FDA) approval for use as monotherapy in advanced non-small cell lung cancer (NSCLC) [126]. Gefitinib received FDA approval in May 2003 as a third-line therapy in locally advanced or metastatic NSCLC after failure of both platinum-based and docetaxel chemotherapies [126]. This followed results from the IDEAL-2 (Iressa Dose Evaluation in Advanced Lung Cancer) phase II trial [127]. Results showed a total response rate of 10.6% and a total symptomatic response rate of 40% when gefitinib was used after platinum-based and docetaxel chemotherapy [127]. However, the manufacturers took the step of advising clinicians to consider other treatment options in patients with recurrent NSCLC after the results of the ISEL (Iressa Survival Evaluation in Lung Cancer) phase III trial, which closed in August 2004 [126]. The ISEL trial randomised gefitinib versus placebo in patients with advanced NSCLC who had progressed or could no longer endure chemotherapy [128]. The primary endpoint was survival, and results showed that gefitinib did not prolong survival in the overall population,

with a median survival of 5.6 months with gefitinib, versus 5.1 months with placebo [128]. Erlotinib received FDA approval in November 2004, for use in patients with locally advanced or metastatic NSCLC after failure of at least one prior chemotherapy regimen [126]. This was following results from the BR.21 phase III study from the National Cancer Institute of Canada Clinical Trials Group (NCIC-CTG), which trialled erlotinib against placebo in patients with advanced NSCLC who had had at least one, but not greater than two, failed chemotherapy regimens [129]. This study found a 27% reduction in risk of death with erlotinib, and a median survival of 6.7 months with erlotinib versus 4.7 months with placebo ($p<0.001$) [129].

1.8.1.3 Predicting clinical response

An important factor to consider when using TKIs to treat human malignancies is that no clear association between ErbB receptor levels and response to ErbB-targeted therapies has been found [130]. Some preclinical studies have noted a relationship between ErbB1 expression and response to TKIs [131], but others haven't [122, 132]. However, selection of patients whose tumours overexpress ErbB2 has proved to be important in the use of Trastuzumab in breast cancer [117]. This discrepancy in reports may be related to the fact that levels of expression of ErbB receptors at the cell surface does not take account of whether mutant receptors are present, whether such receptors are in a more or less active state than wild type receptors, or indeed whether the signalling pathway downstream of the receptors is active. Thus the expression of ErbB1 does not

imply that the tumour cell is solely dependent for growth or survival on this particular signalling pathway, as many alternative mitogenic signalling pathways are available to tumour cells [133].

There is potential for numerous mutations of receptors. The most commonly found ErbB1 mutation is EGFRvIII, which has loss of residues in its ectodomain, and is constitutively active, not downregulated by endocytosis, and is potently transforming [134]. Responsiveness of cells with the EGFRvIII mutation in vitro to gefitinib has been reported [135]. More recently, studies have found subgroups of patients with NSCLC with specific mutations in the ErbB1 gene and improved clinical responsiveness to gefitinib and erlotinib [136, 137].

In view of the uncertainty surrounding the significance of levels of ErbB receptor expression, it has been suggested that until ErbB-based assays predictive of a response to receptor-targeted therapies are available, there is really no justification for stratifying patients by receptor status or excluding patients from clinical trials of such therapies [130].

1.8.2 Lapatinib as a primary chemotherapeutic agent

1.8.2.1 Preclinical data

As previously discussed, ErbB receptors are inactive in monomeric form, and receptor phosphorylation only occurs upon homo- or heterodimerisation in response to ligand binding. ErbB1 preferentially heterodimerises with ErbB2, making dual tyrosine kinase inhibition of these two receptors an attractive therapeutic strategy for epithelial tumours. It is especially attractive in view of the fact that ErbB2 is also the preferred partner for heterodimerisation with ErbB3.

The dual ErbB1/ErbB2 TKI lapatinib has been shown to inhibit cell growth *in vitro* in a number of solid tumour systems, including breast, head and neck, prostate and colon carcinoma cell lines [138 -140], even if ErbB1 and ErbB2 are not overexpressed [138]. Clearly, some tumours with low levels of expression of ErbB1 and ErbB2 remain dependent on these receptors for growth and survival signals. Similar findings were observed *in vivo* in human tumour xenografts [138, 139].

In vitro studies involving treatment with lapatinib have shown that it decreases levels of phosphorylation of ErbB1 and ErbB2, and indirectly down-regulates activated MAPK and activated AKT [138, 139, 141 - 143]. Lapatinib also produces increased levels of apoptosis in breast and colon cancer cell lines [138, 139, 141, 144]. In breast cancer cells, this increase in apoptosis has been linked

with its ability to down-regulate survivin, a member of the inhibitor-of-apoptosis family, in ErbB2 over-expressing cells [141, 144].

The ability of lapatinib to inhibit ErbB3 activation via its heterodimerisation with ErbB2 has been investigated in breast and prostate cancer cell lines [145, 146]. Some breast cancer cell lines express a truncated version of ErbB2 ($p95^{ErbB2}$), in which the extracellular domain of ErbB2 has been cleaved and deleted, and is a feature associated with metastatic disease in breast cancer. In such cell lines, lapatinib inhibited HRG-induced activation of $p95^{ErbB2}$ and AKT, an effect not seen in response to treatment with Trastuzumab [145]. In prostate cancer cell lines, lapatinib inhibited HRG-induced cellular proliferation more potently than the ErbB1 TKI, gefitinib [146]. Lapatinib has also been shown to be superior to gefitinib in prostate cancer cell lines in terms of its ability to impair androgen receptor function [140].

Combining lapatinib with Trastuzumab in breast cancer cell lines showed a synergistic interaction in an *in vivo* study [143], and *in vitro* in oestrogen receptor negative, tamoxifen resistant cells, lapatinib sensitised the cells to tamoxifen [142].

These studies indicate a possible wide range of applications for lapatinib, which require clinical investigation. Of further interest, lapatinib has shown radiosensitising potential *in vitro*, in both Ras-transformed cells, and in ErbB1 overexpressing breast cancer cell lines [147, 148]. To date, lapatinib has not been

42

studied in bladder cancer cell lines, or in combination with chemotherapeutic agents.

1.8.2.2 Clinical data

Phase I studies of lapatinib have been reported, and have shown it to be well tolerated in both healthy patients, and in patients with heavily pretreated, metastatic solid tumours [149 - 151]. The most common side effects, in common with other TKIs, were diarrhoea and rash, with no grade four drug-related adverse reactions reported [149, 150]. In 33 patients with metastatic disease, sequential tumour biopsies were taken. Partial responses occurred in four patients with breast cancer, and disease stabilisation occurred in 11 others with various malignancies. In responders, variable levels of inhibition of phosphorylated ErbB1, ErbB2, MAPK and AKT were seen [151]. Several phase II and phase III trials of lapatinib in a variety of solid tumours, including breast, prostate and oesophageal carcinomas, are currently recruiting

1.8.3 TKIs as adjuncts to chemotherapy

1.8.3.1 Preclinical data

Tyrosine kinase inhibitors have been studied *in vitro* in combination with chemotherapeutic agents in a number of ErbB1-expressing tumour systems,

including breast, ovarian and colon. Growth inhibition has been shown to be enhanced when gefitinib is combined with structurally and functionally different drugs *in vitro*, such as platinum-derived agents (cisplatin, oxaliplatin, carboplatin), taxanes (paclitaxel, docetaxel), topoisomerase I (topotecan) or II (etoposide, topotecan) inhibitors and a thymidylate synthase inhibitor (raltitrexed) [132]. The antiproliferative effect was mainly cytostatic, but treatment with higher doses of gefitinib increased apoptosis. Constitutive activation of AKT has been linked to chemoresistance in NSCLC cells *in vitro* [152]. Since lapatinib is a potent inhibitor of activated AKT [138], it may be an important adjunct to chemotherapy.

In further *in vitro* studies, the importance of the sequence of application of TKIs and chemotherapeutic agents was examined. In the first of these studies, gefitinib was applied in various sequences with cisplatin/5FU to head and neck squamous cell carcinoma cell lines [153]. Results showed a slight synergistic effect when gefitinib was applied first, with optimal results when gefitinib was applied before and during cisplatin/5FU treatment. There appeared to be an antagonistic effect when gefitinib was applied after cisplatin/5FU [153]. However, subsequent studies using colon carcinoma cell lines have contradicted this data [154, 155]. Gefitinib was again applied in various sequences with chemotherapeutic agents, either the topoisomerase I inhibitor SN-38 [154], or oxaliplatin [155]. In both studies there was maximal synergy when gefitinib was applied after chemotherapy, with either only an additive [155], or an antagonistic [154] effect when it was applied before chemotherapy. Clearly, there is need for further investigation of scheduling TKIs and chemotherapeutic agents, and it may be that the optimal schedule varies with cancer cell type and/or chemotherapeutic agent.

In vivo studies have shown that gefitinib in combination with paclitaxel, topotecan or raltitrexed significantly extended survival time in mice bearing colon tumour xenografts [132]. In a further *in vivo* study [122], partial or complete tumour regressions in mice with human squamous, lung and prostate xenografts were observed when treated with combinations of gefitinib, cisplatin, carboplatin, paclitaxel and docetaxel. These regressions were not seen after single-agent treatment. Erlotinib has also improved growth inhibition when combined with cisplatin in head and neck carcinoma xenografts [156].

1.8.3.2 Clinical data

Several large, multicentre, phase III trials of TKIs combined with chemotherapy in patients with NSCLC have now been reported, and all have failed to show any survival benefit of TKI plus chemotherapy over chemotherapy alone [157 - 160]. Two trials, INTACT 1 (Iressa NSCLC Trial Assessing Combination Treatment) and INTACT 2, combined gefitinib with chemotherapy in chemotherapy naïve patients with unresectable, advanced (stage III or IV) NSCLC in phase III, randomised, double-blind, placebo-controlled multicentre trials [157, 158]. INTACT 1 used cisplatin plus gemcitabine as its chemotherapeutic regimen [157], as opposed to paclitaxel plus carboplatin in INTACT 2 [158]. These regimens are commonly used as first line treatments in advanced NSCLC. In both trials, patients received up to six cycles of chemotherapy, plus either 500 mg/day gefitinib, 250 mg/day gefitinib, or placebo, with the gefitinib or placebo

continuing until disease progression. The primary end point was overall survival, with secondary end points of time to progression and response rates. Each trial recruited over 1000 patients, but neither showed any benefit of gefitinib over placebo with respect to their end points (table 1.6) [157, 158]. No significant adverse events were seen in either trial, and in particular there was no increased incidence of interstitial lung disease with gefitinib, despite the fact that AstraZeneca Japan reported that by the end of January 2003, 173 patients who had been treated with gefitinib in Japan (23,500 patients treated in total) had died of acute lung disease and/or interstitial pneumonitis [161]. A subsequent report associated such gefitinib induced interstitial pneumonia with other pulmonary disorders such as previous thoracic irradiation, and poor performance status [162].

	Median survival (months)		Time to progression (months)		Response rate (%)	
	INTACT 1	INTACT 2	INTACT 1	INTACT 2	INTACT 1	INTACT 2
Gefitinib 500 mg/day	9.9	8.7	5.5	4.6	49.7	30.0
Gefitinib 250 mg/day	9.9	9.8	5.8	5.3	50.3	30.4
Placebo	10.9	9.9	6.0	5.0	44.8	28.7

Table 1.6

Table of results from INTACT 1 and INTACT 2 trials, showing the main end points from each trial [157, 158]. No statistically significant differences were seen between the varying treatment combinations.

INTACT 1 and INTACT 2 were established following promising results from phase I and phase II trials, so why was no benefit of gefitinib over placebo seen? Several factors may have contributed. Patients were not selected on the basis of size of tumour, and in fact most of these patients had relatively high tumour volumes. Moreover, survival was higher than expected in the control arm (around 30% survival at one year was expected in the control arm, but approximately 40% survived one year in both arms). Also, ErbB1 status of patients was not assessed, though as previously discussed, at the present time there is no proof that this status would predict response to treatment. A study analysing the frequency of ErbB1 mutations in tumour specimens from both the IDEAL and INTACT trials has been reported [163], in light of the previous data showing a correlation between specific activating mutations in ErbB1 and responses to gefitinib [136]. In the IDEAL trials there was a positive correlation between ErbB1 mutations and response to gefitinib, though no such correlation was found when gefitinib was combined with chemotherapy in the INTACT trials [163]. Other factors to predict response to gefitinib in combination with chemotherapy have been suggested for further study. These include response of the AKT pathway to treatment, and the effect of different sequences of application of gefitinib and chemotherapy [157, 158].

Two similar trials have been reported combining erlotinib with chemotherapy [159, 160]. The study designs were comparable to the INTACT trials, with the TALENT trial combining either erlotinib 150 mg/day or placebo with up to six cycles of cisplatin plus gemcitabine, followed by maintenance erlotinib [159], whilst the TRIBUTE trial used paclitaxel plus carboplatin as the chemotherapeutic regimen [160]. Chemotherapy naïve patients with advanced NSCLC were again

the target population, and over 1000 patients were recruited to each trial. Results were similar to the INTACT trials, with no difference in overall survival, time to progression or response rates seen [159, 160]. Postulated reasons for these results were like those for the INTACT trials.

However, one phase III trial of a TKI combined with chemotherapy has shown a survival benefit [164]. Gemcitabine was combined with either erlotinib 100 mg/day or placebo in a randomised, double-blind, placebo-controlled, multicentre trial in chemotherapy naïve patients with advanced pancreatic cancer [164]. Nearly 600 patients were recruited, and a 23% improvement in overall survival (p=0.025) was found, along with a significant improvement in progression free survival (p=0.003) [164]. This data led the US FDA to approve erlotinib for use with gemcitabine in this group of patients in November 2004. This is the first new therapy in nine years approved for use in pancreatic cancer. This trial gives hope for further investigation of the use of TKIs in combination with chemotherapy in other solid tumours, although more preclinical trials are essential to elucidate the reasons for the poor results from the NSCLC trials.

1.8.4 TKIs as adjuncts to chemotherapy in bladder cancer

There is no preclinical data combining TKIs with chemotherapy in bladder cancer cell lines, though one trial has studied the monoclonal antibody, cetumixab, in combination with paclitaxel [115]. In this *in vivo* study, the combination of cetumixab and paclitaxel resulted in significantly greater regression of tumours compared with

either agent alone [115]. In spite of this lack of data, there are several phase II trials recruiting which are combining gefitinib with chemotherapeutic agents in bladder cancer. These include a SPORE (Specialized Program of Research Excellence) phase II trial combining gefitinib with docetaxel [165], a CALGB (Cancer and Leukaemia Group B) Genitourinary Committee trial of gefitinib and gemcitabine [166], and a trial by AstraZeneca of gefitinib with gemcitabine and cisplatin. However, in view of the disappointing results of the phase III NSCLC trials of TKIs with chemotherapy, preclinical studies into the effect of combining TKIs with clinically relevant chemotherapeutic agents in bladder cancer are essential.

The three chemotherapeutic agents currently under most scrutiny in clinical trials in bladder cancer are cisplatin, gemcitabine and paclitaxel. Cisplatin is an alkylating agent and acts by binding to nuclear DNA. This causes interference with normal transcription and/or DNA replication mechanisms, leading to apoptosis [167]. Cisplatin in not cell cycle dependent. Gemcitabine is a pyrimidine analogue, which exerts its effects by incorporating one of its active metabolites (dFdCTP) into DNA. This leads to inhibition of DNA synthesis and apoptosis, which is specific to S and G1/S phases of the cell cycle [168]. Paclitaxel is a mitotic inhibitor, which causes mitotic arrest followed by apoptosis by creating unusually stable microtubules. This inhibits microtubule depolymerisation and stops cell cycle progression in late G2/M phase [169]. Cancer cells thus show varying responses to the different chemotherapeutic agents according to the alterations they induce in DNA damage checkpoints, usually leading to cell cycle arrest followed by apoptosis when DNA repair cannot be accomplished [170, 171].

Clearly these three agents have very differing modes of action, and adding novel agents such as TKIs to any combination of the chemotherapeutic agents will result in complex interactions. Studies have however shown that all three agents exhibit some effects on the signalling pathways downstream of ErbB receptors. In one study, cisplatin activated ErbB1 and MAPK, but not AKT, in an ErbB1 overexpressing cell line, and it has been postulated that this may be a cell survival response that reduces efficacy of cisplatin [172], although specific effects may be cell type specific. In a recent study, paclitaxel also activated ErbB1 and MAPK, but not AKT in renal cell carcinoma cell lines, six to eight hours after initiation of treatment, an effect that was inhibited by gefitinib [173]. Gemcitabine also activates MAPK, the suppression of which by canertinib or the MAPK inhibitor PD 098059 in combination with gemcitabine, increased apoptosis in breast cancer cell lines [174]. Such activation of ErbB signalling by these chemotherapeutic agents may, as suggested by two of the studies, be the mechanism by which TKIs are able to sensitise cells to chemotherapy. Another group of studies also points towards this idea. As mentioned earlier, constitutive activation of AKT has been linked to chemoresistance [152], and inhibition of AKT has been shown to increase efficacy of paclitaxel in ovarian cancer cell lines [175]. Thus, combining chemotherapy regimens currently in use and under clinical investigation in bladder cancer, with novel targeted therapies such as tyrosine kinase inhibitors, is an attractive and promising prospect for future management of bladder cancer. Preclinical data in this area is necessary before effective clinical trials can be established.

The primary hypothesis for this study is that lapatinib, a dual ErbB1/ErbB2 TKI, will be an adjunct to chemotherapy in bladder cancer cell lines. The second hypothesis is that this interaction is mediated via ErbB receptor signalling pathways, such as the PI3K/AKT and MAPK pathways.

CHAPTER 2

MATERIALS AND METHODS

2.1 Cell lines and tissue culture

Six human bladder cancer cell lines - J82, UMUC3, T24, HT1376, RT4 and RT112 - and the human vulval squamous cell carcinoma cell line A431 were used for initial experiments (American Type Culture Collection and the European Collection of Cell Cultures). The bladder cancer cell lines are of variable grades, with RT4 and RT112 cells being derived from low grade, G1, tumours, and the rest being high grade, G2/3, tumour cell lines. All cells were cultured as a monolayer in DMEM (Dulbecco's Modified Eagle Media [+ 4500 mg/L glucose, + glutamax™ I, + pyruvate] Invitrogen, Carlsbad, CA, USA) supplemented with 10% fetal bovine serum (FBS) (Biowest, Nuaille, France), 1% non-essential amino acids (NEAA) and 1% penicillin-streptomycin (P-S) (Invitrogen, Carlsbad, CA). For some experiments which are discussed later, medium with 1% FBS or serum free medium was used, though both 1% NEAA and P-S were used throughout. All cells were grown in a humidified incubator supplemented with 5% CO_2 (carbon dioxide) at 37°C. Trypsin-EDTA (ethylenediaminetetraacetic acid) was used to lift cells for passaging (Invitrogen, Carlsbad, CA).

2.2 Preparation of drugs for experimental use

Lapatinib, cisplatin, gemcitabine and paclitaxel were prepared in solution in sterile conditions, and stored as below. When used in experiments, these stock solutions were further diluted in medium with the appropriate concentration of FBS.

2.2.1 Lapatinib

Lapatinib was kindly supplied by GlaxoSmithKline as a powder, molecular weight 943.49. This was made up to a 10 mM solution using 9.43 mg powder in 1 ml diethyl sulfoxide (DMSO, Sigma, St. Louis, MO). This stock was solution stored at -20°C.

2.2.2 Cisplatin

Cisplatin (Platinex^{TM}, Bristol-Myers Squibb Pharmaceuticals, Hounslow, England), molecular weight 300.1, was purchased as a 1 mg/ml solution. The molarity of this solution was thus 3.333 mM. A stock solution of 1mM cisplatin was prepared by adding 3 ml of 1 mg/ml solution to 7 ml of 0.9% sodium chloride (NaCl). This was stored at room temperature. Cisplatin is a photosensitive compound and therefore throughout all experiments was used in dimmed light conditions, and stored in the dark.

2.2.3 Paclitaxel

Paclitaxel (Taxol^{TM} Bristol-Myers Squibb Pharmaceuticals, Hounslow, England), molecular weight 853.9, was purchased as a 6 mg/ml solution. The molarity of this solution was thus 7.03 mM. A stock solution of 10 µM paclitaxel was prepared by adding 14.2 µl of 6 mg/ml solution to 10 ml of 0.9% NaCl. This was stored at room temperature.

2.2.4 Gemcitabine

Gemcitabine (Gemzar®, Lilly Pharmaceuticals, Basingstoke, England), molecular weight 299.7, was purchased as a powder (200 mg). This powder was dissolved in 5 ml of 0.9% NaCl to make a solution of 40 mg/ml (133.5 mM). Finally, 75 µl of 40 mg/ml solution was added to 10 ml of 0.9% NaCl to make a 1 mM solution of gemcitabine. This was stored at room temperature.

2.3 Western blot analysis

2.3.1 General methods

2.3.1.1 Preparation of cell lysates

Cells grown as a monolayer and treated according to individual experiments as described below, were lysed when at 70% confluence using standard Laemmli buffer (2% Sodium dodecyl sulphate [SDS], 10% glycerol, 5% β-mercaptoethanol, 0.002% bromophenol blue and 0.125 M Tris HCl, pH approximately 6.8 [from Trizma base], all from Sigma, St Louis, MO, USA) [176]. Laemmli buffer serves to prepare proteins for running on SDS-PAGE (SDS-Polyacrylamide Gel Electrophoresis) gels, and thus electrophoresis to separate the proteins, as follows. SDS detergent denatures the proteins and subunits and gives each an overall negative charge so that each will separate based on size, glycerol increases the density of the sample so that it will layer in the sample wells in the gel, β-mercaptoethanol reduces the intra- and inter-molecular disulfide bonds, and bromophenol blue serves as a dye front that runs ahead of the proteins and serves to make it easier to see the sample during loading. However, lysates were prepared without bromophenol blue and β-mercaptoethanol in the Laemmli buffer initially, as both of these chemicals interfere with the BCA (bicinichoninic acid) Protein Assay to be used to quantify protein content of the lysate. The BCA Protein Assay is colorimetric, and therefore the colour produced by bromophenol blue would interfere with the spectrophotometric analysis of the protein assay

samples. Reducing agents such as β-mercaptoethanol interfere with the BCA Protein Assay by artificially increasing the colour intensity. Both of these chemicals were added to lysates after aliquots for protein assay had been removed.

Initially cells were washed three times in phosphate-buffered saline (PBS, Sigma, St. Louis, MO, USA) prior to addition of Laemmli buffer for 1 minute. Lysate was then scraped from the surface of the flask, pipetted into an eppendorf, boiled for 10 minutes (this increases denaturation of proteins, and deactivates endogenous proteases), and stored in a −20°C freezer.

2.3.1.2 Quantification of lysate protein concentration

It is essential to know the concentration of protein in each lysate, so that equal amounts of protein can be separated by electrophoresis and therefore assessed, using Western blot analysis. This allows a direct comparison of protein levels between samples.

Protein concentration of lysates in these experiments was quantified using the BCA protein assay kit (Pierce, Rockford, IL). This is a detergent compatible, colorimetric assay based on bicinichoninic acid (BCA) and the reduction of Cu^{2+} to Cu^{1+} by protein in an alkaline medium (the biuret reaction) [177]. The purple-coloured reaction product of this assay is formed by the chelation of two molecules of BCA with one Cu^{1+}, and shows a strong absorbance at 562 nm that is nearly linear with increasing protein concentrations over a broad working range

(20 – 2,000 µg/ml). The intensity of the colour produced is actually proportional to the number of peptide bonds participating in the reaction.

The assay was performed in a 96 well plate. A series of dilutions of known concentrations of bovine serum albumin (BSA) were assayed alongside unknowns (the lysates) to allow the experimental sample protein concentrations to be calculated from the standard curve of the known BSA concentrations. Twenty five microlitres of each standard BSA solution or lysate was pipetted into a well (each in duplicate), and 200 µl of working reagent from the kit was added to each sample. The plate was then placed on a plate-shaker for 30 seconds before incubation at 37°C for 30 minutes. Absorbances were analysed using a GENios™ Microplate Reader (Tecan, Mannedorf/Zurich Switzerland). A curve of the BSA standards was plotted and the protein concentration of each lysate determined using Microsoft Excel software.

2.3.1.3 SDS-PAGE

The next step is to separate out the proteins in each lysate, so that the relative quantities of each can be assessed. This is achieved using SDS-Polyacrylamide Gel Electrophoresis (SDS-PAGE). As previously mentioned, the SDS in the Laemmli buffer confers a negative charge to the protein in proportion to its length. It is usually necessary to reduce disulphide bridges in proteins before they adopt the random-coil configuration necessary for separation by size, and this is achieved by the β-mercaptoethanol. As the negative charge conferred on the

protein is in proportion to its length, and the protein is opened out by the β-mercaptoethanol, migration by SDS-PAGE is determined not by intrinsic electrical charge of the polypeptide, but by molecular weight.

There are two types of separating systems in electrophoresis: continuous and discontinuous. A continuous system has only a single separating gel. In a discontinuous system, which was used throughout the current study, a non-restrictive large pore gel, called a stacking gel, is layered on top of a separating gel called a resolving gel. The resolution obtained in a discontinuous system is much greater than that obtained with a continuous system. The stacking gel is slightly acidic (pH 6.8) and has a low acrylamide concentration to make a porous gel, causing proteins to form thin, sharply defined bands. The resolving gel is more basic (pH 8.8), and has a higher acrylamide content which causes the gel to have narrower channels or pores. As a protein, concentrated into sharp bands by the stacking gel, travels through the separating gel, the narrower pores have a sieving effect whereby the resistance to the motion of the particle increases with particle size, allowing smaller proteins to travel more easily, and hence rapidly, than larger proteins. The negatively charged proteins migrate down the gel due to an electric current that is applied across it [176].

Gels were prepared for a discontinuous SDS-PAGE system as follows. Vertical gels made up of 8% resolving gel (2.7 ml 30% acrylamide mix [BDH Electran, Poole, UK], 2.5 ml 1.5 M Tris pH 8.8, 0.1 ml 10% SDS, 0.1 ml 10% ammonium persulfate and 0.006 ml TEMED [*N,N,N',N'*-Tetramethylethylenediamine] [both from Sigma, St Louis, MO, USA], made up to 10 ml with deionised water) and

5% stacking gel (0.5 ml 30% acrylamide mix, 0.38 ml 1.0 M Tris pH 6.8, 0.03 ml 10% SDS, 0.03 ml 10% ammonium persulfate and 0.003 ml TEMED, made up to 3 ml with deionised water), with 1 mm spacers, were prepared. Ammonium persulfate and TEMED were used to catalyse gel polymerisation.

Cell lysates were defrosted at room temperature and 5% β-mercaptoethanol and 0.002% bromophenol blue were added to each sample. Lysates were boiled for 1 minute and placed on ice. Equal amounts of protein from each lysate (calculated from BCA protein assay) were loaded in wells of the previously prepared gel covered in protein-run buffer (3.02 g Tris-base, 18.8 g Glycine and 10 ml 10% SDS, made up to 1000 ml with deionised water) which allowed the appropriate electrical current to be applied across the gel, along with 7 μl marker protein (SeeBlue® Pre-Stained Standard, Invitrogen, Carlsbad, CA), which allowed easy visualisation of protein molecular weight ranges during electrophoresis and evaluation of western transfer efficiency. Electrophoresis was run at 115 V (voltage constant, with at least 15 mA) for approximately 90 minutes.

2.3.1.4 Gel transfer

The next step is to transfer the proteins fractionated by SDS-PAGE to a solid support membrane (Western blotting) [178]. This was accomplished by electroblotting onto Immobilon-P Transfer Membrane (Millipore Corporation, Billerica, MA). This membrane is a polyvinylidene fluoride (PVDF) microporous membrane, which is hydrophobic and offers a uniformly controlled pore structure

with a high binding capacity for biomolecules. The procedure involves a sandwich of gel and membrane compressed in a cassette and immersed in buffer between two parallel electrodes. A current is passed at right angles to the gel, which causes the separated proteins to electrophorese out of the gel and onto the solid support membrane. The addition of methanol (up to 20%) to the transfer buffer has proven to enhance the transfer efficiency of some hydrophobic proteins.

Filter papers (x six) and the membrane were cut to size. The filter papers were soaked in blotting buffer (58.1 g Tris-base, 29.3 g glycine and 37.5ml 10% SDS, made up to 1000 ml with deionised water, further diluted 10 x with 200 ml methanol, 700 ml deionised water and 100 ml of original blotting buffer solution), and the membrane was soaked in methanol to activate it, followed by soaking in the blotting buffer. Three filter papers were placed on the base of the electrophoresis apparatus, on top of which was placed the activated membrane. The SDS-PAGE gel was placed on top of the membrane, with the remaining 3 filter papers on top of this. The resulting sandwich was gently rolled to exclude bubbles, which would interfere with the transfer of current between the gel and the membrane, and the apparatus lid was screwed tightly shut. An electrical field was applied to the apparatus, from top to bottom, at 20 mA (ampage constant, with at least 10 V) and run for variable periods of time (60 minutes for one x gel, and 90 minutes for two x gels). After transfer, the membrane was agitated in Ponceau S solution (Sigma, St. Louis, MO) for approximately five minutes. Ponceau S solution is used for the detection of proteins on membranes such as PVDF membranes. It is a negative stain, which binds reversibly to the positively charged amino groups of the protein, and it detects protein with a clear background and red protein bands. It allows assessment of the relative amounts of protein in each lane,

and ensures that effective blotting has occurred without air bubbles. Finally, the membrane was air dried overnight

2.3.1.5 Western blot staining and immunodetection

Once the membrane has been produced as described, probing of the membrane with primary and secondary antibodies against a specific protein, followed by immunodetection of that protein using chemiluminescence, is undertaken as follows (figure 2.1).

The membrane was divided into appropriate portions, soaked in methanol to reactivate, and transferred to TBS-T (Tris-buffered saline with TWEEN) buffer (18 ml of 1 M Tris pH 8.0, 24.5 ml of 5 M NaCl and 900 µl of TWEEN 20 [Sigma, St. Louis, MO, USA], made up to 1000 ml with deionised water). The membrane was then gently agitated in milk blocking solution (5% skimmed milk powder in TBS-T, milk-TBS-T) for 60 minutes. Incubation in blocking solution is a very important step, as this effectively blocks the unoccupied portions of the membrane, so that antibodies only bind to the proteins of interest. This means that non-specific binding and therefore background staining, is reduced. Both the milk protein and the TWEEN 20 (a non-ionic detergent) are active components in the blocking solution.

Following incubation in blocking buffer, the membrane was incubated with gentle agitation in milk-TBS-T with primary antibody for a further 60 minutes. Primary

antibodies were all at concentration of 1:1000, except for EGFR (1005) 1:4000, and α-tubulin 1:8000. The primary antibody is the antibody that binds the protein of interest. The membrane was next washed in TBS-T buffer (four x 10 minutes), to remove any unbound primary antibody, and thus reduce background staining further.

Next, the membrane was incubated again in milk-TBS-T (with gentle agitation) but this time with the secondary antibody (1:5000), for 45 minutes, followed by repeating washes in TBS-T buffer to remove unbound antibody. The secondary antibody binds to the primary antibody, and is conjugated to an enzyme that is used to indicate the location of the protein. Also, because more than one molecule of the secondary antibody may be able to bind to the primary antibody, a secondary antibody can enhance the signal.

The final step prior to visualising the target protein is immunodetection. This is based on enzyme-linked detection, utilising the secondary antibody covalently bound to an enzyme such as horseradish peroxidase (HRP) or alkaline phosphatase (AP). This enzyme catalyses the degradation of specific substrates, resulting in signal generation. Here chemiluminescent detection was used, which results in generation of a signal of visible light. The chemiluminescent agent was applied to the membrane for the appropriate length of time (SuperSignal West Substrate, Pierce, Rockford, IL, USA, for five minutes; or Amersham ECL, Amersham Biosciences, UK, for one minute). Excess substrate was shaken from the membrane, which was then placed between two sheets of acetate. In dark room conditions the membrane was exposed to X-ray film (Kodak BioMax Light Film,

Amersham Biosciences, Buckinghamshire, UK), which acted to detect the visible light signal generated as above, for varying lengths of time. The films were then processed using a developing machine.
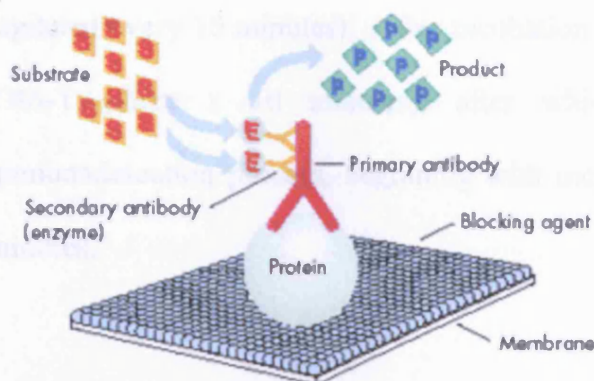
Figure 2.1

Diagrammatic representation of the process of immunodetection of proteins in Western blotting.

2.3.1.6 Stripping of membranes

After chemiluminescence, it is possible to remove all of the reagents from the membrane, a procedure known as stripping. A blot may be stripped and reprobed several times to visualise other proteins without the need for multiple gels and transfers. The key to this process is to use conditions that cause the release of antibody from the protein without causing a significant amount of the protein to be released from the membrane, although some amount of the protein is inevitably lost. Various protocols have been proposed to accomplish this purpose and they generally include some combination of detergent, reducing agent, heat and/or low pH. The stripping buffer that was used here was optimised for use with the antibodies used in these experiments. The membrane was initially washed in

TBS-T buffer (four x 10 minutes) and then submerged in stripping buffer (10 ml 10% SDS, 3.125 ml 1 M Tris pH 6.8, 0.357 ml β-mercaptoethanol and 36.5 ml deionised water) in a glass dish, within a ventilation hood. A lid was applied to the dish and this was then incubated in a water bath at 58°C for 30 minutes (agitated every 10 minutes). After incubation the membrane was washed again in TBS-T (three x 10 minutes), after which it was ready to restart the immunodetection process, beginning with incubation in blocking solution for 60 minutes.

2.3.2 Antibodies for Western blot staining

EGFR (1005), phospho-EGFR (tyr1100), ErbB3 (C-17), ErbB4 (C-18), PTP1B (H-135) and mouse anti-goat IgG-HRP antibodies were from Santa Cruz Biotechnology (Santa Cruz, CA, USA). Phospho-EGFR (tyr845), phospho-EGFR (tyr992), phospho-EGFR (tyr1045), phospho-EGFR (tyr1068), ErbB2, phospho-ErbB2 (tyr1248), phospho-ErbB3 (tyr1289), AKT, phospho-AKT (Ser473), phospho-AKT (Thr308), p42/44 MAP Kinase, phospho-p42/44 MAP kinase (Thr202/Tyr204), PTEN, STAT1 (9H2) monoclonal antibody, phospho-STAT1 (Tyr701), STAT3 and phospho-STAT3 (Tyr705) antibodies were all from Cell Signaling Technology (Beverly, MA, USA). E-cadherin monoclonal antibody was from BD Transduction Laboratories (San Jose, CA). α-tubulin antibody was from Sigma (St. Louis, MO, USA). Goat Anti-Rabbit and Rabbit Anti-Mouse immunoglobulins HRP were from DakoCytomation (Glostrup, Denmark).

2.3.3 Preparation of cells for individual experiments

2.3.3.1 Characterisation of cell lines

Cells were grown in 25 cm^3 flasks in medium with 10% FBS until 70% confluent. Cells were then lysed as described above in 1 ml of Laemmli buffer. Protein levels were quantified and gels were run with 25 μg protein in each well, alongside 7 μl marker protein. Resultant membranes were stained for total levels of proteins.

2.3.3.2 Stimulation of cells with epidermal growth factor (EGF)

Two 25 cm^3 flasks for each cell line were seeded, one control and one for stimulation, and cells were grown in medium with 10% FBS until 70% confluent, at which stage all medium was changed to serum free. Cells were starved for 24 hours. After this time, medium was removed and replaced with a further 3 ml of warm serum free medium for five minutes, along with 100 ng/ml EGF (PeproTech EC, London, UK) in stimulation flasks. Cells were then washed three times in PBS, and lysates were made using 1 ml standard Laemmli buffer and protein quantification was performed. Gels were run with 25 μg protein in each well, alongside 7 μl marker protein. Resultant membranes were stained for total and phosphorylated levels of proteins.

2.3.3.3 Inhibition of EGF-induced stimulation by lapatinib

Four 25 cm^3 flasks each of RT112 and J82 cells were seeded and grown in medium with 10% FBS until 50 – 70% confluent. At this stage medium was changed to serum free, either with or without the IC_{50} (half maximal inhibitory concentration of a drug. This represents the dose of a drug that results in cell viability half-way between the maximum and minimum cell viability levels after treatment with that drug) of lapatinib, and cells were incubated overnight (for 18 hours). After this time period 100 ng/ml EGF was added to the relevant flasks for five minutes. Cells were then washed three times in PBS, and lysates were made using 1 ml standard Laemmli buffer and protein quantification was performed. The lysates obtained were thus of cells treated as in table 2.1. Gels were run with 25 µg protein in each well, alongside 7 µl marker protein. Resultant membranes were stained for total and phosphorylated levels of proteins.

	Flask number			
	1	2	3	4
IC_{50} lapatinib	-	-	+	+
100 ng/ml EGF	-	+	-	+

Table 2.1

Summary of treatment of cells in numbered flasks for experiment investigating effect of lapatinib on EGF stimulation of cells.

2.3.3.4 Inhibition of heregulin(HRG1β)-induced stimulation by lapatinib

Four 25 cm^3 flasks each of RT112 and J82 cells were seeded and grown in medium with 10% FBS until 50 – 70% confluent. At this stage medium was changed to serum free, either with or without the IC$_{50}$ of lapatinib, and cells were incubated overnight (for 18 hours). After this time period 40 ng/ml HRG1β (R & D systems, MN, USA) was added to the relevant flasks for 15 minutes. Cells were then washed three times in PBS, and lysates were made using 1 ml standard Laemmli buffer and protein quantification was performed. The lysates obtained were thus of cells treated as in table 2.2. Gels were run with 25 μg protein in each well, alongside 7 μl marker protein. Resultant membranes were stained for total and phosphorylated levels of proteins.

	Flask number			
	1	**2**	**3**	**4**
IC$_{50}$ lapatinib	-	-	+	+
40 ng/ml HRG1β	-	+	-	+

Table 2.2

Summary of treatment of cells in numbered flasks for experiment investigating effect of lapatinib on HRG stimulation of cells.

2.3.3.5 Inhibition of combination chemotherapy-induced stimulation by lapatinib

Six 25 cm^3 flasks each of RT112 and J82 cells were seeded and grown in medium with 10% FBS until 50 – 70% confluent. At this stage medium was changed to serum free, either with or without IC$_{50}$ of lapatinib. After incubation for 24 hours, IC$_{50}$s of gemcitabine, paclitaxel and cisplatin (GTC) combined was added to the relevant flasks, and finally cells were lysed using standard Laemmli buffer at varying timepoints after addition of chemotherapy. The lysates obtained were thus of cells treated as in table 2.3. Protein assay was performed to quantify protein levels. Gels were run with 25 μg protein in each well, alongside 7 μl marker protein. Resultant membranes were stained for total and phosphorylated levels of proteins.

	Flask number					
	1	**2**	**3**	**4**	**5**	**6**
IC$_{50}$ lapatinib	-	+	-	+	-	+
Length of exposure to chemotherapy	Nil (Control)	Nil (Control)	10 minutes	10 minutes	20 hours	20 hours

Table 2.3

Summary of treatment of cells in numbered flasks for experiment investigating effect of lapatinib on incubation of cells with chemotherapy (GTC).

2.4 <u>Immunoprecipitation</u>

Immunoprecipitation is a method that enables the purification of a protein. An antibody for the protein of interest is incubated with a cell extract so that the antibody will bind the protein in solution. The antibody/antigen complex is then pulled out of the sample using protein A/G-coupled agarose beads. This physically isolates the protein of interest from the rest of the sample (figure 2.2) and any proteins not precipitated by the protein A or G beads are washed away. The protein is removed from the protein A/G by boiling with an SDS-containing buffer. The separated protein sample can then be separated by SDS-PAGE for Western blot analysis.
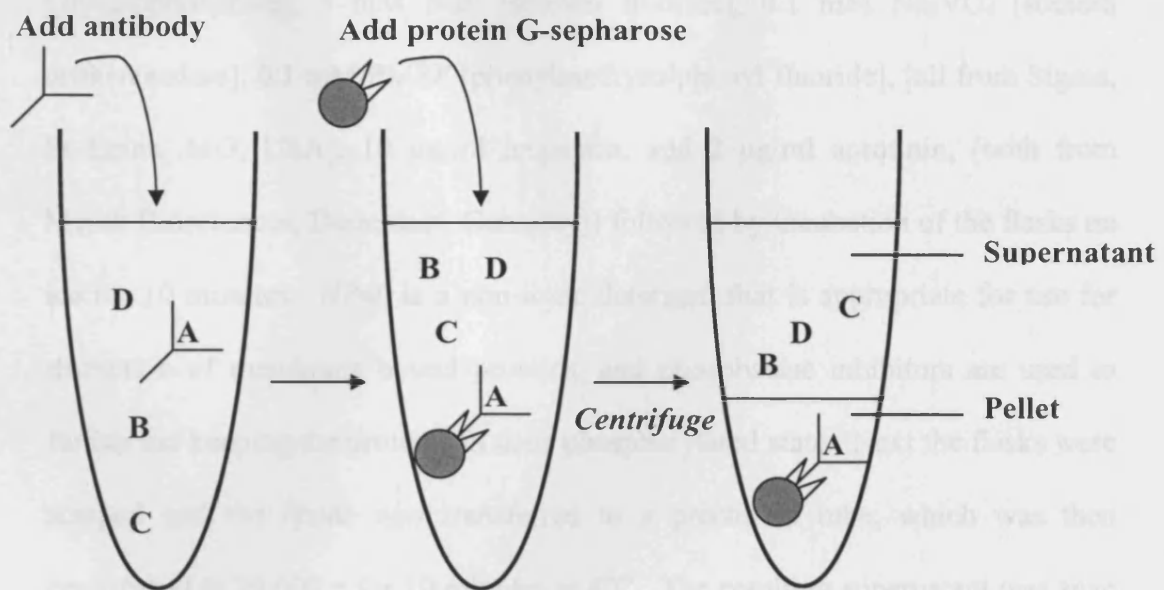
Figure 2.2

Schematic representation of the principle of immunoprecipitation. An antibody added to a solution of cell extract and binds specifically to its antigen (A). Antibody-antigen complex is absorbed from solution through the addition of protein G agarose beads. Upon centrifugation, the antibody-antigen complex is brought down in the pellet. Subsequent liberation of the antigen can be achieved by boiling the sample in the presence of SDS.

2.4.1 General methods

2.4.1.1 Preparation of cell lysates

Cells grown as a monolayer up to 70% confluence (treated according to individual experiments as described below), were washed three times in ice cold PBS. All subsequent stages of immunoprecipitation were carried out on ice or at +4°C to aid keeping proteins in their phosphorylated state. Cells were next immediately covered by 3 ml of Nonidet P40 (NP40) buffer (0.1 M NaCl, 0.5 M NP40 [Sigma, St Louis, MO, USA], 50mM Tris pH 8.0, made up to 50 ml with deionised water) plus phosphatase inhibitors (1 mM DTT [dithiothreitol], 10 mM βGP [β-Glycerophosphate], 5 mM NaF [sodium fluoride], 0.1 mM Na_3VO_4 [sodium orthovanadate], 0.1 mM PMSF [phenylmethysulphonyl fluoride], [all from Sigma, St Louis, MO, USA], 10 μg/ml leupeptin, and 2 μg/ml aprotinin, [both from Merck Biosciences, Darmstadt, Germany]) followed by incubation of the flasks on ice for 10 minutes. NP40 is a non-ionic detergent that is appropriate for use for extraction of membrane bound proteins, and phosphatase inhibitors are used to further aid keeping the proteins in their phosphorylated state. Next the flasks were scraped and the lysate was transferred to a prechilled tube, which was then centrifuged at 20,000 g for 10 minutes at 4°C. The resulting supernatant was snap frozen in liquid nitrogen to again reduce dephosphorylation of the proteins. Equal volumes of lysate were run on SDS-PAGE gels, which were subsequently stained using Simply Blue ™ Safestain (Invitrogen, Carlsbad, CA), a variant on coomassie stains, in order to estimate volumes of lysates required for equal amounts of protein.

2.4.1.2 Immunoprecipitation of proteins

Lysates were thawed on ice and centrifuged at 20,000 g for 10 minutes at 4°C. One microgram of primary antibody (either anti-EGFR antibody Mab13 [Neomarkers, Lab Vision Corporation, Fremont, CA, USA] or anti-ErbB2 antibody [Novagen, Madison, WI, USA]) were added to each lysate and this was incubated overnight with rotation at 4°C. Next 40 μl of protein-G sepharose (Amersham Biosciences, Buckinghamshire, UK) was added and lysates were incubated again with rotation at 4°C for three hours. Lysates were then centrifuged at 300 g for one minute at 4°C. The supernatant was discarded, the pellet was washed in 750 μl of NP40 buffer, and this solution was centrifuged at 300g for one minute at 4°C. This process was repeated a further two times. After the third wash the supernatant was again discarded and 20 μl of standard Laemmli buffer was added to the pellet. The resulting lysates were boiled for five minutes before a final centrifuge at 20,000 g for 5 minutes at 4°C. All of the obtained supernatant was then separated by SDS-PAGE, transferred to a membrane, and proteins were stained for as for Western blot analysis. Primary antibody used for these experiments was anti-phosphotyrosine, clone 4G10, 1:1000 (Upstate, Charlottesville, VA, USA), which was used to detect all phosphorylated tyrosine residues on the extracted receptors.

2.4.2 Preparation of cells for individual experiments

2.4.2.1 Inhibition of combination chemotherapy-induced stimulation by lapatinib

Six 75 cm^3 flasks each of RT112 and J82 cells were seeded and grown in medium with 10% FBS until 50 – 70% confluent. At this stage medium was changed to serum free, either with or without IC_{50} of lapatinib. After incubation for 24 hours, IC_{50}s of gemcitabine, paclitaxel and cisplatin combined was added to the relevant flasks, and cells were then lysed at various timepoints after addition of chemotherapy, using NP40 buffer as above. The lysates obtained were thus of cells treated as in table 2.3. Immunoprecipitation was carried out as described, using either anti-EGFR antibody Mab13 or anti-ErbB2 antibody. Resultant gels were stained using anti-phosphotyrosine, clone 4G10.

2.5 <u>MTT assay</u>

The 3-[4,5-dimethyl(thiazol-2-yl)-3,5-diphery]tetradium bromide (MTT) assay is a semi-automated, colorimetric assay, used to quantify metabolically viable cells through their ability to reduce a soluble yellow tetrazolium salt to blue-purple formazan crystals [179]. The crystals are produced by mitochondrial dehydrogenases and can be dissolved and quantified by measuring the absorbance of the resultant

solution. The absorbance of the solution is related to the number of live cells. Cells are grown in 96-well plates in which the assay is performed, and then the absorbance of the formazan solution is measured using a multiwell spectrophotometer (hence the term semi-automated). This allows a large number of samples to be processed at the same time, and a rapid objective measurement of cell number can be performed [179]. The MTT assay has been validated for use to measure chemosensitivity in human tumour cell lines [180].

2.5.1 General methods

2.5.1.1 Counting cells

Cells were grown in flasks and lysed as described above. Cells were then resuspended in fresh medium and counted using a haemocytometer (all four quarters were counted and an average count obtained to allow for a more accurate result). The number of cells/ml medium was calculated, using the knowledge that each quarter square of the haemocytometer holds 0.1 μl medium below the coverslip.

2.5.1.2 MTT assay

Cells were seeded into 96 well plates at specific cell densities, according to the individual experiment (see below for details). Two hundred microlitres of medium

was the volume used throughout. Cells were initially seeded in medium with 10%

FBS for 24 hours, which was changed after this time period as required. In

experiments where medium in wells was changed, medium was removed using an

eight channel suction pipette used at the edge of the wells. Cells were then grown

under specific conditions, for varying lengths of time, according to the individual

experiment. At the endpoint of the experiment, 20 µl MTT solution (made up to 5

mg/ml solution in deionised water, and filtered to sterilise; Sigma, St. Louis, MO),

as added to each experimental well. The plate was then incubated at 37°C, 5%

CO_2, for three hours. Next, all medium was removed from wells, and 200 µl

DMSO was added to each well. Plates were incubated for 10 minutes as before,

followed by gentle agitation for 10 minutes to allow tetrazolium crystals to first

dissolve and then mix evenly throughout the solution. The absorbance in each

experimental well was then immediately measured using a microplate reader, at a

wavelength of 560 nm. All MTT assays were repeated in triplicate.

2.5.2 Details of individual MTT assays

2.5.2.1 Calculation of absorbance per number of cells for each cell line

MTT assays were performed to characterise each cell line in terms of activity of

mitochondrial dehydrogenase and therefore absorbance per well for specific

numbers of cells. One 96 well plate was seeded per cell line, and repeated in

triplicate. Eight concentrations of cells ranging from 500 cells/200 µl medium

(i.e. 500 cells per well) to 64000 cells/200 µl medium were prepared using serial

dilutions, and five wells of each concentration were seeded per 96 well plate. Plates were incubated overnight to allow seeding of the cells, and then MTT assay was performed as described.

2.5.2.2 Determination of optimal conditions for incubation of cells over a 96 hour period

It was important to reduce the content of serum in medium as much as possible whilst maintaining adequate rates of cell growth, to reduce the exogenous growth factors that would interfere with the assay. Therefore, assays were performed to determine optimal concentration of cells seeded, and optimal concentration of serum in medium, for growth of each cell line over a period of four days in 96 well plates. After analysing the results from the assays looking at absorbance values for each concentration of cells for all cell lines, and estimating cell numbers after four days growth using theoretical doubling times, it was decided to seed cells at concentrations of 500 and 1500 cells/200 μl medium (i.e. cells/well of 96 well plate). Four rows, each with five wells, were seeded for both numbers of cells, and 24 hours after seeding medium was changed from that with 10% FBS, to that with either 0% FBS (serum free), 1% FBS, 2.5% FBS or 5% FBS (figure 2.3). Plates were incubated for a further 72 hours before MTT assay was performed (figure 2.4).

| 0 % FBS | 1 % FBS | 2.5 % FBS | 5 % FBS | Key | 500 cells/well seeded |
| | | | | | 1500 cells/well seeded |
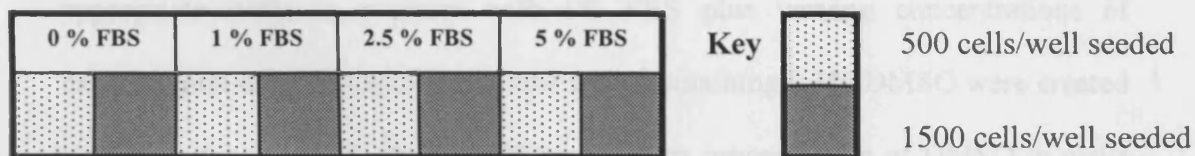
Figure 2.3

Diagrammatic representation of layout of columns in 96 well plate for determination of optimal

conditions for growth of cells over 96 hours (each column contained 5 wells).

Time (hours after seeding)

| 0 | 24 | 48 | 72 | 96 |

| Seed cells in 10% FBS | Change to varying % FBS | | | Perform MTT assay |
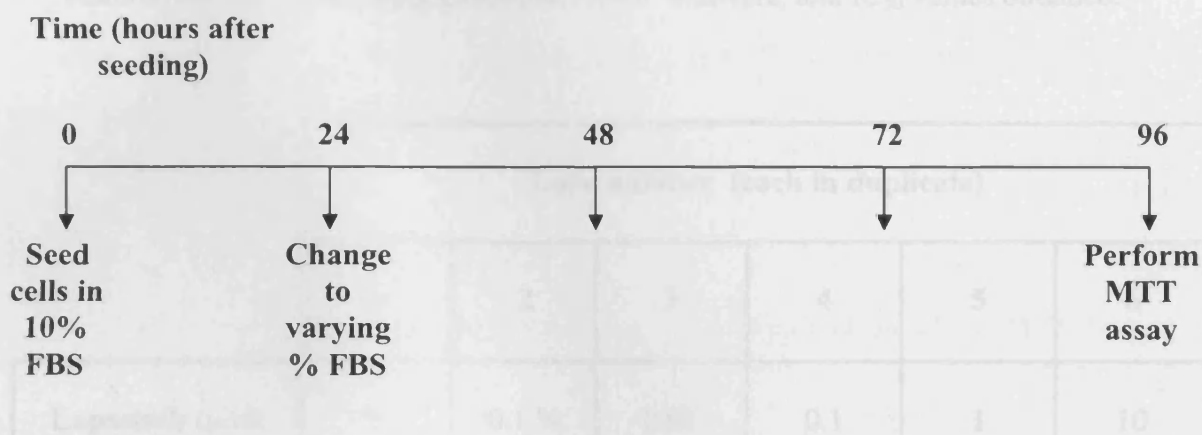
Figure 2.4

Schematic demonstrating timescale of treatment of cells in MTT assays to determine optimal conditions

for growth of cells over 96 hours

2.5.2.3 Assays to determine IC_{50}s of lapatinib and chemotherapeutic agents on RT112 and J82 cells

Cells were seeded at a concentration of 1000 cells/200 µl medium into 96 well

plates (200 µl per well and therefore 1000 cells/well). Ten wells were seeded for

each planned concentration of drug and were initially grown in medium with 10%

FBS. Twenty four hours after seeding, medium in all experimental wells was

changed to 1% FBS. A further 24 hours later, medium was again changed in the appropriate wells to medium with 1% FBS plus varying concentrations of experimental drug (table 2.4). Control wells containing 0.1% DMSO were created in plates with lapatinib, to reflect the maximum concentration of DMSO in wells treated with lapatinib, as lapatinib was made up in solution with DMSO. MTT assay was performed 48 hours after addition of experimental drugs (96 hours after seeding of cells – figure 2.5). All experiments were performed in triplicate. Results were analysed using Graphpad Prism® software, and IC_{50} values obtained.

	Lane number (each in duplicate)					
	1	2	3	4	5	6
Lapatinib (µM)	0	0.1 % DMSO	0.01	0.1	1	10
Cisplatin (µM)	0	0.01	0.1	1	10	100
Gemcitabine (µM)	0	0.1	1	10	100	1000
Paclitaxel (nM)	0	0.1	1	10	100	1000

Table 2.4

Concentrations of experimental drugs used in MTT experiments to determine IC_{50}s (each lane equals 10 wells, or 2 columns each with 5 wells). Ranges for each drug used were chosen after studying concentrations used in other cell lines *in vitro* in published studies.

Time (hours after seeding)

0	24	48	72	96

Seed
cells in
10%
FBS

Change
to 1%
FBS

Change
to 1%
FBS +
drug

Perform
MTT
assay
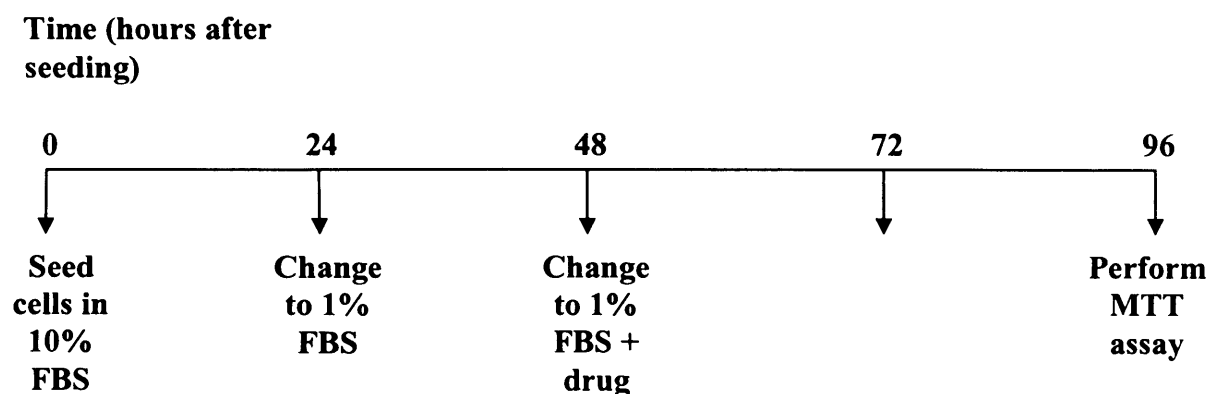
Figure 2.5

Schematic demonstrating timescale of treatment of cells in MTT assays to determine $IC_{50}s$ of experimental drugs

2.5.2.4 Assays to determine optimal sequences of application of lapatinib and chemotherapy

RT112 and J82 cells were used throughout, and all experimental combinations were performed in triplicate in each cell line. The aim of these assays was to determine the optimal sequence of application of lapatinib with respect to the chemotherapeutic agents. Lapatinib was added either prior and during, concomitant with or after chemotherapy. Chemotherapy used was either single agent cisplatin, gemcitabine or paclitaxel (C, G or T), gemcitabine plus cisplatin (GC), or the triplet gemcitabine, paclitaxel plus cisplatin (GTC). Throughout all assays, lapatinib was at a constant IC_{50} dose (as this was the constant drug throughout all experiments, and therefore keeping its dose constant allowed easier and more reliable comparison between assays), but chemotherapy dose varied. Where combinations of chemotherapeutic agents were used, drugs were combined

at their IC_{50} doses. Solutions of chemotherapeutic agents at their IC_{50} doses (either single agent or combination) were serially diluted and final solutions with 1/8 x, 1/4 x, 1/2 x and 1 x IC_{50} doses of chemotherapy were obtained, and these were the solutions used in the experiments. All experiments with cisplatin were carried out in dimmed lighting conditions. All plates were incubated in the dark. Cells were seeded onto 96 well plates at 1000 cells/well as above, in medium with 10% FBS. Four wells per plate were used for each experimental combination of drugs (figure 2.6). After 24 hours, all wells were changed to medium with 1% FBS (this concentration was used throughout for the rest of each experiment). At this stage, IC_{50} concentration of lapatinib was added to those wells where lapatinib was to be added prior and during chemotherapy. A further 24 hours later, chemotherapy at varying concentrations was added to all relevant wells, along with IC_{50} of lapatinib in wells to be treated with lapatinib prior and during, or lapatinib concomitant with chemotherapy. Plates were then incubated for a further 48 hours prior to performing MTT assay. In those wells where lapatinib was to be added after chemotherapy, IC_{50} of lapatinib was added 24 hours after addition of chemotherapy, and therefore 24 hours prior to MTT assay (figure 2.7). At the end of the experiment, MTT assay was performed as previously described. Results were analysed using analysis of variance (ANOVA test, using MINITAB™ statistical software, PA, USA) to look for statistical significance, and then interactions plots were performed to look for synergy between drug combinations.

Column:	A	B	C	D	E / A	B	C	D	E
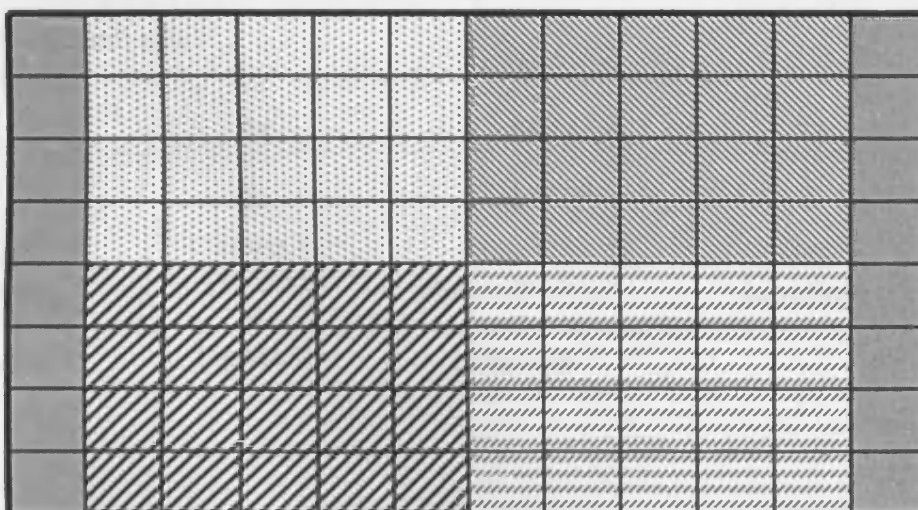
Key

Columns:

A – control (no chemotherapy, no lapatinib); B – 1/8 IC_{50} chemotherapy; C – 1/4 IC_{50}

chemotherapy; D – 1/2 IC_{50} chemotherapy; E - IC_{50} chemotherapy.

Wells:

Medium only, no cells, no treatment

Chemotherapy only, no lapatinib

Lapatinib prior and during chemotherapy

Lapatinib concomitant with chemotherapy

Lapatinib after chemotherapy

Figure 2.6

Diagrammatic representation of layout of each 96 well plate in experiments to determine the optimal

sequence of application of lapatinib and varying combinations of chemotherapeutic agents.

Time (hours after seeding)

0	24	48	72	96
Seed cells in 10% FBS	Change to 1% FBS +/- lapatinib	+ chemotherapy +/- lapatinib	+/- lapatinib	Perform MTT assay
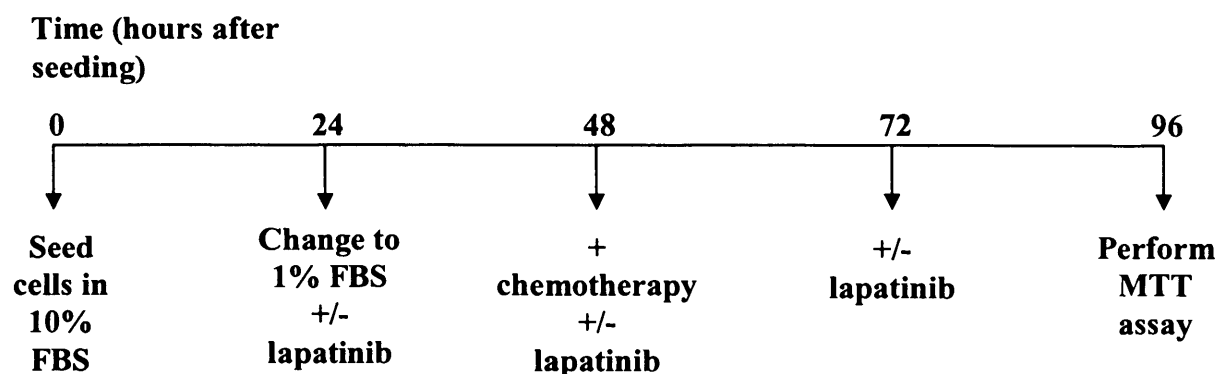
Figure 2.7

Schematic demonstrating timescale of treatment of cells in experiments to determine the optimal sequence of application of lapatinib and varying combinations of chemotherapeutic agents.

2.6 Apoptosis assays

Apoptosis is a tightly regulated form of cell death, originally defined as the orderly and characteristic sequence of structural changes resulting in the programmed death of the cell [181]. Morphologically, it is characterised by chromatin condensation and cell shrinkage in the early stage. Then the nucleus and cytoplasm fragment, forming membrane-bound apoptotic bodies, which can be engulfed by phagocytes. Apoptosis is an important process during normal development. It is also involved in aging and various diseases including cancer. A number of assays to assess apoptosis *in vitro* have been developed, and are used to evaluate the ability of agents to induce apoptosis

in cell lines, and thus to help understand their modes of action in disease processes, including cancer.

Two different assays were used to attempt to assess the presence and level of apoptosis in RT112 and J82 cells treated with lapatinib and chemotherapeutic agents, as described below.

2.6.1 Apoptosis detection by fluorescence microscopy

The Mitocapture™ mitochondrial apoptosis detection kit (Merck Biosciences, Darmstadt, Germany) was used to look for apoptosis using fluorescence microscopy. The Mitocapture™ reagent is a cationic dye that is reported to exhibit distinct fluorescence in viable cells versus apoptotic cells. In viable cells, the reagent accumulates and aggregates in the mitochondria, giving off a bright red fluorescence. In apoptotic cells, the reagent cannot aggregate in the mitochondria due to the disruption of the mitochondrial transmembrane potential that is one of the earliest intracellular events occurring following induction of apoptosis. Thus the reagent remains in the cytoplasm in its monomer form, generating green fluorescence [182]. The fluorescent signals are reported to be easily detected by fluorescence microscopy.

J82 and RT112 cells were seeded at 1000 cells/well in a 96 well plate, in medium with 10% FBS. Four columns of cells with three wells each were seeded for each cell line. Cells in column 1 were untreated, in column 2 were treated with 100 ng/ml EGF, in column 3 were treated with IC_{50} of lapatinib, and in column 4 were treated with lapatinib and EGF (table 2.5). After 24 hours in medium with 10% FBS, medium was

changed in all wells to that with 1% FBS, and IC_{50} of lapatinib was added to cells in columns 3 and 4. A further 24 hours later, 100 ng/ml EGF was added to wells in columns 2 and 4. Finally, 48 hours later, apoptosis was detected as follows using the Mitocapture detection kit (figure 2.8). A volume of 2 ml of incubation buffer was pre-warmed to 37°C. Just prior to use, 1 µl Mitocapture reagent was diluted to 1 ml using the pre-warmed incubation buffer, and the solution was vortexed. Next, as the reagent is poorly soluble in aqueous solution, the diluted reagent was repeatedly pipetted and then centrifuged for 5 minutes at 15,000 rpm, and the supernatant was carefully transferred without disturbing the pellet. Medium was removed from all experimental wells and 200 µl of the Mitocapture solution was added to each well. The plate was then incubated at 37°C, in 5% CO_2, for 15 – 20 minutes, followed by removal of the mitocapture solution. Further pre-warmed incubation buffer was applied to each well and cells were immediately observed under a fluorescence microscope using a band-pass filter, to look for red fluorescence in healthy cells, and green fluorescence in apoptotic cells. The experiment was repeated in duplicate.

	Column number			
	1	2	3	4
IC_{50} lapatinib	-	-	+	+
100 ng/ml EGF	-	+	-	+

Table 2.5

Summary of treatment of cells in 96 wells plate (each column contained three wells) for Mitocapture

apoptosis assay.

Time (hours after seeding)

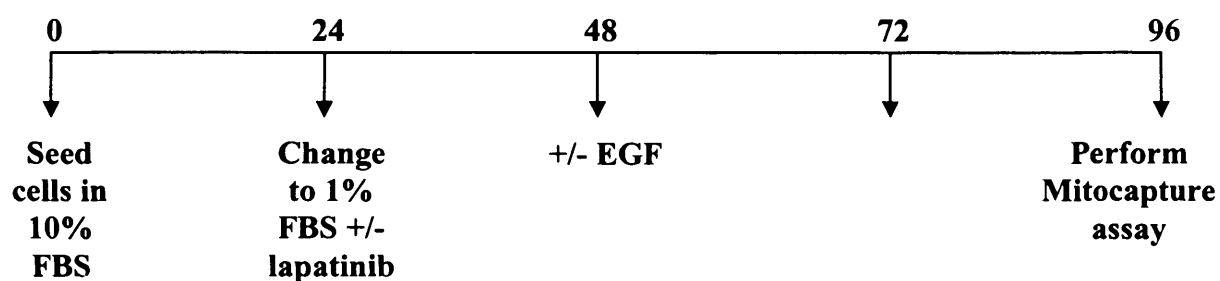| 0	24	48	72	96
↓	↓			↓
Seed cells in 10% FBS	Change to 1% FBS +/- lapatinib	+/- EGF		Perform Mitocapture assay

Figure 2.8

Schematic demonstrating timescale of treatment of cells for Mitocapture apoptosis assay.

2.6.2 Apoptosis detection using Annexin V staining

2.6.2.1 Background

The Annexin V-FITC (fluorescein isothiocyanate) apoptosis detection kit (Merck Biosciences, Darmstadt, Germany) was used to detect apoptosis using flow cytometry. In viable cells phosphatidyl serine (PS) is located on the cytoplasmic surface of the cell membrane. Upon induction of apoptosis, rapid alterations in the organisation of phospholipids in cells occurs leading to exposure of PS on the external surface of the cell membrane [183]. *In vitro* detection of externalised PS can be achieved through interaction with the anticoagulant Annexin V [184]. In the presence of calcium, rapid high affinity binding of Annexin V to PS occurs. Translocation of PS precedes nuclear breakdown, DNA fragmentation, and the appearance of most apoptosis-associated molecules and so making Annexin V binding a marker of early-stage apoptosis.

The Annexin V-FITC apoptosis detection kit utilises a fluorescein isothiocyanate (FITC) conjugate of Annexin V, allowing detection of apoptosis by flow cytometry. Since membrane permeabilisation is observed in necrosis, necrotic cells will also bind Annexin V-FITC. Therefore, propidium iodide (PI) is used to distinguish between viable, early apoptotic, and necrotic or late apoptotic cells. PI is a membrane-impermeable chemical that is excluded from viable cells, but is admitted to necrotic cells or cells in late stages of apoptosis that have permeabilised membranes. PI binds to DNA by intercalating between the bases, and when excited by a laser light at 488 nm, PI emits a signal that can be detected

by flow cytometry. Necrotic and late apoptotic cells thus bind Annexin V-FITC and stain with PI, while PI is excluded from viable (FITC negative) and early apoptotic (FITC positive) cells.

Flow cytometry is a means of measuring certain physical and chemical characteristics of cells as they travel in suspension one by one past a sensing point. The cells to be analysed are placed in suspension and injected into a fluid stream (figure 2.9). Cells then emerge in single file to form a narrow jet. This stream then sequentially intersects one or more laser beams. The laser beams are focused such that they only illuminate a single particle at any given time. If the given cell contains a fluorescent tag excited by the laser, it will fluoresce, emitting a measurable pulse of photons of a specific wavelength. Signals are collected by photodetectors, processed by specialised electronics, digitised, and stored on a computer. At constant laser power, the intensity of emission will be dependent on the number of fluorophores present, thereby making flow cytometry both a qualitative and highly quantitative analysis tool [185]. In this experiment, the flow cytometer was set up to detect the FITC signal by FL1 at 518 nm, and to detect the PI signal by FL2 at 620 nm (FL1 and 2 are sensors on the flow cytometer), after excitation at 488 nm.
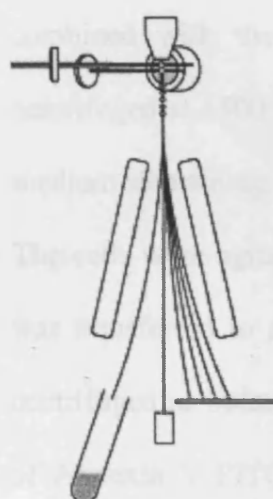
Principles of cell sorting

- Particles are placed in a fluid stream
- Lasers excite particle fluorescence
- Signals are collected
- Stream is broken into drops
- Drops containing desired particles are deflected in an electric field
- Drops with particles are collected

Current Opinion in Biotechnology

Figure 2.9

Diagrammatic representation of principles of cell sorting [185].

2.6.2.2 Experimental details

For each cell line, four 75 cm^3 flasks were seeded with cells at low densities in medium with 10% serum. When cells were 30 - 40% confluent, medium in all flasks was changed to serum free medium. Twenty four hours later, IC$_{50}$ dose of lapatinib was added to flasks 2 and 4, and a further 24 hours later either GC, or GTC were added at their IC$_{50}$ doses to flasks 3 and 4 (table 2.6). Forty eight hours after the addition of chemotherapy all flasks were prepared as follows for flow cytometry (figure 2.10). Experiments were repeated in duplicate. Medium from flasks containing floating cells was reserved, and plates were washed twice in PBS. Remaining cells were trypsinised for as short a time as possible in 1ml 1 x trypsin/EDTA. Plates were given a sharp tap to aid detachment, and an equivalent volume of medium containing 10% FBS was immediately added. This was

combined with the medium containing floating cells and the solution was centrifuged at 1500 rpm for five minutes. Cells were resuspended in 10 ml fresh medium containing 10% FBS and incubated at 37°C, 5% CO_2, for 30 minutes. The cells were agitated to ensure they were resuspended, 2 ml of this suspension was transferred to a FACS (fluorescence-activated cell sorting) tube, cells were centrifuged as before, and then resuspended in 1 ml Annexin buffer. Next, 2.5 µl of Annexin V-FITC conjugate was added, the solution was vortexed and then incubated at room temperature for 10 minutes. PI (from the Annexin V kit) was then added to a final concentration of 1.5 µg/ml and the suspension was incubated again at room temperature for 1 minute. Samples were stored on ice whilst awaiting analysis on the flow cytometer. Data was acquired and analysed using Cell Quest software (BD Biosciences, CA, USA).

	Flask number			
	1	2	3	4
IC_{50} lapatinib	-	+	-	+
IC_{50} chemotherapy (GC or GTC)	-	-	+	+

Table 2.6

Summary of treatment of cells in preparation for the Annexin V apoptosis assay/FACS analysis of cell cycle.

Time (hours after seeding)

0	24	48	72	96

Seed cells in 10% FBS | Change to 1% FBS +/- lapatinib | +/- chemotherapy | | Perform Annexin V assay
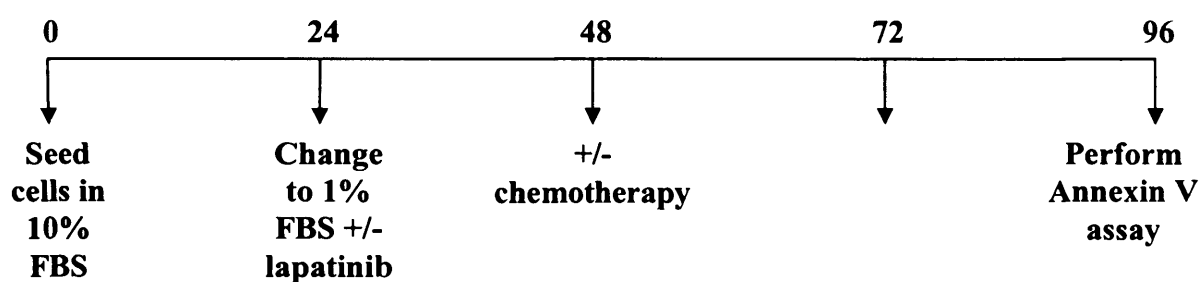
Figure 2.10

Schematic demonstrating timescale of treatment of cells for Annexin V assay/FACS analysis of cell cycle.

2.7 Cell cycle analysis using FACS

Fluorescence-activated cell sorting (FACS) analysis is a type of flow cytometry. It sorts cells, one cell at a time, based upon specific light scattering and fluorescent characteristics. This technique can be used to study cell DNA content when cells are stained with fluorescent dyes such as PI. DNA staining can be used to study the cell division cycle, as the relative quantity of PI-DNA staining corresponds to the proportion of cells in G0/G1, S, and G2/M phases, with lesser amounts of staining indicating apoptotic/necrotic cells. This can be quantified using FACS analysis

2.7.1 Analysis of effects of lapatinib and chemotherapy on cell cycle

Effects on cell cycle of lapatinib combined with combination chemotherapy were investigated using FACS analysis with PI. For each cell line, four x 25 cm^3 flasks were seeded with cells at low densities in medium with 10% serum. When cells were 40 – 50% confluent, medium in all flasks was changed to serum free medium. After 24 hours, IC_{50} dose of lapatinib was added to flasks 2 and 4, and a further 24 hours later either gemcitabine, paclitaxel and cisplatin, or gemcitabine and cisplatin alone, were added at their IC_{50} doses to flasks 3 and 4 (table 2.6). Forty eight hours after the addition of chemotherapy all flasks were prepared as follows for flow cytometry (figure 2.10). Experiments were repeated in duplicate. Medium from flasks containing floating cells was reserved, so as not to miss any part of the cell population, and plates were washed in PBS. Remaining cells were trypsinised for as

short a time as possible in 1ml 1 x trypsin/EDTA. Plates were given a sharp tap to aid detachment, and the medium with floating cells was added. This cell suspension was centrifuged at 1500 rpm for five minutes, cells were resuspended in 10 ml PBS and then centrifuged again as previously. Next the cell pellet was resuspended in 200 µl PBS and 2 ml of ice cold 70% ETOH (ethanol, Sigma, St Louis, MO, USA)/PBS was added whilst vortexing. The ETOH fixes the cells to prevent any change in composition, and vortexing whilst adding the ETOH ensures there is no clumping of cells. Cells were thus incubated at 4°C for at least two hours. Following incubation, the cells were centrifuged for 10 minutes at 1400 rpm, resuspended in 800 µl PBS, and then transferred to a 1.5 ml eppendorf. Next, 100 µl of boiled RNase A (ribonuclease A [Sigma, St Louis, MO, USA], acts to degrade RNA and thus eliminate or reduce RNA contamination in preparations of DNA, 10 mg/ml prepared in 10 mM Tris-HCl, pH 7.5, and boiled for 5 minutes) was added, followed by 100 µl PI (500 µg/ml solution, [Sigma, St Louis, MO, USA], to a final concentration of 50 µg/ml). The cells were then incubated for one hour at 37°C, 5% CO_2, and samples were analysed using the FACS machine and data analysed using Cell Quest Software.

2.8 Genetic approaches to down-regulation of ErbB1 expression and signal transduction

Two methods were attempted to genetically modify J82 and RT112 cells to down-regulate ErbB1 expression and signal transduction in the cell lines, to further study the effects of lapatinib *in vitro*.

2.8.1 RNAi-based approach to suppress *ErbB1* gene expression

2.8.1.1 General background

RNA interference (RNAi), or double-stranded RNA (dsRNA)-dependent post-transcriptional gene silencing, is a mechanism of sequence-specific, post-transcriptional gene silencing by dsRNA homologous to the gene being suppressed. However, in most mammalian cells dsRNA provokes a strong cytotoxic effect [186]. More recently a small interfering RNA (siRNA) has been developed, which can induce a similar RNA interference in mammalian cells but without the cytotoxicity [187]. Unfortunately, the gene silencing produced by siRNA effects is short-lived, which severely limits its application to cellular systems. An alternative to this was reported in 2002, which is a vector system, named pSuper that directs the synthesis of siRNA in mammalian cells [188]. The expression of siRNA by this vector results in efficient and specific down-regulation of gene expression, which is stable. Such stable expression of siRNAs

using this vector mediates persistent suppression of gene expression, allowing the analysis of loss-of-function phenotypes that develop, over longer periods of time.

A pSuper RNAi vector against ErbB1 was obtained, along with a control vector, in order to attempt to down-regulate ErbB1 expression so that specific effects of lapatinib on RT112 and J82 cells lines with loss of this receptor could be studied. The aim of this was to gain further knowledge of the mode of action of lapatinib in these cell lines.

2.8.1.2 Experimental methods

2.8.1.2.1 Transformation of plasmid

In order to genetically manipulate cells, large quantities of pSuper RNAi vector is needed. One of the easiest ways to get large amounts of the vector is to place the desired vector into bacteria, grow the bacteria, then harvest the bacteria and isolate the vector. The process of introducing the vector to the bacteria is called transformation, and the most commonly used bacterium for this purpose is Escherichia Coli (E-Coli). Uptake of vectors by E-Coli can only be achieved when the recipient cells have been made "competent". One method of achieving this is by a heat shock in the presence of Ca^{2+} ions [189].

An ErbB1-pSuper RNAi vector along with a control vector were obtained (a pSuper RNAi specific for plasmid expressing short hairpin *ErbB1*, pSuper-ErbB1, provided by Professor Ozanne at the Beaton Institute for Cancer Research,

Glasgow, UK). Transformation of the plasmids was performed as follows. Vector (1.5 μl) made up from10 μg in 50 μl of deionised water was put into an eppendorf on ice. E-Coli (competent cells, Bioline, MA, USA) were removed from the – 80°C freezer and 20 μl was added to the vector. This mixture was incubated on ice for 10 minutes, and then heat shocked in a water bath at exactly 42°C for 45 seconds, followed by further incubation on ice for two minutes. Next, 200 μl of LB medium (Lysogeny Broth medium, a nutritionally rich medium which is primarily used for the growth of bacteria) without antibiotic was added and the cells were incubated at 37°C for 60 minutes, with shaking at 300 revolutions/minute. All of the sample was then plated onto an agar plate (with ampicillin) and spread until dry. The plate was stored upside-down overnight at 37°C. A small number of colonies were transferred to 100 ml of LB medium with ampicillin, and this was incubated overnight with mixing, again at 37°C. Ampicillin was added to the agar plates and LB medium as the vector is ampicillin-resistant, and therefore adding ampicillin allowed for selection of cells containing the vector. Following this, plasmid was isolated at described below.

2.8.1.2.2 Making agar plates (with ampicillin)

Agar powder (Invitrogen, Carlsbad, CA, USA) was dissolved in deionised water in a conical flask, to a concentration of 32 g/l, in a fume cupboard. The solution was heated in a microwave oven for one minute, shaken, and then heated for a further one minute before shaking again. When the agar was dissolved and the solution boiling it was boiled for a further three minutes in the microwave. This was left to

cool for a few minutes before adding a volume of 100mg/ml ampicillin to make 100 μg/ml final solution (Sigma, St Louis, MO, USA). Twenty millilitres of agar were pipetted into each petri dish, ensuring no bubbles were formed, and this was allowed to set.

2.8.1.2.3   Isolation of vector from E-Coli

In order to use the vector transformed in the E-Coli, it needs to be isolated and purified. This was achieved by using the PureYield™ Plasmid Midiprep System (Promega Corporation, WI, USA). Contents of the flask containing the E-Coli were centrifuged at 4150 rpm for 20 minutes at 4°C, and the supernatant discarded. The pellet was suspended in Cell Resuspension Fluid, transferred into a 50 ml tube, and 3 ml cell lysis solution was added. This was inverted gently up to five times to mix, and then incubated at room temperature for three to five minutes to ensure thorough clearing. The resultant lysate was filtered through a clearing column to remove cellular debris, and the filtrate was incubated again at room temperature for two minutes to allow debris to rise. The clearing column was next centrifuged at 1500 rpm for five minutes and discarded. The lysate was poured into a binding column, to bind the plasmid and remove it from solution, in a 50 ml tube, which was centrifuged at 1500 rpm for three minutes. Next, the binding column was washed with Endotoxin Removal Wash, designed to remove substantial amounts of protein, RNA and endotoxin contaminants from purified vector, and was again centrifuged at 1500 rpm for three minutes. The column was removed from the tube, the flowthrough in the tube was discarded and the column

replaced in the tube. Twenty millilitres of Column Wash solution was added to the binding column, this was centrifuged at 1500 rpm for five minutes, the flowthrough was again discarded and the column placed into a new 50 ml tube. Elution was next performed by adding 600 μl of Nuclease-Free Water to the binding column, which was then centrifuged again at 5000 rpm for five minutes. Elution is a process that causes the separation, by washing, of one solid from another. In this case, the vector was being eluted from the binding column. The flowthrough from this step was the vector. The concentration of the vector was measured in the spectrophotometer, after 100 x dilution in water.

2.8.1.2.4 Cutting of vector to ensure correct transformation

This was performed as below to ensure that purification of the vector was accurate. This procedure is specific to the pSuper-ErbB1 and control vector used. The DNA plasmids were spliced using the restriction enzymes (a restriction enzyme recognizes and cuts DNA only at a particular sequence of nucleotides) EcoR1 and HindIII (New England Biolabs, Ipswich, MA, USA), which in a positive clone would result in a fragment of 281 bp that could be detected by a gel electrophoresis. In a 1.5 ml eppendorf on ice, 0.5 μl plasmid (either control or ErbB1) was mixed with 11.4 μl deionised water, 1.5 μl of 10 x incubation buffer M (50 mM Tris-HCl, 10 mM $MgCl_2$ [magnesium chloride, Fluka, Switzerland], 100 mM NaCl, 1 mM Dithioerythritiol [DTE, Sigma, St Louis, MO, USA], pH 7.5), 0.8 μl HindIII and 0.8 μl EcoR1. This was incubated for one hour at 37°C,

and following this the spliced samples were analysed using agarose gel electrophoresis.

2.8.1.2.5   Agarose gel electrophoresis

Agarose gel electrophoresis is the easiest and commonest way of separating and analysing DNA. The purpose of the gel might be to look at the DNA, to quantify it or to isolate a particular band. The DNA is visualised in the gel by addition of ethidium bromide (EtBr). This binds strongly to DNA by intercalating between the bases and is fluorescent meaning that it absorbs invisible ultraviolet (UV) light and transmits the energy as visible orange light.

The Horizon-58 Horizontal Electrophoresis Kit (Biometra, Göttingen, Germany) was used. A solution of TBE electrophoresis buffer (Tris/Borate/EDTA made as 10 x buffer using: 108 g Tris Base, 55 g Boric acid [Prolabo, Normapur, Paris, France], 20 ml 0.5 M EDTA [Sigma, St Louis, MO, USA] and deionised water to 1.0 l) plus EtBr (Sigma, St Louis, MO, USA) was made by adding 5 μl EtBr to 500 ml of 1 x TBE (450ml deionised water and 50 ml 10 x TBE). Tris is an effective buffer for slightly basic solutions, which keeps DNA deprotonated and soluble in water. EDTA binds to divalent cations, which are necessary co-factors for many enzymes, and particularly magnesium (Mg^{2+}). Forty millilitres of TBE + EtBr was aliquoted and 500 mg of agarose (Bioline, MA, USA) added. This was heated in a microwave oven for a total of one min (shaking at intervals when boiling). The agarose solution was then poured into the electrophoresis kit and

allowed to set. The gel and reservoir was covered with TBE + EtBr. A 1/4 volume of DNA loading buffer (60% glycerol, EDTA and bromophenol blue) was added to the restriction mixture, and this was loaded into the wells in the gel. The loading buffer gives colour via the bromophenol blue, and the glycerol gives density to the sample to make it easy to load into the wells. Also, the dyes are negatively charged in neutral buffers and thus move in the same direction as the DNA during electrophoresis. This allows monitoring of the progress of the gel easier. A marker lane was also used (100 bp DNA ladder, Invitrogen, Carlsbad, CA), to allow accurate assessment of the size of the vector samples. The gel was run at 120 V constant (approx 50 mA), for around 30 minutes. The gel was visualised using UV light to ensure the correct vectors had been purified.

2.8.1.2.6 Transfection via electroporation

Transfection is the introduction of nucleic acids into eukaryotic cells. Electroporation is a physical tool used to transfect DNA into cells via an electric field. This exposes the cell membrane to high-intensity electrical pulses that can cause transient and localised destabilisation of the membrane. During this perturbation, the cell membrane becomes highly permeable to exogenous molecules, such as DNA, present in the surrounding medium [190]. Permeabilisation requires that the externally applied electrical field surpasses a critical threshold value. For a cell suspension, this requires around the order of 1 V, although the absolute potential depends upon a number of factors. The transient increase in permeability is believed to result from the creation of electric

field-induced pores, although the precise mechanism by which they are made is unclear. It is also unclear as to what the mechanism of DNA uptake is [190].

Green fluorescent protein (GFP) is a protein produced by a jellyfish, *Aequorea*, which fluoresces in the lower green portion of the visible spectrum. Several mutants of the GFP gene have been constructed that fluoresce more reliably than wild-type, at 509 nm. In order to determine the percentage of cells that have been successfully transfected with DNA in an experiment (transfection efficiency), a reporter gene can be used. EGFP (enhanced green fluorescent protein) is a convenient reporter in this setting as its expression can be easily detected by fluorescence microscopy or flow cytometry.

A 175 cm^3 flask of either J82 or RT112 cells at around 80% confluence was trypsinised (3 ml trypsin), and then when cells had lifted this was neutralised with 10 ml media with 10 % FBS. The cell suspension was centrifuged at 1500 rpm for five minutes, the pellet was washed with 10 ml PBS and centrifugation was repeated. The cells were then resuspended in 450 µl PBS (solution pipetted around 20 x to separate out cells) and at this stage 5 µg pEGFP (BD Biosciences, CA, USA) was added if necessary. This cell solution was transferred to sterile cuvettes (100 µl per cuvette), plasmid was added, and the solution was gently mixed whilst avoiding formation of bubbles. This was placed on ice for 20 minutes. During this time, 5 ml media with 10% FBS was placed in a 5 cm Petri dish and incubated at 37°C, 5% CO_2, 95% O_2, for around 15 minutes. After the cell solution had been on ice for 20 minutes it underwent electroporation (Gene Pulser Xcell, BioRad, CA, USA), followed by resuspension of cells in 800 µl

medium. The cells were then placed in the pre-incubated medium in the Petri dish, which was again incubated as above. Once cells were around 50% confluent, dishes were examined using the fluorescence microscope to assess transfection efficiency.

2.8.1.2.7 Chemical transfection

The chemical transfection of DNA is based on complex formation between positively charged chemicals (usually polymers) and negatively charged DNA molecules, leading to introduction of DNA into the cell by endocytosis. A variety of chemicals for this purpose have been developed. One such chemical is GeneJammer® system (Stratagene, CA, USA). GeneJammer is a polyamine chemical transfection agent. The major limitation of early chemicals was toxicity, but polyamines are capable of condensing DNA and delivering it to a variety of cell lines with minimum toxicity [191].

Chemical transfection was performed using the GeneJammer system. J82 or RT112 cells were seeded in 2 ml of medium with 10 % FBS in a small Petri dish and grown until 50% confluent. One hundred microlitres of serum free medium was placed into an eppendorf and 5 µl GeneJammer was added. This was left at room temperature for 10 minutes, followed by addition of 1 µg of vector and/or 1 µg pEGFP (to assess transfection efficiency) and a further incubation for 10 minutes at room temperature. During this incubation period, the medium on the cells was changed to 900 µl of fresh medium with 10 % serum and the

GeneJammer/vector mixture was added dropwise. This was incubated for six hours before addition of a further 1 ml of medium with 10% serum, and incubation for a further 18 hours. Plates were then examined using the fluorescence microscope to assess transfection efficiency.

2.8.1.2.8 Western blot analysis to look for downregulation of ErbB1 following transfection

RT112 cells transfected by electroporation, and J82 cells transfected using GeneJammer were lysed as previously described with 200 μl standard Laemmli buffer. Cells transfected with either pEGFP (control), control vector, or pSuper-ErbB1 were used. Protein quantification was performed, and Western blot was performed as previously. Membranes were stained for ErbB1 (as previously) to assess for downregulation after transfection with the ErbB1 vector.

2.8.2 Dominant-negative approach to suppression of ErbB1 function

2.8.2.1 General background

A dominant-negative gene contains a mutation whose product adversely affects the normal, wild-type gene product within the same cell. This effect usually occurs if the dominant-negative gene product can still interact with the same elements as the wild-type product, but blocks some aspect of its function. The

dominant-negative vector used in these experiments, CD533, is a deletion mutant which produces a truncated ErbB1 receptor lacking most of its cytoplasmic domain, but retaining the dimerisation domain, causing formation of inactive heterodimers [192]. The aim of its transfection into RT112 and J82 cells was to negate the effects of wild-type ErbB1, thus allowing further studies of the mode of action of lapatinib in these cell lines.

2.8.2.2 Experimental methods

2.8.2.2.1   Description of CD533 plasmid DNA

An original plasmid, pRK5-HER NA8, containing an N-terminal fragment of human ErbB1 was obtained (from the laboratory of A. Ullrich, Germany). The ErbB1 fragment contains a deletion of the last 533 C-terminal amino acids [193]. This fragment DNA was then subcloned in pcDNA 4/V5-His eukaryotic expression vector (Invitrogen, Carlsbad, CA, USA. Subcloning performed by E. Tulchinsky, University of Leicester). Subcloning is a technique used to move a gene of interest from a parent vector to a destination vector in order to further study its functionality. A eukaryotic vector was used here as the destination vector, as this is a form of plasmid DNA that contains signalling sequences that are recognised by enzymes in eukaryotic cells for mRNA and protein synthesis. The resulting vector used throughout this experiment contains C-terminal tags (V5 and 6xHis) allowing the use of anti-V5 and/or anti-6xHis tag antibodies to distinguish expressed ErbB1 mutant from the endogenous wild-type receptor. The

vector also encodes the *Sh ble* gene, the product of which is a protein that confers resistance to an antibiotic, Zeocin™ (Invitrogen, Carlsbad, CA, USA). Thus cells that express this gene product can be selected by their resistance to Zeocin [194].

2.8.2.2.2 Transfection

The CD533 plasmid DNA was transfected into RT112 and J82 cells using electroporation (see section 2.8.1.2.6 for method of electroporation). After transfection, cells were seeded onto 96-well plates and incubated at 37°C, 5% CO_2. Cells were grown in medium with 10% FBS and 500 µg/ml Zeocin. Selection of stable clones (cells that constantly express the gene of interest, here selected by resistance to Zeocin) over 14 days was thus performed. Obtained clones were split and screened for the expression of the V5-epitope by immunocytostaining.

2.8.2.2.3 Immunocytostaining

Immunocytostaining involves the visualisation of specific proteins in cells using light microscopy. The principle is similar to that of Western blot staining, and involves probing the protein of interest with primary and secondary antibodies, followed by addition of a substrate that stains the protein of interest via the adherent antibodies. The protocol for detecting the V5-epitope, and thus cells expressing the CD533 vector, is as follows.

Clones were grown in petri dishes, until around 50% confluent. Medium was removed and cells were washed in 3 ml PBS. The cells were then fixed using 2 ml of acetone/methanol solution (1:1 ratio, stored at $-20^{\circ}C$, VWR International, West Chester, PA/Sigma, St. Louis, MO), for 10 minutes at room temperature, before it was removed and cells were left to dry at room temperature for 5 – 10 minutes. A small number of cells (approximately 1 cm diameter) were sectioned off used a wax pen, and these were then stained. Initially, the cells were rinsed in 100 μl PBS, and the primary antibody, anti-V5 MAb (Invitrogen, Carlsbad, CA, USA), was diluted to 1:200 in medium with 10% FBS, and 100 μl was added to cells for one hour at room temperature, with gentle agitation. Cells were then washed three times with 100 μl PBS, applied for five minutes each time, with gentle agitation. The secondary antibody, Rabbit Anti-Mouse immunoglobulin HRP (as used for Western blot analysis), was diluted to 1:200 in medium with 10% FBS, and 100 μl was added to cells for one hour at room temperature, with gentle agitation. Three washes with PBS were repeated as previously. Staining of cells with substrate to allow visualisation of V5 positive cells was next performed. The substrate was formed from an AEC (3-Amino-9-ethylcarbazole) chromogen kit (AEC-101, Sigma, St Louis, MO), which is used for staining peroxidase labelled compounds. Two drops of acetate buffer were added to 4 ml of deionised water, followed by one drop of AEC chromogen, and finally one drop of 3% hydrogen peroxide (all pre-made solutions). The solution was mixed and 100 μl was added to cells for 10 minutes at room temperature. The cells were then rinsed with deionised water, and cells were checked under the light microscope for staining.

2.8.2.2.4   Western blot analysis to look for effects of dominant-negative plasmid on ErbB1 signalling following transfection

V5-positive clones of both RT112 and J82 cells were chosen for further analysis, alongside cells negative for the V5-epitope. Cells were grown in flasks in medium with 10% FBS as previously until 50 - 70% confluent, medium was changed to serum free, and cells were starved for 24 hours. Cells were then either stimulated with 100ng/ml EGF for five minutes, or left untreated, and subsequently lysed as previously described with 200 µl standard Laemmli buffer. Protein quantification was performed, and Western blot was performed as previously. Resultant membranes were stained for expression of V5-epitope (anti-V5 MAb, as used for immunocytostaining, at 1:5000 dilution), ErbB1, p-ErbB1, AKT and p-AKT (all as used previously), to assess for effects of the dominant-negative CD533 plasmid on ErbB1 signalling.

CHAPTER 3

RESULTS

3.1 Molecular actions of lapatinib and chemotherapeutic agents in bladder cancer cell lines

3.1.1 Characterisation of expression of ErbB receptors and downstream signalling proteins

Expression of proteins involved in ErbB signalling in the six different bladder cancer cell lines of varying grades and in the vulval epidermoid carcinoma cell line A431 (known to express an artificially high level of ErbB1) were assessed using Western blot analysis. Morphologically, these cell lines represented two distinct types, epithelial (RT4, RT112, HT1376 and A431) and mesenchymal (T24, UMUC3 and J82). Cells belonging to the first group exhibited typical polarised epithelial morphology, formed tight cell-cell contacts, and expressed high levels of the epithelial marker E-cadherin (figure 3.1a). Cells of the second group had elongated fibroblastoid phenotype and were E-cadherin negative. ErbB1 and ErbB2 were highly expressed in epithelioid cells, and were present but at much lower levels in mesenchymal cells (figure 3.1a). In contrast, expression of ErbB3 was similar, and the expression of ErbB4 was hardly detectable, throughout all cell lines. AKT, a protein kinase responsible for ErbB-mediated anti-apoptotic response, was expressed at higher levels in mesenchymal cell lines, with two of these (J82 and UMUC3) expressing very low levels of PTEN (a tumour suppressor protein responsible for down-regulation of AKT) (figure 3.1b). Expression of other proteins involved in ErbB signalling and examined in this study (p42/44 MAPK, STAT1 and STAT3 [all involved with regulation of cell cycle progression and apoptosis], and PTP1B [protein tyrosine

phosphatase 1B, which is involved in the dephosphorylation and deactivation of receptor tyrosine kinases, 195]) did not correlate with morphological characteristics of cells (Figures 3.1a and 3.1b).
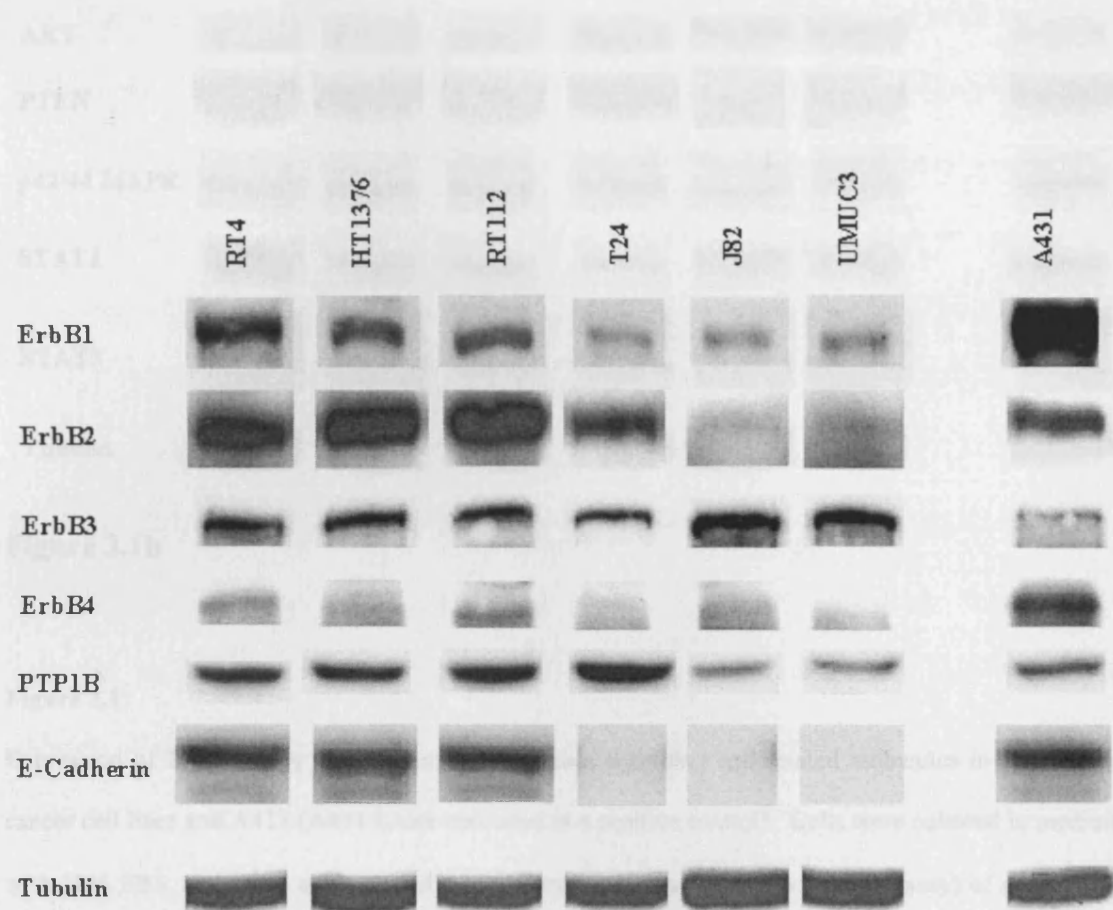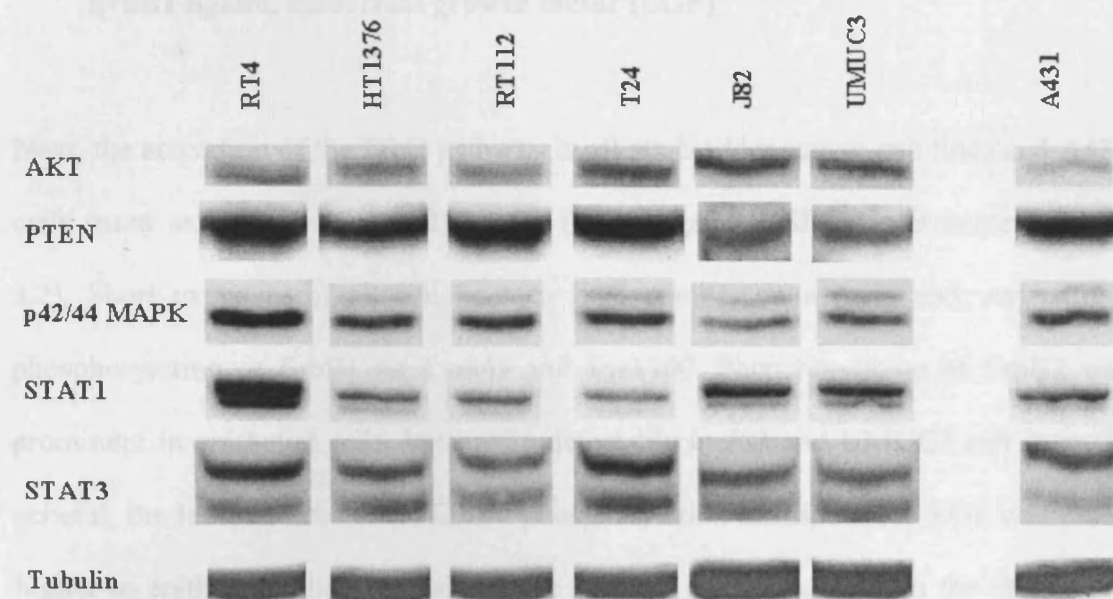

Figure 3.1a

Figure 3.1b

Figure 3.1

Expression of ErbB family of receptors, downstream signalling and related molecules in six bladder cancer cell lines and A431 (A431 lysate was used as a positive control). Cells were cultured in medium with 10% FBS, and lysed as described. 25 µg protein (as quantified by protein assay) of each lysate was resolved by SDS-PAGE and Western blot analysis was performed. Figure 3.1a shows the expression of ErbB family members, PTP1B and E-cadherin. Figure 3.1b shows the expression of downstream signalling pathways. Detection of α-tubulin was used as a loading control.

3.1.2 Activation of ErbB receptors and downstream signalling pathways by the ErbB1 ligand, epidermal growth factor (EGF)

Next, the activation of the ErbB pathway in all six bladder cancer cell lines and A431 cells (used as a positive control) by the ErbB1 ligand, EGF, was examined (figure 3.2). Short exposure of all cell lines to EGF resulted in a rapid and very strong phosphorylation of ErbB1 on Tyr845 and Tyr1100. Phosphorylation of ErbB2 was prominent in epithelial cells, but hardly detectable in J82 and UMUC3 cell lines. In general, the level of ErbB1 and ErbB2 phosphorylation in response to EGF was much higher in epithelial cells expressing more of these receptors. Even in the absence of EGF, all cell lines expressed detectable levels of phosphorylated ErbB3 with the higher p-ErbB3 levels in epithelial cells. ErbB3 phosphorylation levels were, however, variable after EGF stimulation. Whereas in RT112 cells EGF enhanced phosphorylation of ErbB3, in the two remaining epithelial cell lines, RT4 and HT1376, phosphorylation of this receptor was not affected by EGF. Furthermore, in mesenchymal cells, EGF actually decreased the basal level of p-ErbB3 expression.

Exposure to EGF resulted in the activation of both p42/44MAPK and AKT in all mesenchymal cell lines, and in RT112 cells, but not in RT4 or HT1376 cells. Activation of the STAT pathway was considerably less effective. Although all non-stimulated cell lines expressed phosphorylated STAT1 and STAT3, their level was mostly unaffected by EGF, except for increased activation of STAT3 seen in RT112 cells.
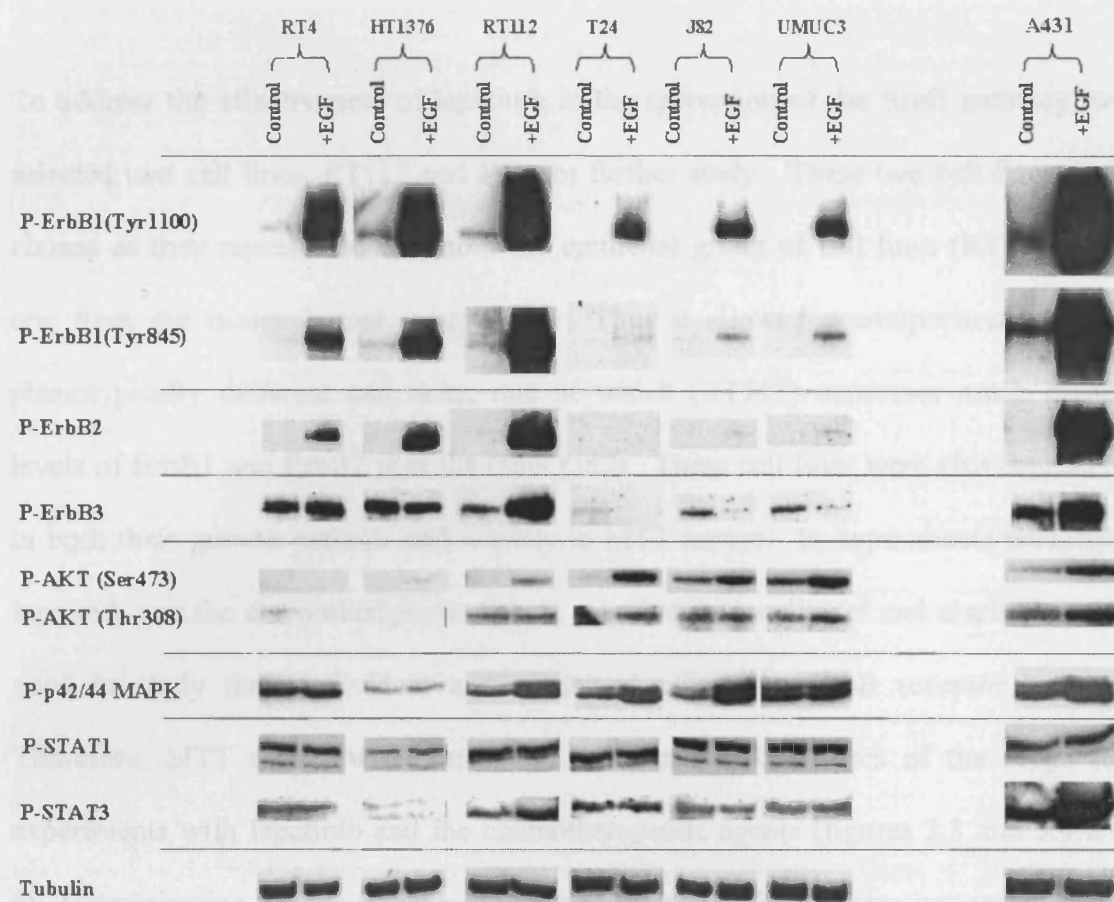
Figure 3.2

Activation of ErbB receptors and downstream signalling pathways. Cells were starved for 24 hours prior to either stimulation with 100 ng/ml EGF for five minutes, or no treatment (controls). Lysates were made, and protein content quantified by protein assay. 25 μg protein of each lysate was resolved by SDS-PAGE and Western blot analysis was performed. Detection of α-tubulin was used as a loading control.

3.1.3 Determination of IC_{50}s of lapatinib and chemotherapeutic agents

To address the effectiveness of lapatinib in the repression of the ErbB pathway, we selected two cell lines, RT112 and J82, for further study. These two cell lines were chosen as they represented one from the epithelial group of cell lines (RT112), and one from the mesenchymal group (J82). Thus it allowed a comparison between phenotypically different cell lines, one of which (RT112) expresses much higher levels of ErbB1 and ErbB2 than the other (J82). These cell lines were also consistent in both their growth patterns and activity in MTT assays. In experiments hereafter, lapatinib and the chemotherapeutic agents gemcitabine, paclitaxel and cisplatin, were used to study their individual and combined effects on ErbB receptor activity. Therefore, MTT assays were performed to calculate IC_{50} doses of the drugs for experiments with lapatinib and the chemotherapeutic agents (figures 3.3 and 3.4 a – d). Determination of the correct protocol for performing these assays was investigated as described in later sections. Results from the assays were analysed using Graphpad Prism software and IC_{50} values obtained (table 3.1).

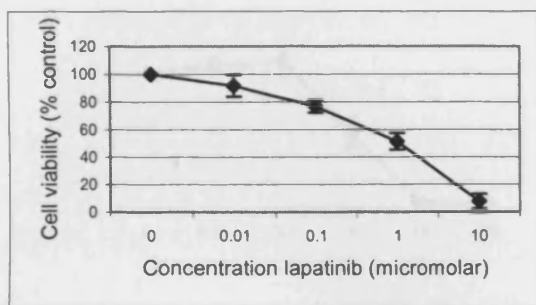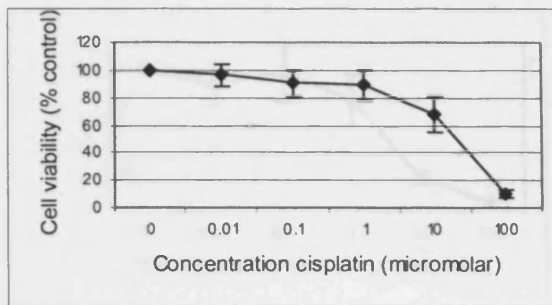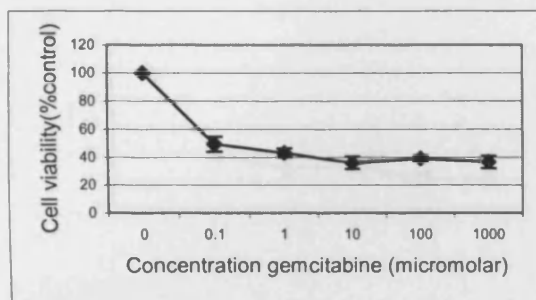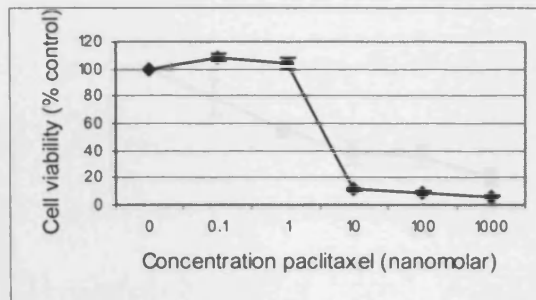Figure 3.3a

Figure3.3b

Figure 3.3c

Figure 3.3d

Figure 3.3

MTT analysis of RT112 cell viability following application of varying doses of lapatinib and chemotherapy. Cells were seeded in 96 well plates in medium with 10% FBS, which was changed to 1% FBS 24 hours later. A further 24 hours later, varying doses of lapatinib (a), cisplatin (b), gemcitabine (c) or paclitaxel (d) were added. MTT assay was performed 48 hours after addition of drugs. Assays were performed in triplicate.

	Lapatinib	Cisplatin	Gemcitabine	Paclitaxel
RT112	0.19	22.5	0.004	0.0054
J82	1.22	8.55	0.025	0.0005

Table 3.1

IC50 values (µmol/l) of lapatinib and chemotherapeutic agents in RT112 and J82 cells. IC50 were calculated on GraphPad Prism, using data from MTT assays (figures 3.3 and 3.4).

114

Figure 3.4a

Figure 3.4b

Figure 3.4c
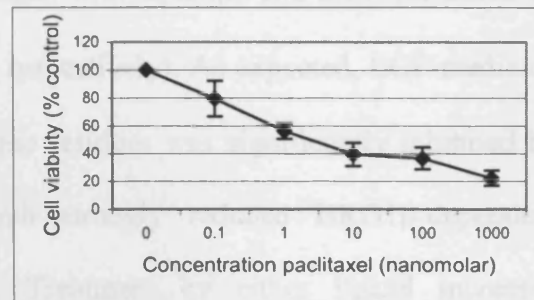
Figure 3.4d

Figure 3.4

MTT analysis of J82 cell viability following application of varying doses of lapatinib and chemotherapy. Cells were seeded in 96 well plates in medium with 10% FBS, which was changed to 1% FBS 24 hours later. A further 24 hours later, varying doses of lapatinib (a), cisplatin (b), gemcitabine (c) or paclitaxel (d) were added. MTT assay was performed 48 hours after addition of drugs. Assays were performed in triplicate.

	Lapatinib	**Cisplatin**	**Gemcitabine**	**Paclitaxel**
RT112	1.1	29.2	0.004	0.0034
J82	1.22	3.55	0.022	0.0005

Table 3.1

IC_{50} values (μmol/L) of lapatinib and chemotherapeutic agents in RT112 and J82 cells. IC_{50}s were calculated on GraphPad Prism, using data from MTT assays (figures 3.3 and 3.4).
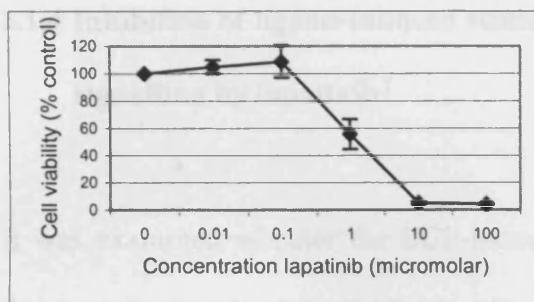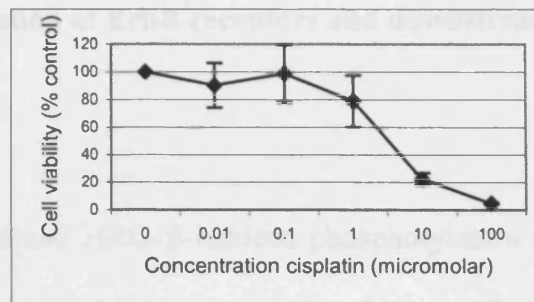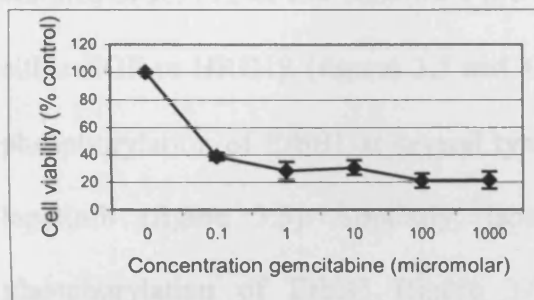
115

3.1.4 Inhibition of ligand-induced stimulation of ErbB receptors and downstream signalling by lapatinib

It was examined whether the EGF-induced and HRG1β-induced phosphorylation of the proteins involved in ErbB signalling is sensitive to lapatinib. Semi-confluent cultures of RT112 or J82 cells were pre-treated with lapatinib and then stimulated by either EGF or HRG1β (figures 3.5 and 3.6 respectively). As expected, EGF-mediated phosphorylation of ErbB1 at several tyrosine residues was significantly inhibited by lapatinib (figure 3.5). Similarly, lapatinib strongly reduced HRG1β-dependent phosphorylation of ErbB3 (figure 3.6). Treatment by either ligand increased phosphorylation of ErbB2 in RT112, but not in J82 cells, and this was again inhibited by prior treatment with lapatinib. A similar effect was seen with activation of ErbB1 by HRG1β in RT112 but not J82 cells, with activation being inhibited by lapatinib. Subsequent activation of AKT by either ligand was sensitive to lapatinib, with pAKT being inhibited back to basal levels. Lapatinib produced minimal (in RT112 cells) or no (in J82 cells) effect on ligand-dependent phosphorylation of p42/44MAPK.
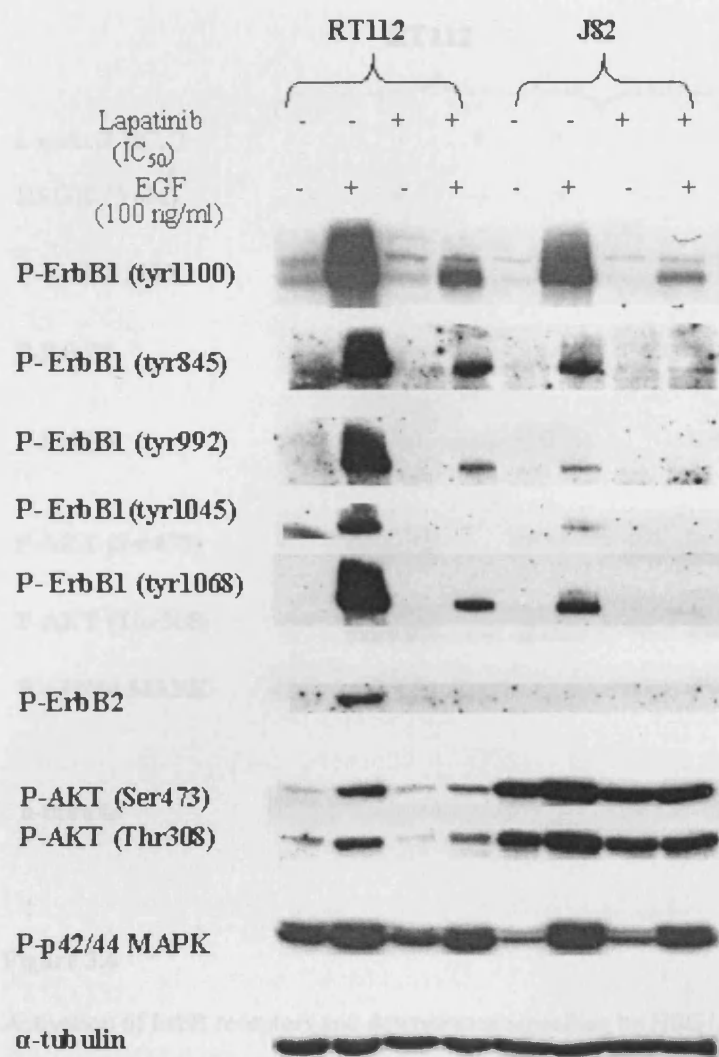
Figure 3.5

Inhibition of EGF activation of ErbB1, ErbB2 and downstream signalling by lapatinib. Cells at 50% confluence were starved in serum-free medium, and IC_{50} dose of lapatinib was added overnight (18 hours). Stimulation with EGF (100 ng/ml) was performed for five minutes. Lysates were made, and protein content quantified by protein assay. 25 µg protein of each lysate was resolved by SDS-PAGE and Western blot analysis was performed. Detection of α-tubulin was used as a loading control.

Figure 3.6

Activation of ErbB receptors and downstream signalling by HRG1β, and inhibition of this activation by lapatinib. Cells at 50% confluence were starved in serum-free medium, and IC$_{50}$ dose of lapatinib was added overnight (18 hours). Stimulation with 40 ng/ml HRG1β was performed for 15 minutes. Lysates were made, and protein content quantified by protein assay. 25 μg protein of each lysate was resolved by SDS-PAGE and Western blot analysis was performed. Detection of α-tubulin was used as a loading control.
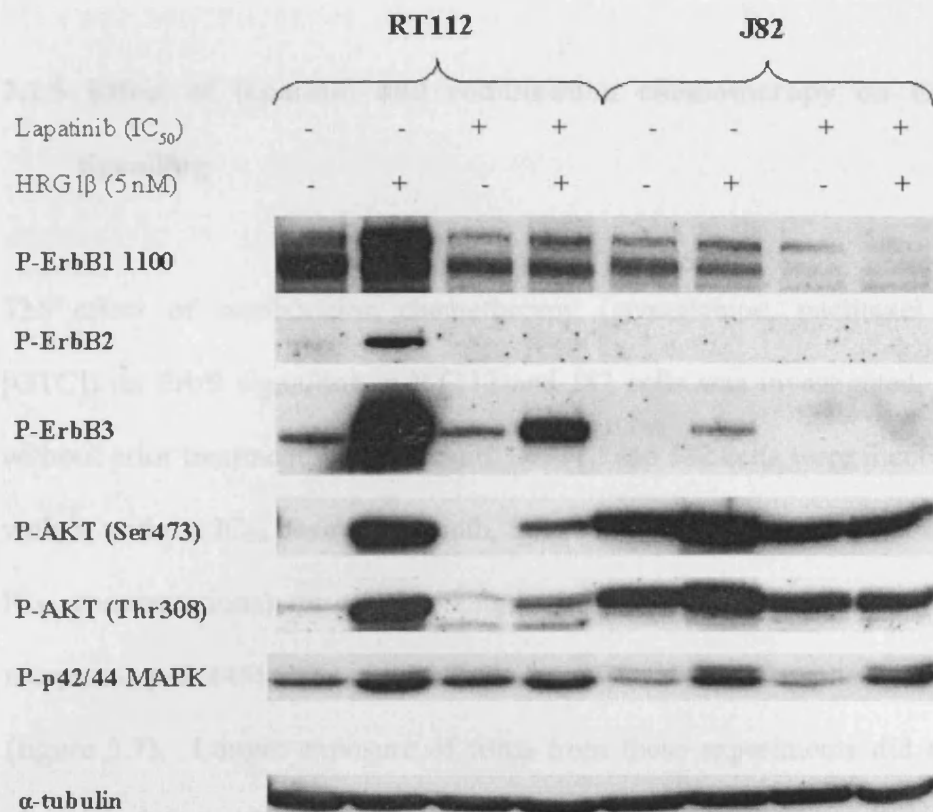
3.1.5 Effect of lapatinib and combination chemotherapy on ErbB receptor signalling

The effect of combination chemotherapy (gemcitabine, paclitaxel and cisplatin [GTC]) on ErbB signalling in RT112 and J82 cells was investigated, both with and without prior treatment with lapatinib. RT112 and J82 cells were incubated overnight with or without IC_{50} dose of lapatinib, followed by GTC (combined at their individual IC_{50} concentrations) for varying lengths of time. Phosphorylation status of ErbB receptors, p42/44MAPK and AKT was analysed with phospho-specific antibodies (figure 3.7). Longer exposure of films from these experiments did not reveal any phosphorylation of ErbB1 at some timepoints of GTC treatment, or ErbB2 at all timepoints of GTC treatment, despite some activation of downstream signalling proteins. To increase the sensitivity of the detection method, total ErbB1 and ErbB2 was immunoprecipitated using corresponding antibodies, followed by Western blotting to detect phosphorylated forms of the receptors. It was demonstrated that GTC produced a mild increase in the levels of phospho-ErbB1 in both cell lines at 10 minutes but not at the later timepoint, and also caused a mild increase in ErbB3 activation at 10 minutes in J82 cells only (figure 3.7a and 3.7b). Lapatinib completely blocked phosphorylation of ErbB1 and ErbB3 in J82 cells (figure 3.7b). In RT112 cells, while phosphorylation of ErbB1 and ErbB2 was similarly abolished by lapatinib, its effect on ErbB3 phosphorylation was only partial (figure 3.7a).

GTC treatment induced phosphorylation of AKT but not p42/44MAPK in both cell lines. The effect was particularly evident in J82 cells (figure 3.7b), in which GTC-

mediated phosphorylation of two residues, Ser473 and Thr308 was observed, especially at the later timepoint. This phosphorylation at 20 hours was not affected by lapatinib, and was therefore ErbB-independent. In contrast, GTC-dependent AKT phosphorylation on Ser473 in RT112 cells at both 10 minutes and 20 hours (figure 3.7a), and in J82 cells at 10 minutes (figure 3.7b), was inhibited by lapatinib.
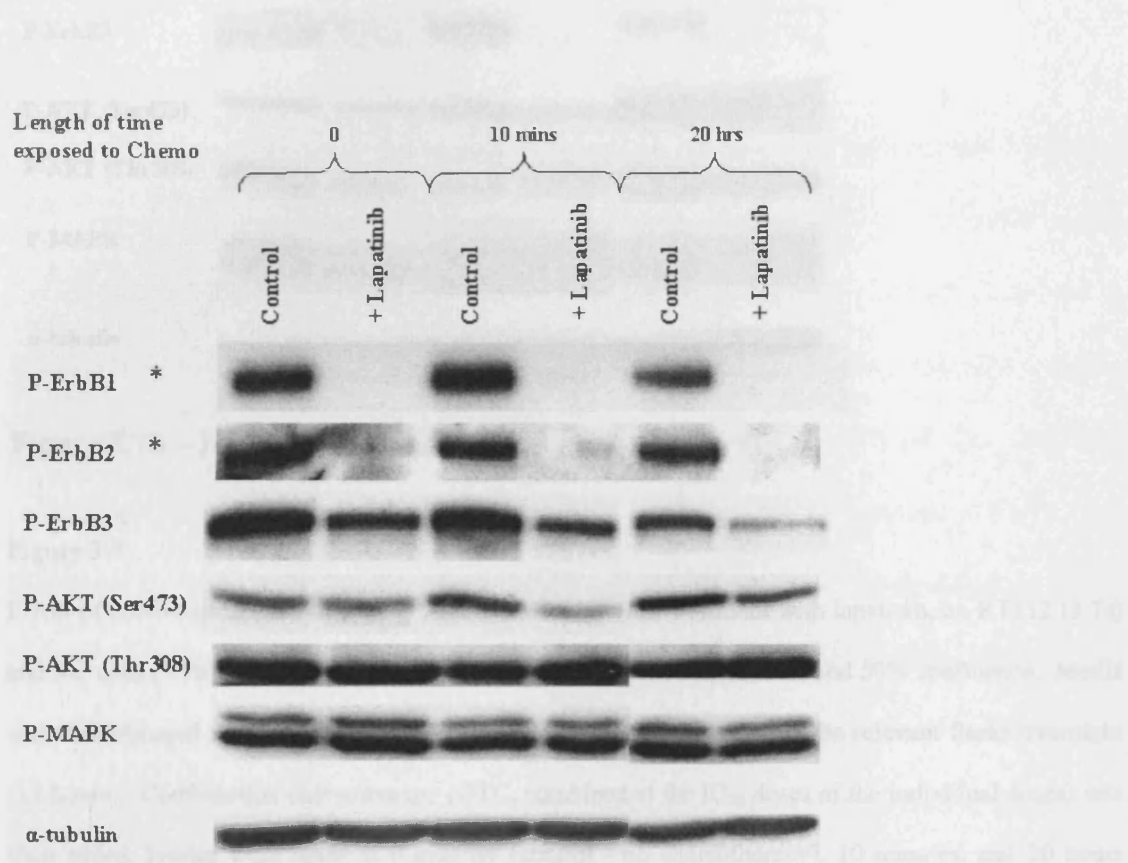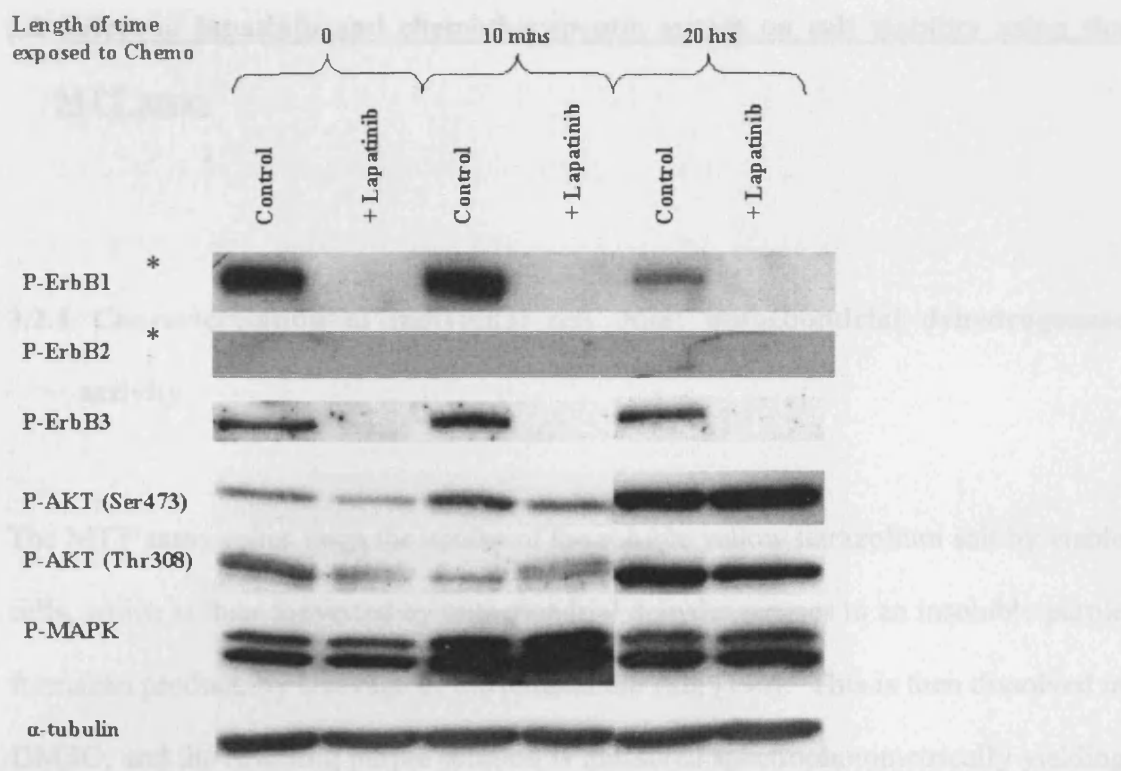

Figure 3.7a – RT112 cells

Figure 3.7b – J82 cells

Figure 3.7

Effect of combination chemotherapy, with and without prior treatment with lapatinib, on RT112 (3.7a) and J82 cells (3.7b). Cells were cultured in media with 10% FBS, until around 50% confluence. Media was then changed to serum-free, and IC$_{50}$ dose of lapatinib was added to the relevant flasks overnight (18 hours). Combination chemotherapy (GTC, combined at the IC$_{50}$ doses of the individual drugs) was then added, lysates were made at 0 minutes (control - no chemotherapy), 10 minutes, and 20 hours later, and protein content quantified by protein assay. 25 μg protein of each lysate was resolved by SDS-PAGE and Western blot analysis was performed. Detection of α-tubulin was used as a loading control.

* Western blot analyses performed using lysates prepared by immunoprecipitation with either ErbB1 or ErbB2 specific antibodies. Treatment timepoints were the same as used in lysates prepared with standard Laemmli buffer.

3.2 Effect of lapatinib and chemotherapeutic agents on cell viability using the MTT assay

3.2.1 Characterisation of individual cell lines: mitochondrial dehydrogenase activity

The MTT assay relies upon the uptake of the soluble yellow tetrazolium salt by viable cells, which is then converted by mitochondrial dehydrogenases to an insoluble purple formazan product, by cleavage of the tetrazolium ring [196]. This is then dissolved in DMSO, and the resulting purple solution is measured spectrophotometrically yielding an absorbance value, which represents the concentration of converted dye, and thus cellular activity. Each cell type has different levels of dehydrogenase activity, and therefore it is important to characterise each cell line with respect to absorbance levels per cell number. In the assays shown in figure 3.8, all six bladder cancer cell lines and A431 were thus assessed. 96 well plates were seeded with a range of cell densities and MTT assay performed. All assays were performed in triplicate, and it was found that the assay results were on the whole very reproducible, with low standard deviations (figure 3.8). However, at higher cell numbers there was slightly increased variation in absorbance in two cell lines (HT1376 and J82 – figures 3.8 b and 3.8 e), and this was particularly marked in the HT1376 cell line. The spectrophotometer used for all experiments did not produce an absorbance reading if the colour density of the solution was too high, with the highest attainable reading being around 3.5 absorbance units. It was found that dehydrogenase activity was particularly high in HT1376 and T24 cells (figures 3.8 b and 3.8 d), where cell densities above 16000 cells/well

produced solution densities above 3.5 absorbance units. In contrast, RT4, J82 and UMUC3 cells (figures 3.8 a, 3.8 e and 3.8 f) had much lower levels of dehydrogenase activity, with cell densities of 64000 cells/well producing readings of less than 3 absorbance units. This data allowed planning for future experiments, including number of cells/well to seed at the beginning of assays to be carried out over a number of days.
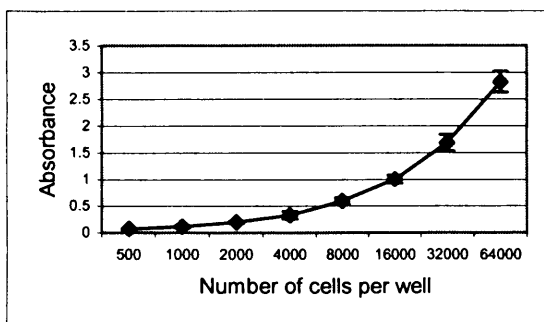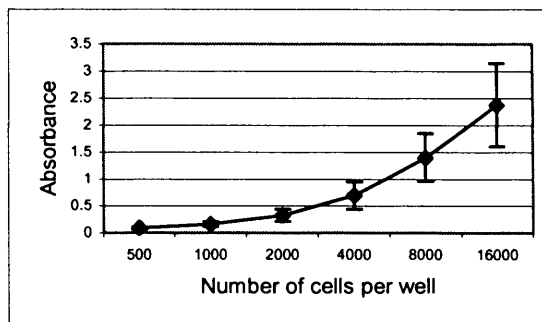
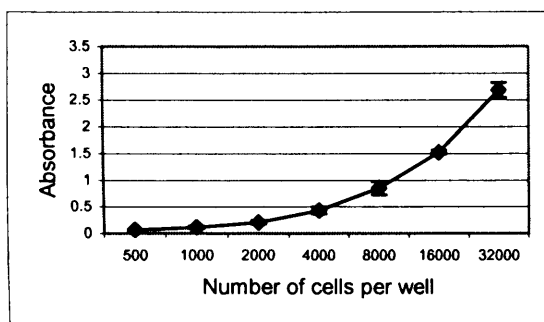**Figure 3.8a** – RT4 cells

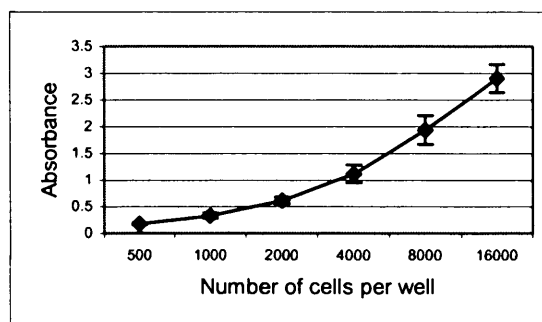**Figure 3.8b** – HT1376 cells

Figure 3.8c – RT112 cells

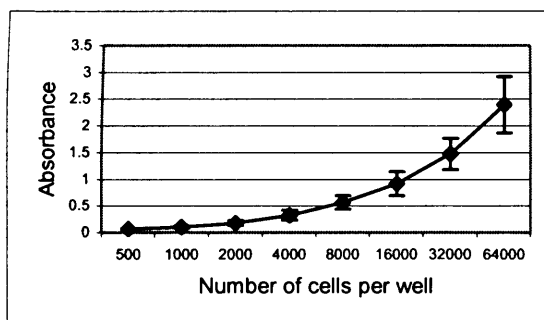**Figure 3.8d** – T24 cells

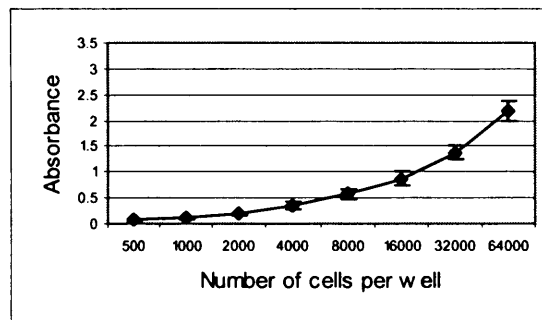**Figure 3.8e** – J82 cells
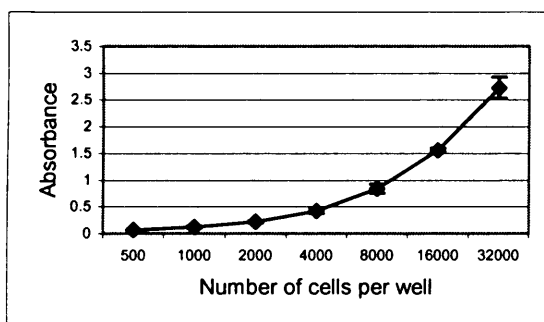

Figure 3.8f – UMUC3 cells

Figure 3.8g – A431 cells

124

Figure 3.8

MTT assays investigating the relation of cell numbers to absorbance in all six bladder cancer cell lines, and A431 cells. Cells were seeded at varying densities in 96 well plates, in medium with 10% FBS. Plates were incubated overnight, and then MTT assay was performed as described. All assays were performed in triplicate. Six bladder cancer cell lines and A431 cells were investigated: a – RT4 cells; b – HT1376 cells; c – RT112 cells; d – T24 cells; e – J82 cells; f – UMUC3 cells; g – A431 cells.

3.2.2 Assessment of optimal numbers of cells seeded and growing conditions for cells for assays over a period of 96 hours

It was necessary to assess the optimal growing conditions for cell lines over a period of 96 hours in 96 well plates, as future assays to investigate the effects of lapatinib and chemotherapeutic agents on cells would run over this time period. Therefore cells were grown in varying serum concentrations, and were seeded at various densities, in order to carry out this assessment. After considering cell numbers which created solutions too concentrated for spectrophotometer readings after incubation with MTT, and after predicting cell numbers 4 days after seeding using theoretical doubling times, it was decided to seed 500 and 1500 cells/well, for each cell line. Both numbers of cells were grown in medium with different concentrations of FBS for the final 72 hours of the assay. It was shown that throughout all cell lines (all six bladder cancer cell lines, and A431), there was little cell growth in serum-free medium, and that cell growth generally increased with increasing concentrations of FBS (figure 3.9). However, two cell lines, RT4 and UMUC3, showed slight decreases in cell growth after 96 hours with serum concentrations over 1% FBS (figures 3.9 a and 3.9 f). Without exception, wells with 1500 cells/well seeded produced final absorbance

values higher than those with the lower density of cells. In T24 cells, the cells with the greatest dehydrogenase activity (figure 3.8 d), it was found that when serum concentrations were higher than 1% FBS, cell growth was such that absorbance levels were too high to be readable by the spectrophotometer, except with 500 cells/well and 2.5% FBS (figure 3.9 d). From these results it was clear that the optimal serum concentration for growth of cells over a 96 hour period was 1% FBS. It was also decided that seeding density should be 1000 cells/well, as this number would provide adequate absorbance levels at the end of the assays, without danger of exceeding recordable absorbance levels when allowing for natural variation of cell growth.
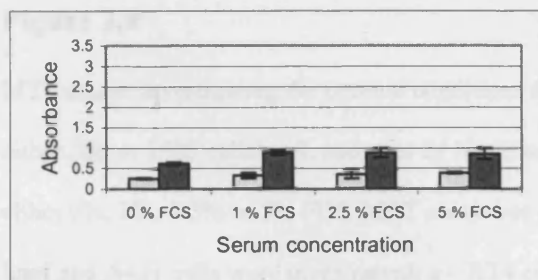
Figure 3.9a – RT4 cells

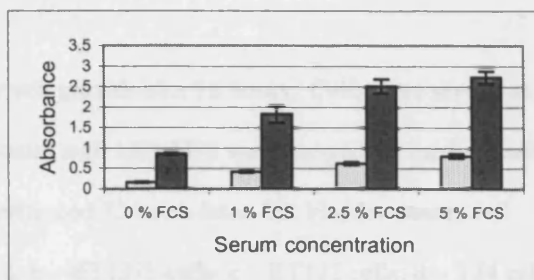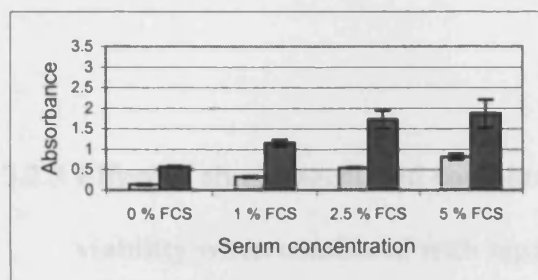**Figure 3.9b** – HT1376 cells

Figure 3.9c – RT112 cells
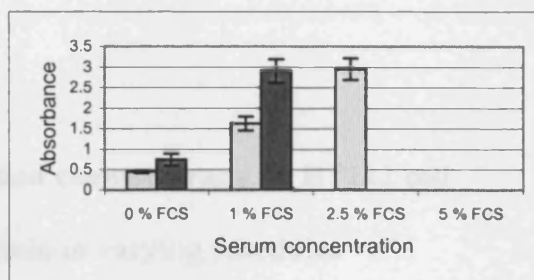
Figure 3.9d – T24 cells
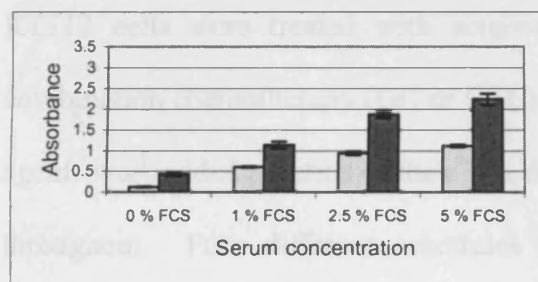
Figure 3.9e – J82 cells
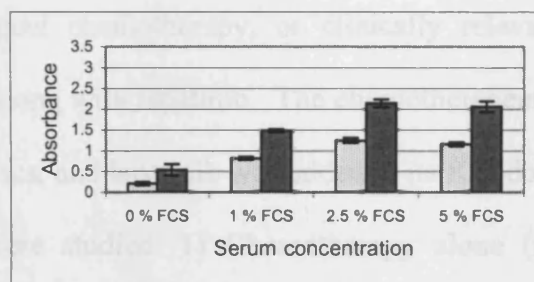
Figure 3.9f – UMUC3 cells
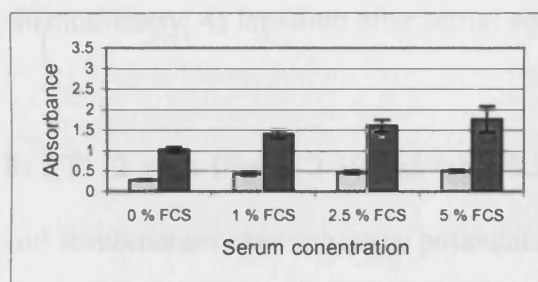
Figure 3.9g – A431 cells

Key

500 cells per well seeded

1500 cells per well seeded

Figure 3.9

MTT assays investigating the optimal conditions for cell growth over 96 hours. Cells were seeded at either 500 or 1500 cells/well, and after 24 hours medium with 10% FBS was changed for medium with either 0%, 1%, 2.5% or 5% FBS. MTT assay was performed 72 hours later. Six bladder cancer cell lines and A431 cells were investigated: a – RT4 cells; b – HT1376 cells; c – RT112 cells; d – T24 cells; e – J82 cells; f – UMUC3 cells; g – A431 cells.

3.2.3 Effect of single-agent and combination chemotherapy on RT112 cell viability when combined with lapatinib in varying schedules

RT112 cells were treated with single-agent chemotherapy, or clinically relevant combination chemotherapy (GC or GTC) along with lapatinib. The chemotherapeutic agents were added at ratios of their IC_{50} doses, and lapatinib was added at its IC_{50} dose throughout. Four different schedules were studied: 1) Chemotherapy alone (no lapatinib); 2) lapatinib before chemotherapy; 3) lapatinib concomitant with chemotherapy; 4) lapatinib after initial application of chemotherapy.

In RT112 cells (figure 3.10 and table 3.2), addition of lapatinib to both single-agent and combination chemotherapy potentiated efficacy. When single-agent cisplatin was combined with lapatinib (figure 3.10 a), the cell viability was less at 1/8 IC_{50} dose of cisplatin than when the IC_{50} dose of cisplatin was applied alone, independent of the sequence of application of the agents. A similar result was seen when gemcitabine alone was compared with differing sequences of lapatinib and gemcitabine (figure 3.10 b). Lapatinib reduced cell viability by more than 30% at all doses of gemcitabine. When lapatinib was combined with paclitaxel (figure 3.10 c), a

reduction of paclitaxel dose to 1/2 IC_{50} could be achieved whilst still maintaining the same level of cell viability as the IC_{50} dose of paclitaxel alone. The ability to decrease the chemotherapy dose to 1/8 IC_{50} with addition of lapatinib and still maintain rates of cell viability observed at IC_{50} doses was also seen in the experiments with combination chemotherapy (GC – figure 3.10 d, GTC – figure 3.10 e). However this was only observed when lapatinib was applied before, or concomitant with GC, and only before and during GTC.

Table 3.2 demonstrates the results of pairwise Tukey's tests (from the analysis of variance test), comparing the different sequences of application of lapatinib and chemotherapy, for all the different chemotherapy regimens in RT112 cells. From this, it is clear that efficacy was significantly enhanced when lapatinib was given before, concomitant with or after any of the chemotherapy regimens compared with chemotherapy alone (all p-values <0.001). Overall, a comparison of lapatinib-chemotherapy combinations revealed that prior application of lapatinib was significantly better than any other sequence (p-values range from $p < 0.05$ to $p < 0.001$), and concomitant lapatinib was significantly better than lapatinib after chemotherapy regimens (p-values range from $p < 0.01$ to $p < 0.001$). There were two exceptions. Lapatinib before single-agent cisplatin showed similar efficacy to lapatinib concomitant with cisplatin, and lapatinib concomitant with single-agent cisplatin showed similar efficacy to lapatinib after cisplatin.
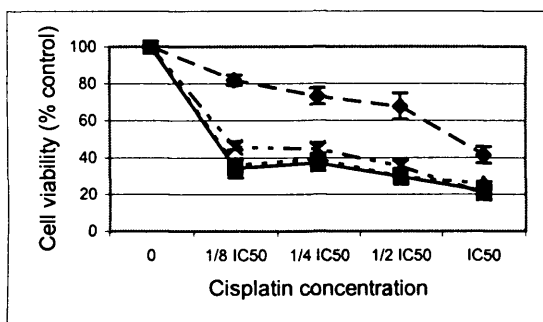
Figure 3.10a
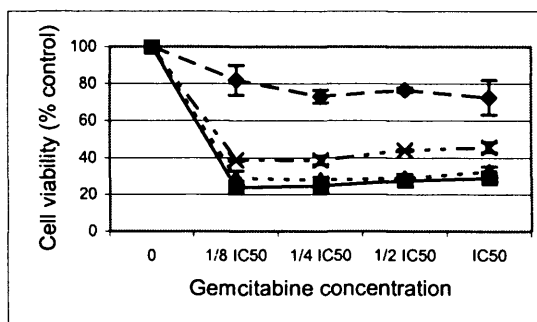
Figure 3.10b
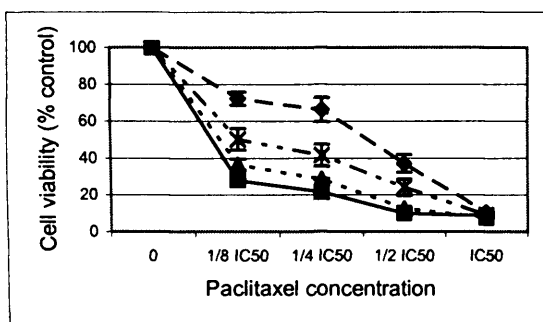
Figure 3.10c
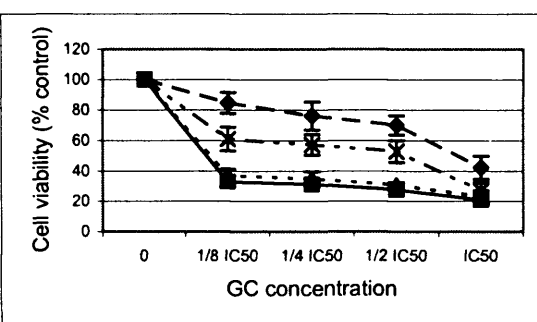
Figure 3.10d
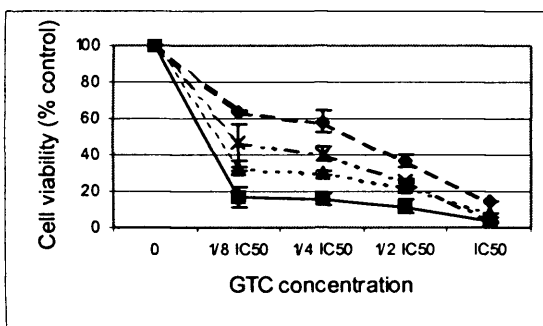
Figure 3.10e

Key

— — — — — Chemotherapy alone

——————— Lapatinib prior to chemotherapy

·················· Lapatinib concomitant with chemotherapy

— ·· — ·· — Lapatinib after chemotherapy

Figure 3.10

MTT analysis of RT112 cell viability following treatment with chemotherapy and lapatinib in varying combinations and sequences of application. Cells were seeded in 96 well plates at 1000 cells/well, medium was changed from that with 10% FBS to that with 1% FBS after 24 hours, and cells were then treated with lapatinib and chemotherapeutic agents in varying sequences of application over the next 72 hours prior to MTT assay; a – cisplatin; b – gemcitabine; c – paclitaxel; d – GC; e – GTC.

130

		Chemotherapy regimen				
Lapatinib schedules		Cisplatin only	Gemcitabine only	Paclitaxel only	GC	GTC
Lapatinib before chemotherapy	No lapatinib, chemotherapy only	**<0.001**	**<0.001**	**<0.001**	**<0.001**	**<0.001**
	Lapatinib concomitant with chemotherapy	0.1	**<0.05**	**<0.001**	**<0.01**	**<0.001**
	Lapatinib after chemotherapy	**<0.01**	**<0.001**	**<0.001**	**<0.001**	**<0.001**
Lapatinib concomitant with chemotherapy	No lapatinib, chemotherapy only	**<0.001**	**<0.001**	**<0.001**	**<0.001**	**<0.001**
	Lapatinib after chemotherapy	0.5	**<0.001**	**<0.001**	**<0.001**	**<0.01**
Lapatinib after chemotherapy	No lapatinib, chemotherapy only	**<0.001**	**<0.001**	**<0.001**	**<0.001**	**<0.001**

Significant p-values are highlighted in bold.

Table 3.2

Statistical differences (p-values) in cell viability between lapatinib schedules (columns 1 versus 2) with respect to chemotherapy in RT112 cells (Analysis of Variance using pairwise Tukey method).

3.2.4 Effect of single-agent and combination chemotherapy on J82 cell viability when combined with lapatinib in varying schedules

Similar experiments were carried out using J82 cells, using the same methodology as above in RT112 cells. In J82 cells (figure 3.11 and table 3.3), addition of lapatinib to both single-agent and combination chemotherapy again generally enhanced a reduction in cell viability. Addition of lapatinib to cisplatin (figure 3.11 a) decreased cell viability throughout all sequences of application, although this was more apparent when it was applied before or concomitant with single-agent cisplatin. Lapatinib plus 1/8 IC_{50} dose of cisplatin had similar efficacy to single-agent cisplatin at its IC_{50} dose. Similar results were observed with lapatinib and gemcitabine (figure 3.11 b), lapatinib and paclitaxel (figure 3.11 c), and lapatinib and GC (figure 3.11 d), though only lapatinib prior to gemcitabine showed less cell viability at 1/8 IC_{50} dose of gemcitabine compared with the IC_{50} dose of gemcitabine alone. The combination of the three chemotherapy agents (GTC) with lapatinib in J82 cells (figure 3.11 e) showed the least enhancement of efficacy compared with chemotherapy alone. This was because even at 1/8 IC_{50} doses of GTC, cell viability was only approximately 30%, which decreased to 20% when lapatinib was added prior to GTC. However, lapatinib again facilitated dose reduction of the chemotherapeutic agents; lapatinib prior to the 1/8 IC_{50} dose of the chemotherapeutic agents led to the same level of cell viability as the IC_{50}s of GTC alone.

Table 3.3 shows the results of pairwise Tukey's tests, comparing the effects of different schedules of lapatinib and chemotherapy regimens on cell viability in J82 cells. Similar to RT112 cells, it is clear in J82 cells that efficacy was significantly

enhanced when lapatinib was given before any of the chemotherapy regimens compared with chemotherapy alone (all p-values < 0.001). However unlike our results for RT112 cells, lapatinib concomitant or after chemotherapy did not always enhance efficacy compared with chemotherapy alone. Indeed, lapatinib concomitant with GTC was no better than GTC alone, and lapatinib after single-agent paclitaxel or GC was no better than paclitaxel alone. Overall, a comparison of lapatinib-chemotherapy combinations revealed that prior application of lapatinib was significantly better than any other sequence in J82 cells (p < 0.05 to p < 0.001). There were three exceptions. Lapatinib before cisplatin or GC was similar to lapatinib concomitant with cisplatin or GC; lapatinib before GTC was similar to lapatinib after GTC. Concomitant application of lapatinib was significantly better than lapatinib after chemotherapy (p < 0.01 to p < 0.001) for most schedules except GTC. Lapatinib after GTC was superior to concomitant lapatinib (p< 0.01).

Figure 3.11a
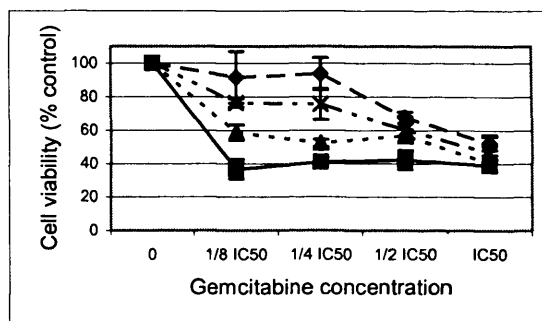
Figure 3.11b
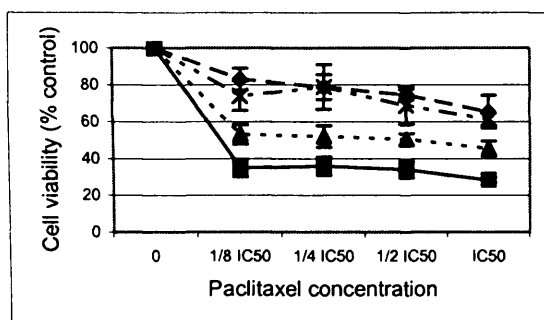
Figure 3.11c
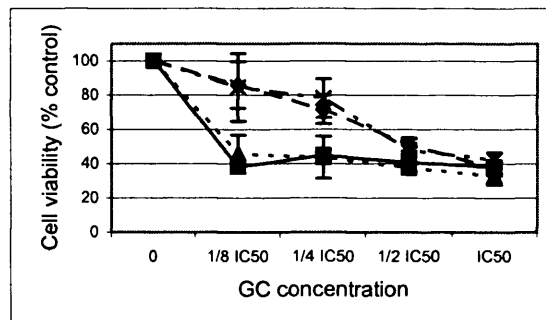
Figure 3.11d
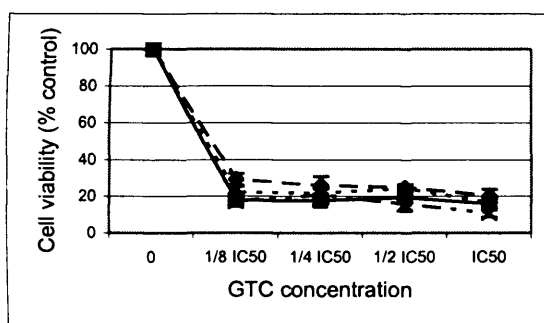
Figure 3.11e

Key

– – – – – Chemotherapy alone

———— Lapatinib prior to chemotherapy

·················· Lapatinib concomitant with chemotherapy

–··–··–··– Lapatinib after chemotherapy

Figure 3.11

MTT analysis of J82 cell viability following treatment with chemotherapy and lapatinib in varying combinations and sequences of application. Cells were seeded in 96 well plates at 1000 cells/well, medium was changed from that with 10% FBS to that with 1% FBS after 24 hours, and cells were then treated with lapatinib and chemotherapeutic agents in varying sequences of application over the next 72 hours prior to MTT assay; a – cisplatin; b – gemcitabine; c – paclitaxel; d – GC; e – GTC.

		Chemotherapy regimen				
Lapatinib schedules		Cisplatin only	Gemcitabine only	Paclitaxel only	GC	GTC
Lapatinib before chemotherapy	No lapatinib, chemotherapy only	**<0.001**	**<0.001**	**<0.001**	**<0.001**	**<0.001**
	Lapatinib concomitant with chemotherapy	0.3	**<0.01**	**<0.001**	0.4	**<0.05**
	Lapatinib after chemotherapy	**<0.001**	**<0.001**	**<0.001**	**<0.001**	0.9
Lapatinib concomitant with chemotherapy	No lapatinib, chemotherapy only	**<0.001**	**<0.001**	**<0.001**	**<0.001**	0.3
	Lapatinib after chemotherapy	**<0.001**	**<0.001**	**<0.001**	**<0.01**	**<0.01***
Lapatinib after chemotherapy	No lapatinib, chemotherapy only	**<0.05**	**<0.001**	0.6	0.5	**<0.001**

Significant p-values are highlighted in bold.

*Lapatinib after GTC showed less cell viability than lapatinib concomitant with GTC.

Table 3.3

Statistical differences (p-values) in cell viability between lapatinib schedules (columns 1 versus 2) with respect to chemotherapy in J82 cells (Analysis of Variance using pairwise Tukey method).

3.2.5 Synergism between lapatinib and various chemotherapeutic regimens

Having established that lapatinib before chemotherapy is overall the most promising schedule for these two cell lines, we then determined whether prior lapatinib had an additive or synergistic effect with the various chemotherapy combinations. Results were analysed as interactions plots, using the ANOVA test (figures 3.12 and 3.13). Lapatinib prior to the various chemotherapy regimens demonstrated synergism in both cell lines in all except one combination (lapatinib and cisplatin in J82 cells [figure 3.13 a]). For this combination, the effect of lapatinib was additive.
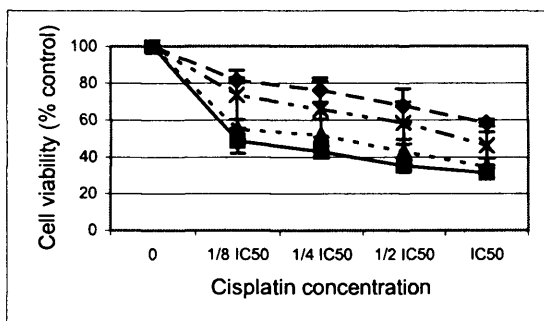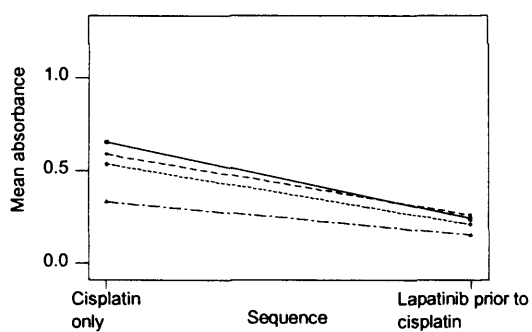
Figure 3.12a
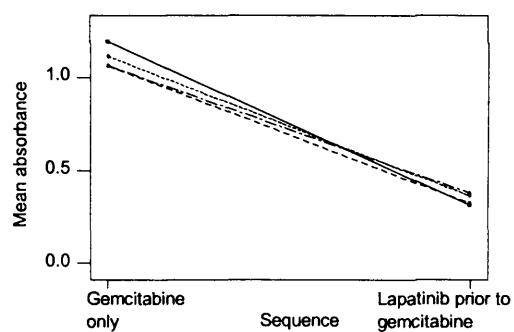
Figure 3.12b
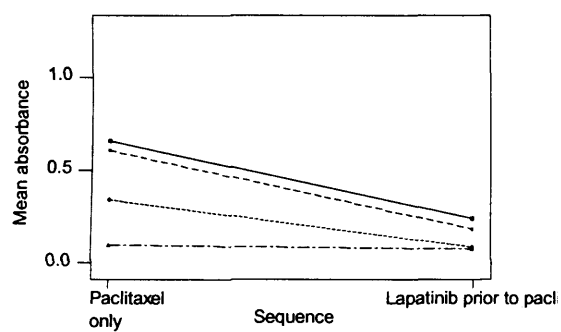
Figure 3.12c
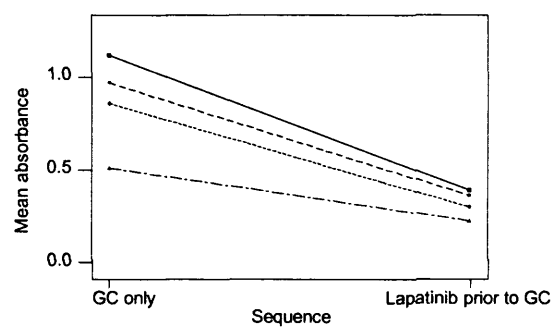
Figure 3.12d
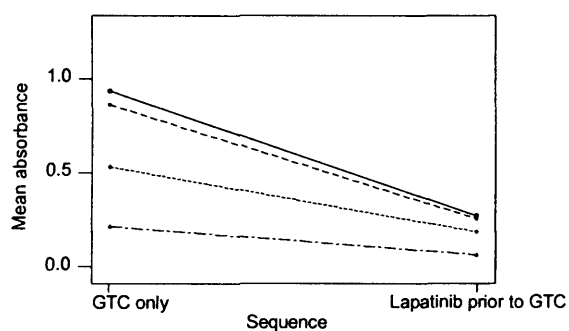
Figure 3.12e

Key

—————	1/8 IC50 chemotherapy
— — — — —	1/4 IC50 chemotherapy
··················	1/2 IC50 chemotherapy
— · — · — · —	IC50 chemotherapy

Figure 3.12

Interactions plots of cell viability comparing application of chemotherapy only against lapatinib before

chemotherapy in RT112 cells: a – cisplatin only; b – gemcitabine only; c – paclitaxel only; d – GC; e –

GTC. Interactions plots were produced from the ANOVA test.
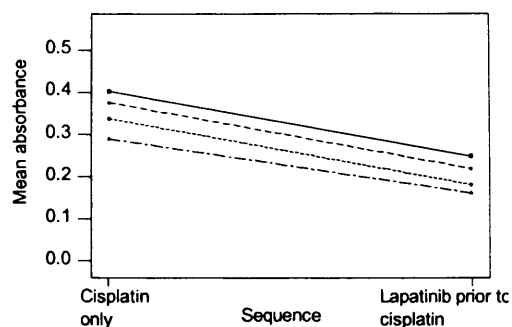
Figure 3.13a
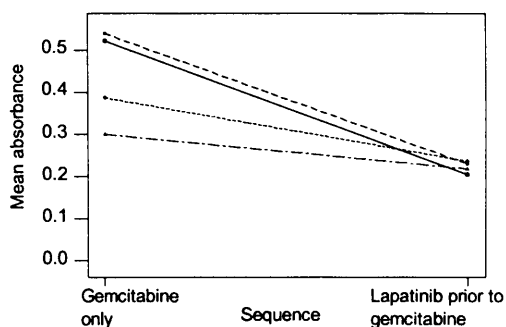
Figure 3.13b

Figure 3.13c

Figure 3.13d

Figure 3.13e

Figure 3.13

Interactions plots of cell viability comparing application of chemotherapy only against lapatinib before

chemotherapy in J82 cells: a – cisplatin only; b – gemcitabine only; c – paclitaxel only; d – GC; e –

GTC. Interactions plots were produced from the ANOVA test.

3.3 Effect of lapatinib and chemotherapy on cell survival and cell cycle

3.3.1 Apoptosis assays

3.3.1.1 Assessment of apoptosis using fluorescence microscopy

Attempts were made to investigate whether lapatinib caused apoptosis in RT112 and J82 cells, using fluorescence microscopy. The MitoCapture™ apoptosis detection kit was used. The basis of the assay, as previously described, is that MitoCapture, a cationic dye, fluoresces differently in healthy cells than in apoptotic cells. In healthy cells, there is bright red fluorescence due to accumulation and aggregation in the mitochondria. In apoptotic cells, there is green fluorescence which represents the dye remaining in its monomer form in the cytoplasm due to altered mitochondrial transmembrane potential. Initial attempts with the assay were inconclusive. Cells were seeded in a 96 well plate at 1000 cells/well, and 24 hours later medium was changed to that with 1% FBS along with IC_{50} of lapatinib in relevant wells. A further 24 hours later 100 ng/ml EGF was added to relevant wells and the plate was incubated for 48 hours before the assay was performed. Therefore there were untreated cells, cells with lapatinib or EGF alone, and cells with a combination of lapatinib and EGF. After performing the assay as described, cells were inspected using a fluorescent microscope. All cells showed both green and red fluorescence, so that a distinction could not be made between living and apoptotic cells. Communications were made with the company supplying the assay kit, and slight modifications to the method of

performing the assay, mainly involving extra mixing of the reagent and buffer mixer, were made. The assay was repeated. Again, results were inconclusive as with the previous assay (pictures weren't taken of the results, and therefore no results are available to show). A decision was made to discontinue using this assay, and after discussion with apoptosis experts in neighbouring laboratories, the Annexin V assay was undertaken.

3.3.1.2 Assessment of apoptosis using the Annexin V assay

Induction of apoptosis was next investigated in RT112 and J82 cells using the Annexin V-FITC apoptosis assay. As described, this assay is based around the binding of Annexin V to early apoptotic cells, due to externalisation of phosphatidyl serine on cell membranes. Both Annexin V and propidium iodide used in this assay bind to late apoptotic and dead cells due to disruptions in cell membranes, but are excluded from viable cells with intact membranes. In these experiments, treated and untreated cells were grown in serum-free medium. Two clinically relevant combinations of chemotherapeutic agents were studied: GC and GTC. Fluorescence was measured using a flow cytometer as described. In RT112 cells, lapatinib alone caused a minor increase in apoptosis rate of 1.2 - 1.4 x the apoptosis rate in untreated cells (figure 3.14 a and b). Interestingly, GC actually led to a 0.7 x decrease in apoptosis rate (figures 3.14 a and c), whereas when paclitaxel was added to this combination, there was a 1.8 x increase in apoptosis rate (figures 3.14 b and e), as compared to untreated cells. When lapatinib was added prior to the chemotherapy regimens, there was again some disparity, with lapatinib prior to GC causing a 1.3 x increase in apoptosis rate

when compared to GC alone (figures 3.14 c and d), but lapatinib prior to GTC led

to a 0.6 x decrease in apoptosis rate when compared to GTC alone (figures 3.14 e

and f). Overall, lapatinib seemed to marginally increase apoptosis rates in RT112

cells, except when added prior to GTC, which on its own had caused the greatest

increase in apoptosis rate. In J82 cells, lapatinib consistently led to a decrease in

apoptosis rates (figure 3.15). Lapatinib alone caused a 0.5 x decrease in apoptosis

rate when compared to untreated cells (figures 3.15 a and b). Unlike in RT112

cells, both combinations of chemotherapy led to a similar increase in apoptosis

rates in J82 cells when compared to untreated cells of around 1.6 – 1.7 x (figures

3.15 b, c and e). When lapatinib was added prior to the chemotherapeutic

regimens, a small decrease in apoptosis rates was seen when compared to the

chemotherapy alone (figures 3.15 c – f). Therefore, looking at results in both cell

lines, lapatinib had only very minor effects on apoptosis rates, but the marginal

decreases in apoptosis rates seen with lapatinib were of a greater factor than when

an increase in apoptosis rate was witnessed. To investigate the reasons behind the

disparity between these findings and the synergism seen between lapatinib and the

chemotherapeutic agents in MTT assays, FACS analysis was undertaken to look

further at the effect of lapatinib and chemotherapy on the cell lines.
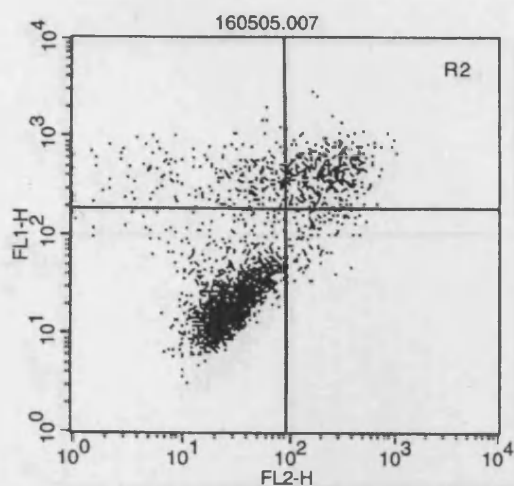
Quadrant	Events (% cells)
UL (apoptotic cells)	**7.56**
UR (dead cells)	13.28
LL (viable cells)	75.62
LR (others)	3.64

Figure 3.14a –control
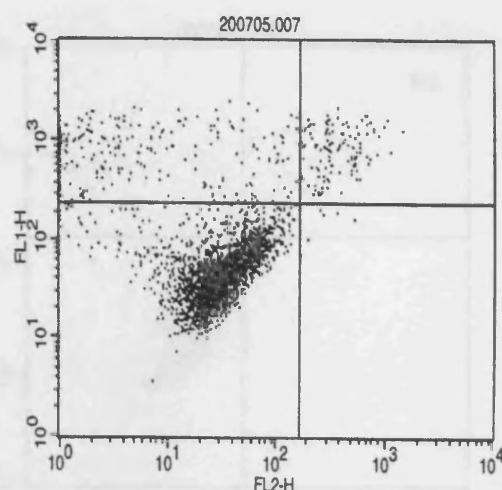
Quadrant	Events (% cells)
UL (apoptotic cells)	**10.80**
UR (dead cells)	5.00
LL (viable cells)	83.95
LR (others)	0.25

Figure 3.14b – lapatinib
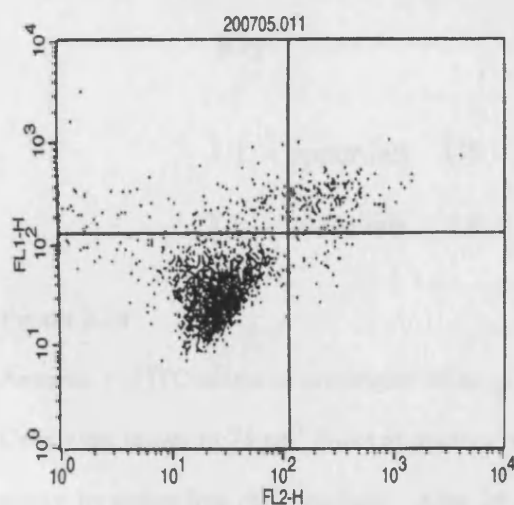
Quadrant	Events (% cells)
UL (apoptotic cells)	**5.32**
UR (dead cells)	7.12
LL (viable cells)	86.34
LR (others)	1.22

Figure 3.14c – GC
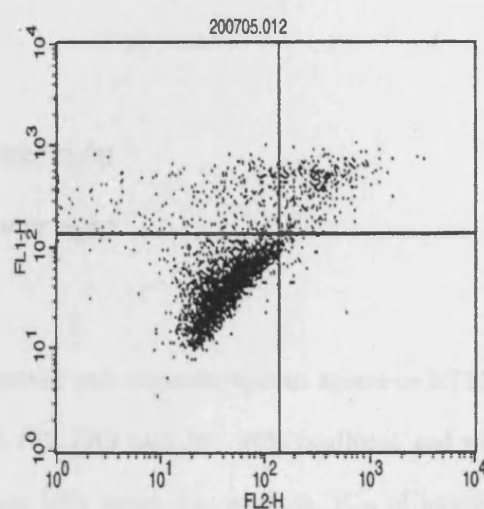
Quadrant	Events (% cells)
UL (apoptotic cells)	**7.13**
UR (dead cells)	8.32
LL (viable cells)	83.41
LR (others)	1.14

Figure 3.14d – GC and lapatinib

142

Quadrant	Events (% cells)
UL (apoptotic cells)	**13.65**
UR (dead cells)	10.08
LL (viable cells)	74.65
LR (others)	1.62

Quadrant	Events (% cells)
UL (apoptotic cells)	**7.86**
UR (dead cells)	3.77
LL (viable cells)	87.38
LR (others)	0.98
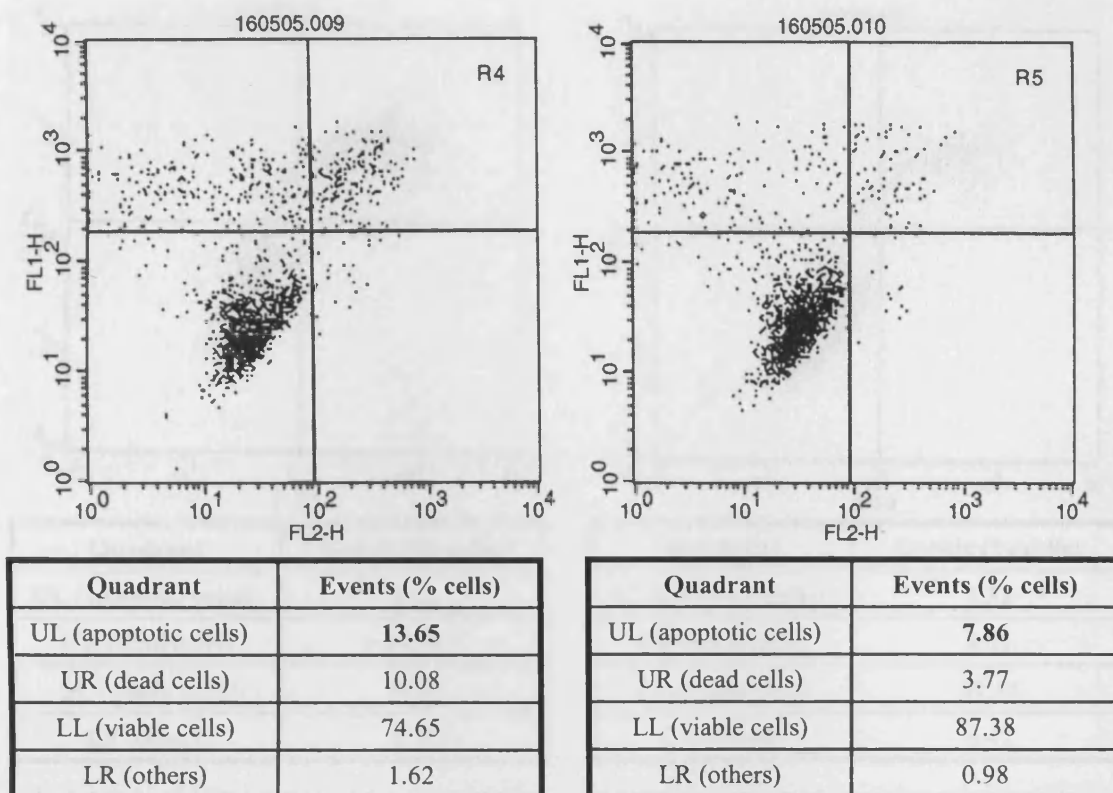
Figure 3.14e – GTC

Figure 3.14f – GTC and lapatinib

Key

UL – upper left   UR – upper right

LL – lower left   LR – lower right

Figure 3.14

Annexin V–FITC assays to investigate effect of lapatinib and chemotherapeutic agents on RT112 cells. Cells were grown in 75 cm³ flasks in medium with 10% FBS until 30 – 40% confluent, and were then grown in serum-free (SF) medium. After 24 hours with serum-free medium, IC_{50} of lapatinib was added to relevant flasks, followed by either GC or GTC 24 hours later. Annexin V assay was performed 48 hours later, with results being obtained by the fluorescence microscope. FITC was detected by FL1 (y – axis) and propidium iodide was detected by FL2 (x – axis), which meant that quadrants represent cells as explained in the figures above. Cells were treated as follows: a– control; b – lapatinib; c – GC; d – lapatinib and GC; e – GTC; f – lapatinib and GTC.

143
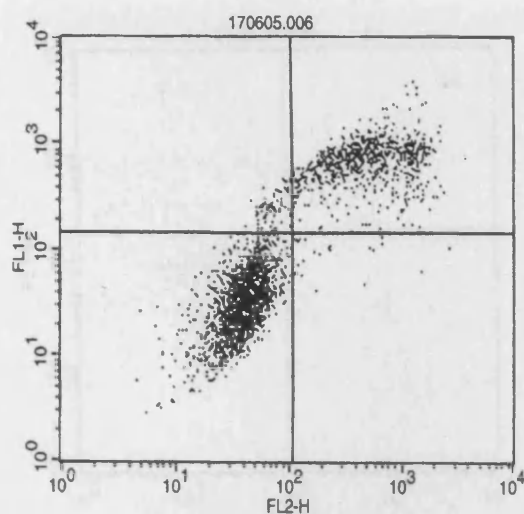
Quadrant	Events (% cells)
UL (apoptotic cells)	**2.63**
UR (dead cells)	25.79
LL (viable cells)	70.80
LR (others)	0.78

Figure 3.15a – control
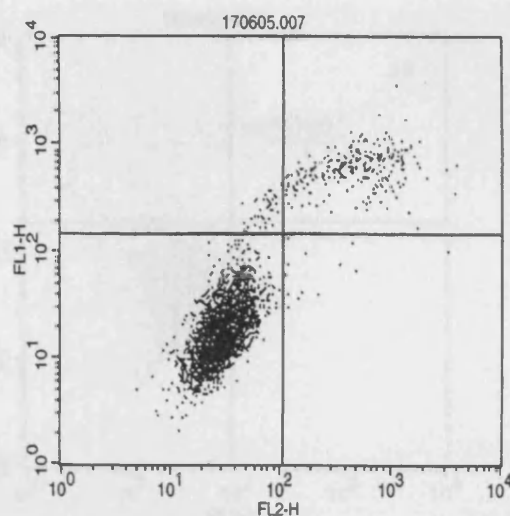
Quadrant	Events (% cells)
UL (apoptotic cells)	**1.32**
UR (dead cells)	8.81
LL (viable cells)	89.44
LR (others)	0.42

Figure 3.15b – lapatinib
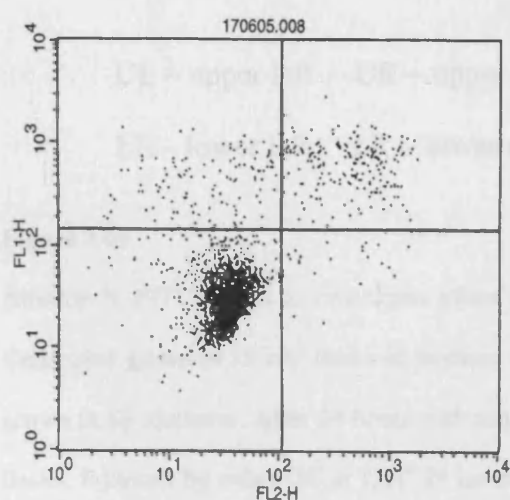
Quadrant	Events (% cells)
UL (apoptotic cells)	**4.13**
UR (dead cells)	6.63
LL (viable cells)	88.46
LR (others)	0.78

Figure 3.15c – GC
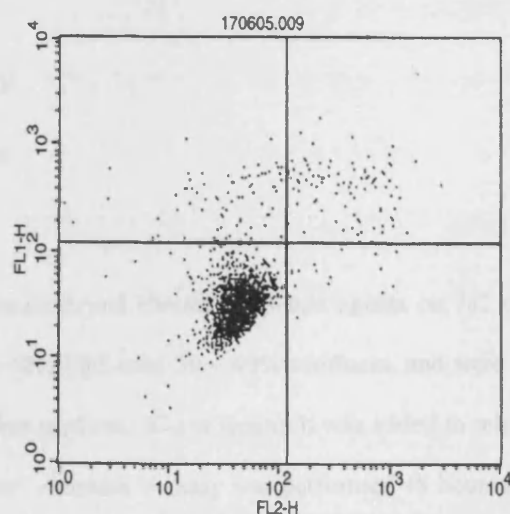
Quadrant	Events (% cells)
UL (apoptotic cells)	**3.91**
UR (dead cells)	4.58
LL (viable cells)	90.59
LR (others)	0.92

Figure 3.15d – GC and lapatinib

144
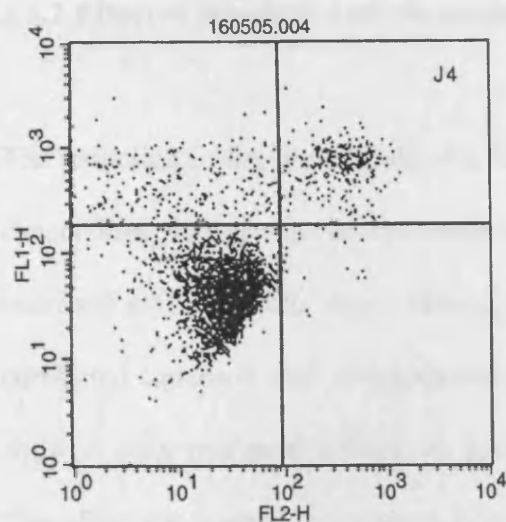
Quadrant	Events (% cells)
UL (apoptotic cells)	**8.45**
UR (dead cells)	9.03
LL (viable cells)	81.65
LR (others)	0.87
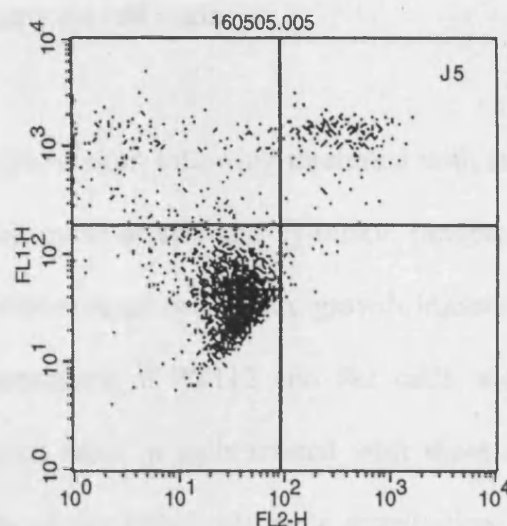
Quadrant	Events (% cells)
UL (apoptotic cells)	**7.64**
UR (dead cells)	7.02
LL (viable cells)	84.50
LR (others)	0.84

Figure 3.15e –GTC   **Figure 3.15f – GTC and lapatinib**

Key

UL – upper left   UR – upper right

LL – lower left   LR – lower right

Figure 3.15

Annexin V–FITC assays to investigate effect of lapatinib and chemotherapeutic agents on J82 cells.

Cells were grown in 75 cm^3 flasks in medium with 10% FBS until 30 – 40% confluent, and were then

grown in SF medium. After 24 hours with serum-free medium, IC$_{50}$ of lapatinib was added to relevant

flasks, followed by either GC or GTC 24 hours later. Annexin V assay was performed 48 hours later,

with results being obtained by the fluorescence microscope. FITC was detected by FL1 (y – axis) and

propidium iodide was detected by FL2 (x – axis), which meant that quadrants represent cells as

explained in the figures above. Cells were treated as follows: a – control; b – lapatinib; c – GC; d –

lapatinib and GC; e – GTC; f – lapatinib and GTC.

145

3.3.2 Effect of lapatinib and chemotherapy on cell cycle

The reduction in the growth rate of a cell population following treatment with an anti-cancer drug is the sum of cytostatic (cell cycle arrest) and cytotoxic (apoptosis or necrosis) effects of this drug. Having demonstrated synergistic growth inhibition by combined lapatinib and chemotherapy treatment of RT112 and J82 cells, we then showed only marginal effects on apoptosis rates in cells treated with these drugs. Therefore we wished to examine how the drugs affect cell cycle distribution, using FACS analysis. Flow cytometric analysis of the effects of lapatinib alone on cell cycle distribution revealed a significant shift into the G_0/G_1 phase of the cell cycle in both cell lines (figures 3.16 b and 3.17 b). In contrast, effect of combination chemotherapy was cell-specific. In RT112 cells, both GC and GTC treatment resulted in the increased proportion of cells in the G_0/G_1/early S phase (figures 3.16 c and e). Combined lapatinib and chemotherapy treatment further strengthened this tendency, a trend that was much more pronounced with GTC (> 80% cells in G_0/G_1 phase) than just GC (just > 50% in G_0/G_1 phase) (figures 3.16 d and f). In J82 cells treated with GC or GTC, the majority of cells were accumulated in S phase with decreased proportion of cells in G_0/G_1 and G_2/M (figures 3.17 c and e). Either chemotherapeutic combination added to the cells pre-incubated with lapatinib also demonstrated accumulation of cells in the S phase. However, this treatment revealed a trend towards restoration of higher proportions of the cells accumulated in G_0/G_1 and G_2/M phases as compared with the cells treated with chemotherapy only (figures 3.17 d and f). In all treatment schemes, we observed no or very small sub-G1 cell population.
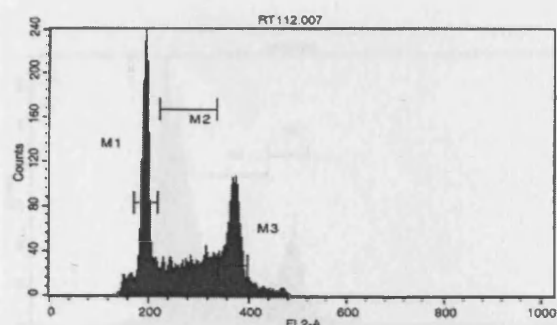
Marker	% Gated
M1	37.80
M2	29.92
M3	32.28

Figure 3.16a – control
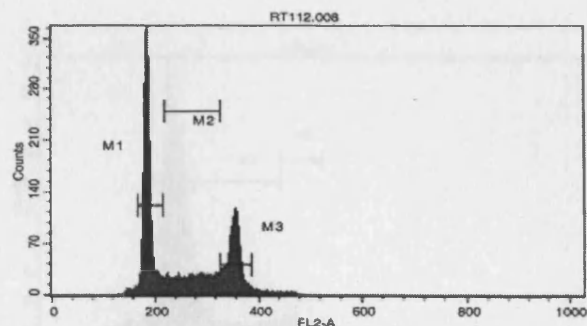
Marker	% Gated
M1	47.19
M2	24.11
M3	28.70

Figure 3.16b – lapatinib
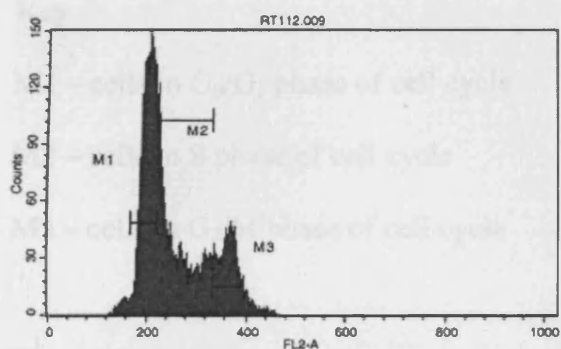
Marker	% Gated
M1	47.96
M2	33.89
M3	18.15

Figure 3.16c – GC
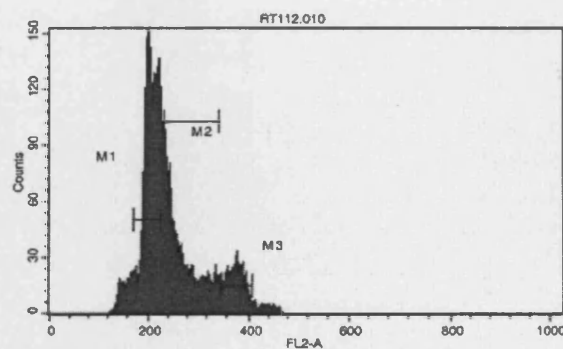
Marker	% Gated
M1	53.31
M2	34.80
M3	11.89

Figure 3.16d – GC and lapatinib

Marker	% Gated
M1	51.78
M2	29.32
M3	18.90

Marker	% Gated
M1	80.24
M2	14.38
M3	5.38
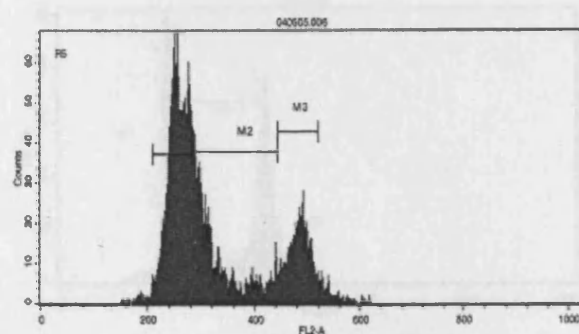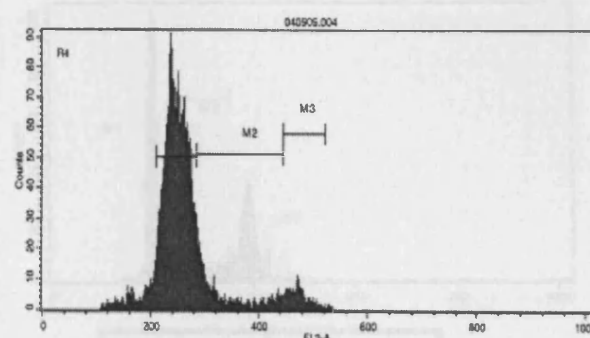
Figure 3.16e – GTC   **Figure 3.16f** – GTC and lapatinib

Key

M1 – cells in G_0/G_1 phase of cell cycle

M2 – cells in S phase of cell cycle

M3 – cells in G_2/M phase of cell cycle

Figure 3.16

FACS analysis to assess the effect of lapatinib and combination chemotherapy on cell cycle in RT112 cells. Cells were seeded in 25 cm^3 flasks and starved in SF medium when 50% confluent. Lapatinib (IC_{50} dose) was added 24 hours later, and IC_{50} doses of combination chemotherapy (GC or GTC) were added a further 24 hours later. FACS analysis was performed 48 hours later, a total of 96 hours after starving cells. The samples were treated as follows: a – control; b – lapatinib; c – GC; d – lapatinib and GC; e – GTC; f –lapatinib and GTC.
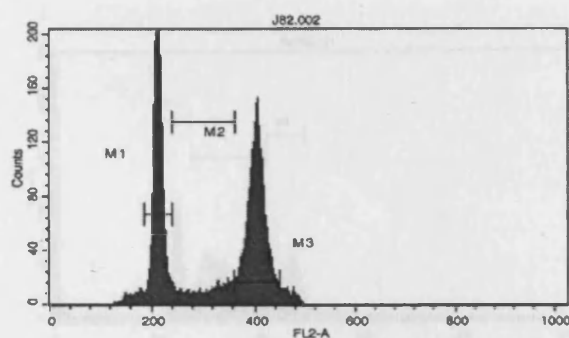
Marker	% Gated
M1	39.32
M2	10.48
M3	50.20

Figure 3.17a – control
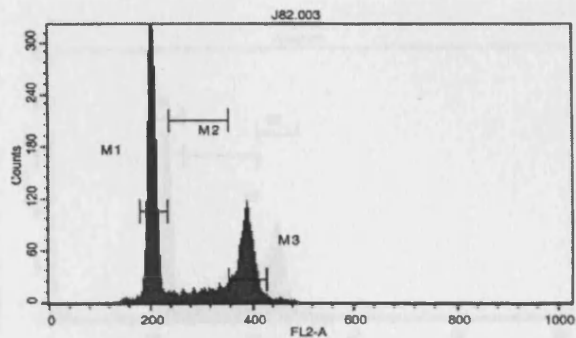
Marker	% Gated
M1	54.91
M2	11.88
M3	33.21

Figure 3.17b – lapatinib
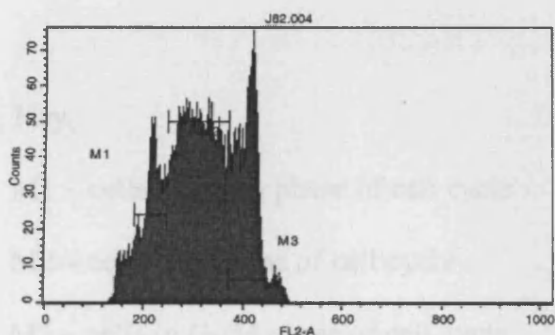
Marker	% Gated
M1	18.86
M2	53.00
M3	28.14

Figure 3.17c – GC
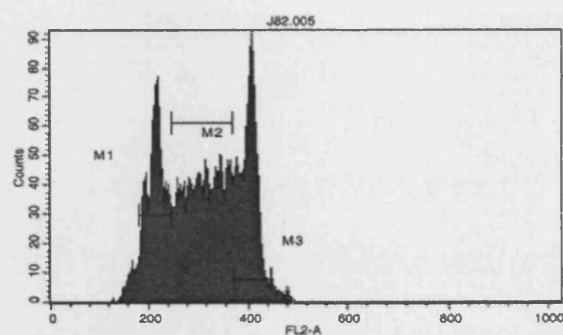
Marker	% Gated
M1	26.69
M2	44.08
M3	29.23

Figure 3.17d – GC and lapatinib
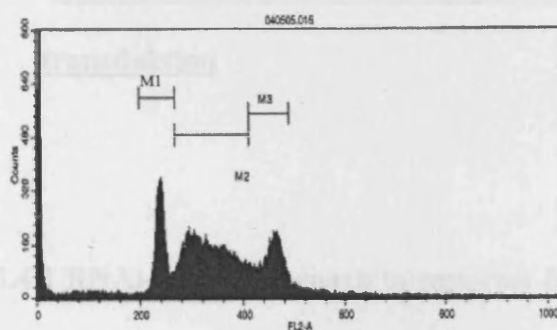
Marker	% Gated
M1	22.13
M2	53.45
M3	24.42
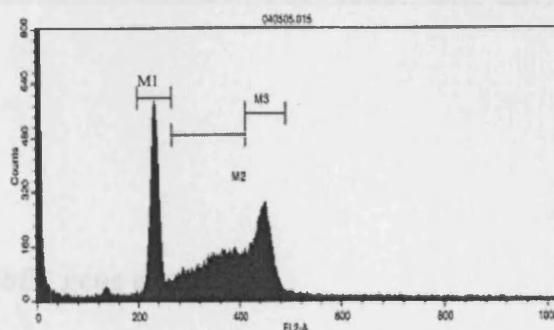
Marker	% Gated
M1	30.73
M2	38.60
M3	30.67

Figure 3.17e – GTC   **Figure 3.17f** – GTC and lapatinib

Key

M1 – cells in G_0/G_1 phase of cell cycle

M2 – cells in S phase of cell cycle

M3 – cells in G_2/M phase of cell cycle

Figure 3.17

FACS analysis to assess the effect of lapatinib and combination chemotherapy on cell cycle in J82 cells. Cells were seeded in 25 cm^3 flasks and starved in SF medium when 50% confluent. Lapatinib (IC$_{50}$ dose) was added 24 hours later, and IC$_{50}$ doses of combination chemotherapy (GC or GTC) were added a further 24 hours later. FACS analysis was performed 48 hours later, a total of 96 hours after starving cells. The samples were treated as follows: a – control; b – lapatinib; c – GC; d – lapatinib and GC; e – GTC; f – lapatinib and GTC.

150

3.4 Genetic approaches to down-regulation of ErbB1 expression and signal transduction

3.4.1 RNAi-based approach to suppress *ErbB1* gene expression

3.4.1.1 Preparation of plasmid DNA samples for transfection

Control vector and a pSuper RNAi vector specific for plasmid expressing short hairpin *ErbB1,* pSuper-ErbB1, were propagated in E.coli using standard transformation and purification protocols as described in Materials and Methods.

To confirm the identity of purified plasmids, samples of plasmid DNA were digested by restriction enzymes, run on an agarose gel in the presence of Ethidium Bromide (EtBr), and visualised in UV light. Results showed that the digests corresponded to plasmid DNA maps. As expected, double HindIII/EcoRI digestions excised 1 kb and 0.3 kb fragments from the wild type vector and pSuper-ErbB1 respectively (figure 3.18). These plasmids were therefore applicable for transfection.
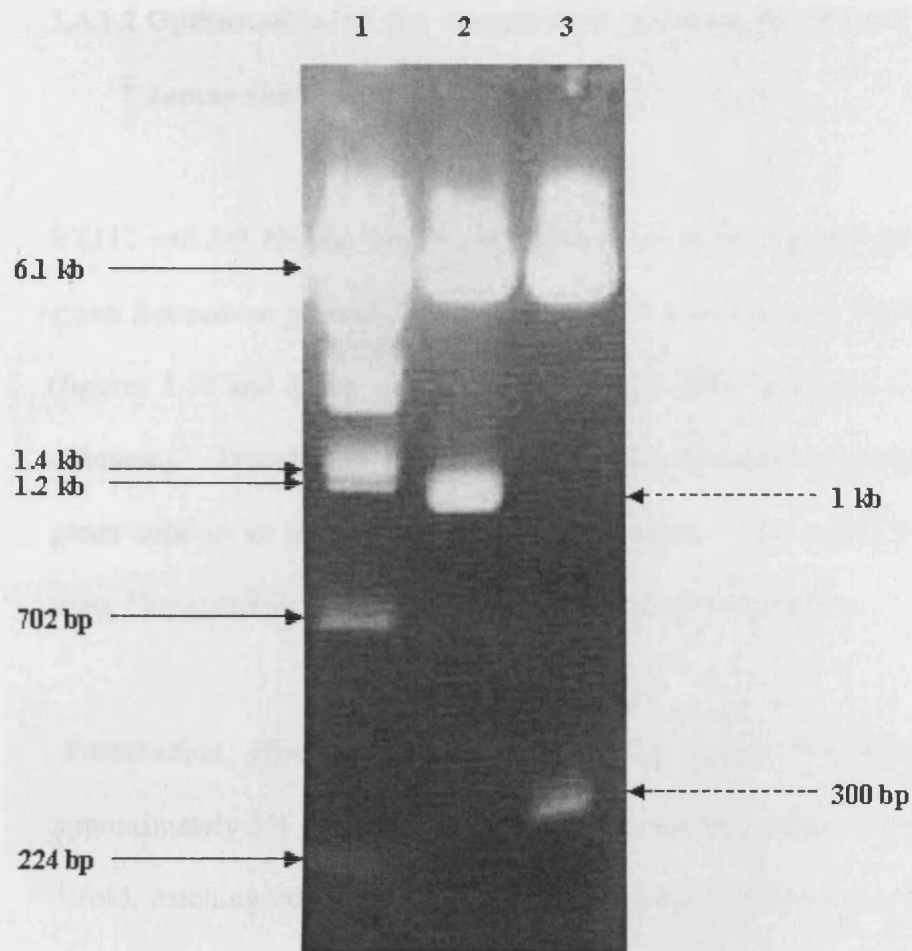
Key

1. DNA ladder

2. Plasmid Control

3. Plasmid pSuper-ErbB1

Figure 3.18

Restriction analysis of control vector and pSuper-ErbB1 plasmid. Samples of plasmid DNA (control vector and pSuper-ErbB1) were isolated, digested by EcoR1 and HindIII restriction enzymes and resolved in an agarose gel, along with a 100 bp DNA ladder (120 V constant, 50 mA, for 30 min). To visualise DNA fragments, the gel was exposed to UV light.

3.4.1.2 Optimisation of the transfection protocol for RT112 and J82 bladder cancer cell lines

RT112 and J82 bladder cancer cells were transfected with pEGFP plasmid, encoding green fluorescent protein, alone, or in a mixture with pSuper-ErbB1 or control vector (figures 3.19 and 3.20). Application of pEGFP alone was used to assess transfection efficiency. Transfected cells expressing green fluorescent protein were detected as green cells in an inverted fluorescent microscope. Two transfection protocols were used, GeneJammer (chemical transfection) and electroporation.

Transfection efficiency of RT112 cells using the GeneJammer protocol was approximately 5% (figure 3.19 a). However, electroporation increased the efficiency 4-fold, reaching 20% (figure 3.19 b). Transfection efficiency of J82 cells was much higher than that in RT112 cells, with more than 50% efficiency, independent of the protocol used (figure 3.20 a and b).

In parallel, cells were transfected with the mixtures of pEGFP and pSuper-ErbB1 or control vector by different methods. Again, efficiency of transfection of RT112 cells using GeneJammer protocol was low (figure 3.19 c and d). Results were to some extent improved with electroporation (approximately 10% transfection efficiencies for the control plasmid, and 7.5% for the pSuper-ErbB1plasmid [figures 3.19 e and f]). As the transfection efficiency in J82 cells was high independent of the protocol used, but possibly marginally higher using the GeneJammer protocol, GeneJammer reagent alone was chosen for transfection of plasmids in J82 cells. Transfection efficiencies were again greater than 50% (figures 3.20 c and d).
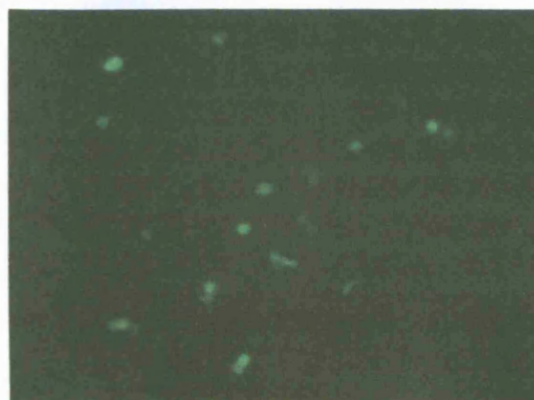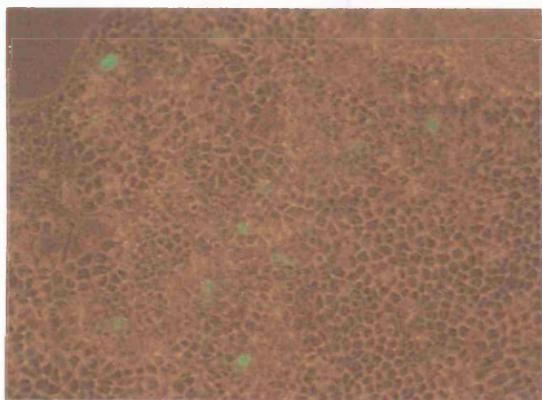
Figure 3.19a – pEGFP transfection, GeneJammer
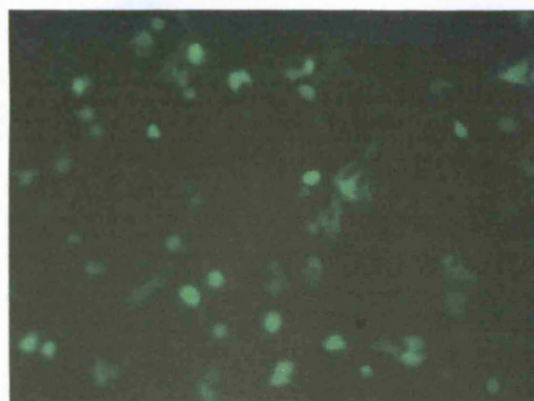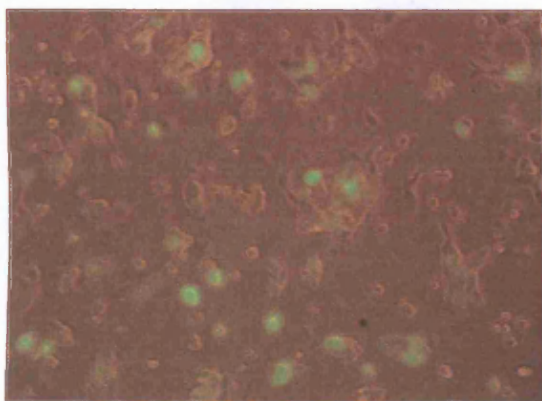
Figure 3.19b – pEGFP transfection, electroporation

Figure 3.19c – Transfection with the mixture of control plasmid and pEGFP, GeneJammer
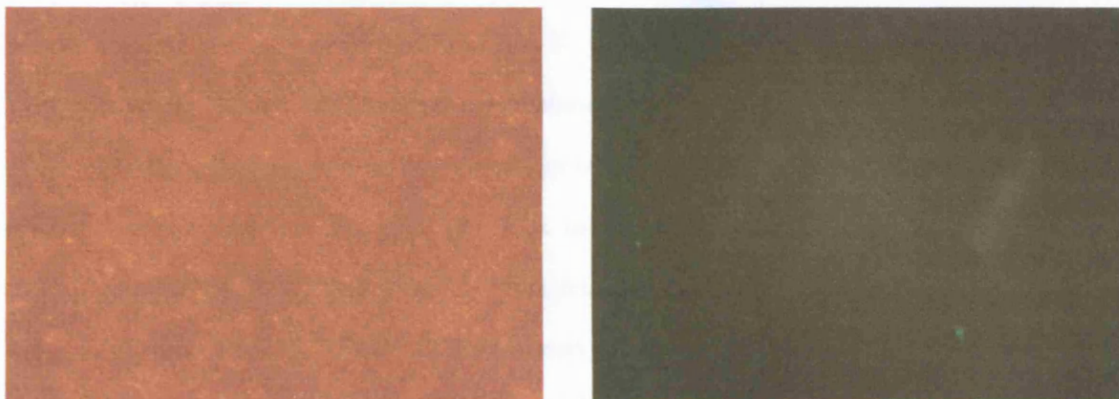
Figure 3.19d – Transfection with the mixture of pSuper-ErbB1 and pEGFP, GeneJammer
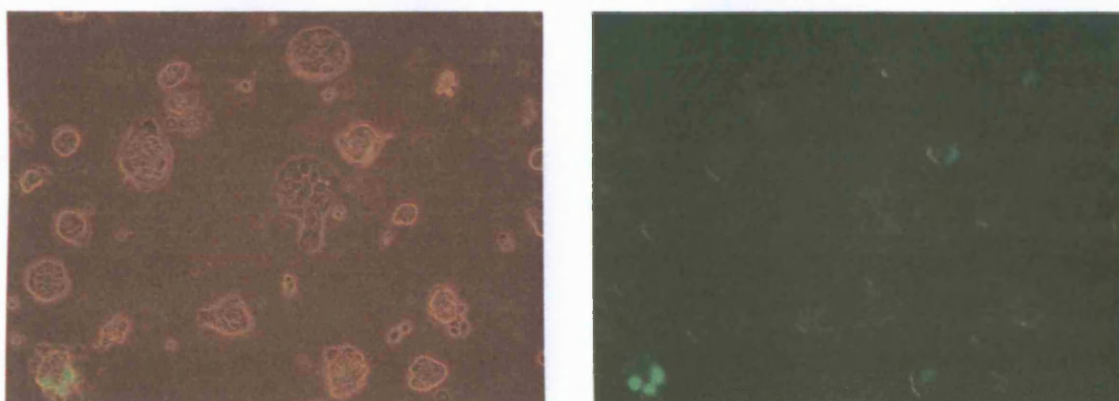
Figure 3.19e – Transfection with the mixture of control plasmid and pEGFP, electroporation
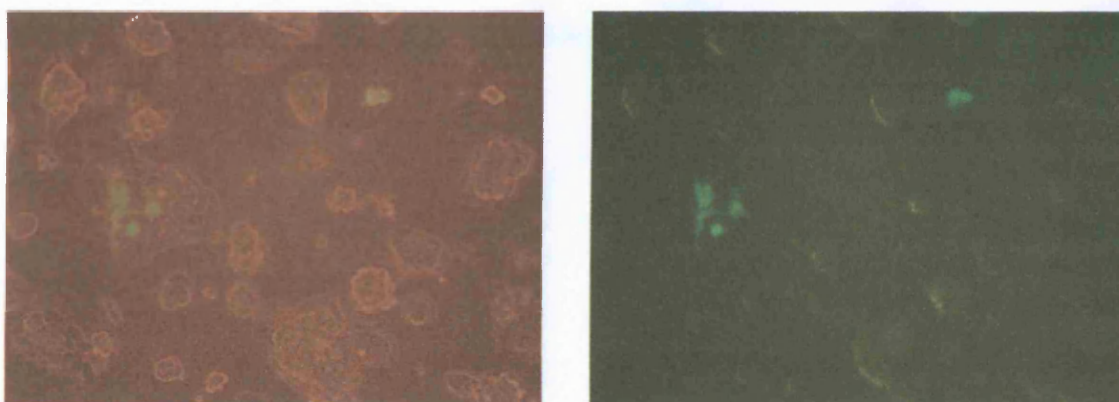
Figure 3.19f – Transfection with the mixture of pSuper-ErbB1 and pEGFP, electroporation

Figure 3.19

Images showing transfection efficiencies of RT112 cells using chemical transfection (GeneJammer) or electroporation. The left hand pictures are combined images of live cells in phase contrast and UV light, whilst the right hand pictures are UV images only. Cells after transfection with either pEGFP or with mixture of plasmid DNA were grown in petri dishes. Transfections were as follows: a – transfection with pEGFP (GeneJammer); b – transfection with pEGFP (electroporation); c – mixture of the control plasmid and pEGFP (GeneJammer); d – mixture of pSuper-ErbB1 and pEGFP (GeneJammer); e – mixture of control plasmid and pEGFP (electroporation); f – mixture of pSuper-ErbB1 and pEGFP (electroporation).
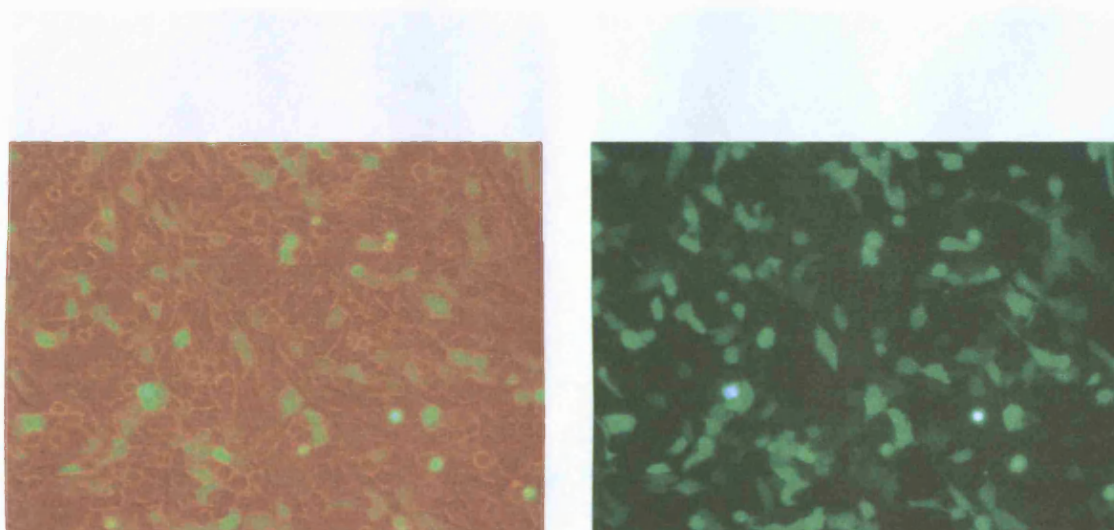
Figure 3.20a – pEGFP transfection, GeneJammer
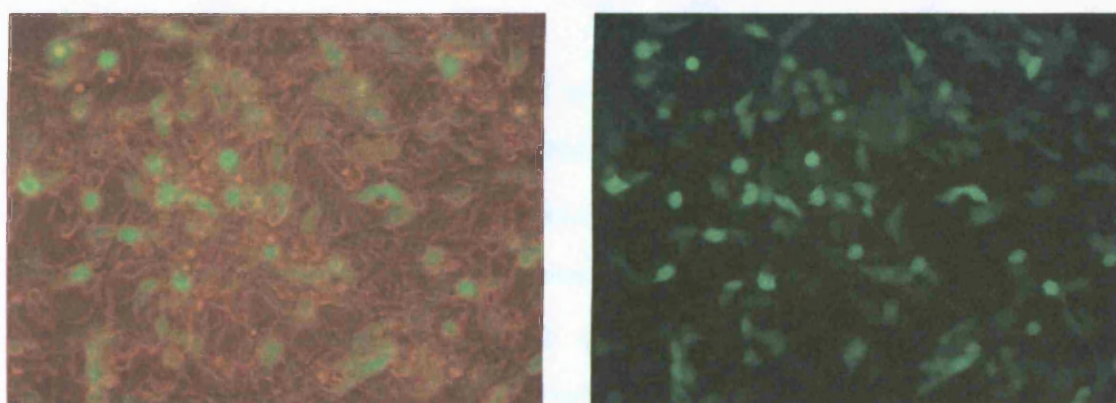
Figure 3.20b – pEGFP transfection, electroporation
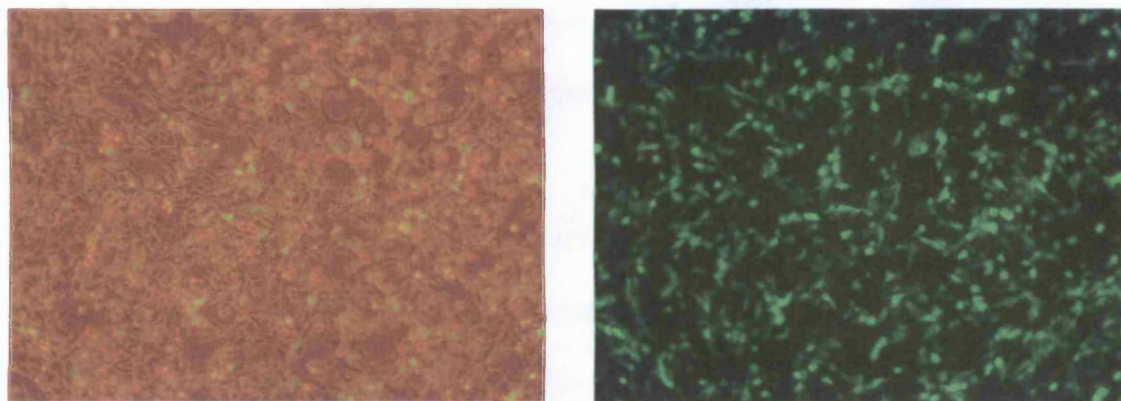
Figure 3.20c – Transfection with the mixture of control plasmid and pEGFP, GeneJammer
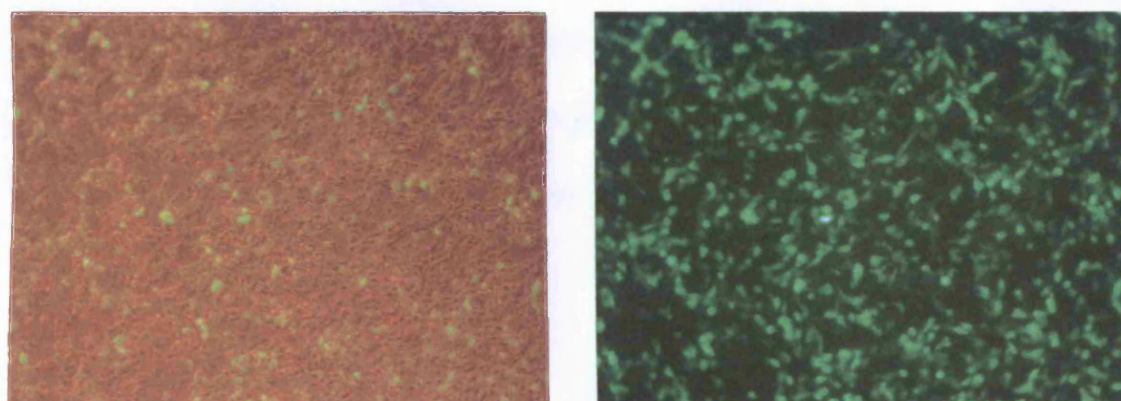
Figure 3.20d – Transfection with the mixture of pSuper-ErbB1 and pEGFP, GeneJammer

Figure 3.20

Images showing transfection efficiencies of J82 cells using chemical transfection (GeneJammer) or electroporation. The left hand pictures are combined images of live cells in phase contrast and UV light, whilst the right hand pictures are UV images only. Cells after transfection with either pEGFP or mixture of plasmids were grown in petri dishes. Transfections were as follows: a – pEGFP (GeneJammer); b – pEGFP (electroporation); c – mixture of control plasmid and pEGFP (GeneJammer); d – mixture of pSuper-ErbB1 and pEGFP (GeneJammer).

157

3.4.1.3 Assessment of downregulation of ErbB1 expression following transfection of cells with pSuper-ErbB1

As described, after assessing transfection efficiencies in the cell lines by both chemical transfection and electroporation, it was decided to use electroporation in RT112 cells, and the GeneJammer system in J82 cells, for further experiments. Cells were transfected with both control and pSuper-ErbB1 plasmid, and once cells reached around 80-90% confluence they were lysed for western blot analysis. Resultant membranes were stained for ErbB1. In both cell lines, no evidence of downregulation of ErbB1 was seen with the pSuper-ErbB1 plasmid (figure 3.21). This approach of potential downregulation of the receptor using plasmid containing short hairpin *ErbB1* was therefore not pursued further.
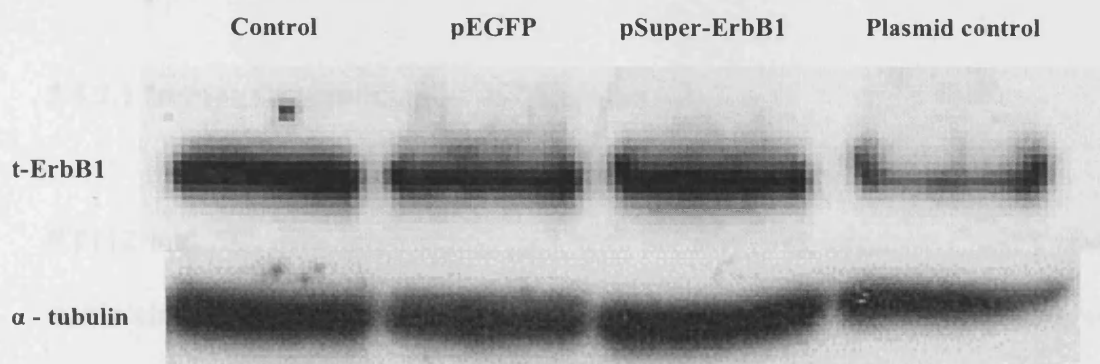
Figure 3.12a - RT112 cells
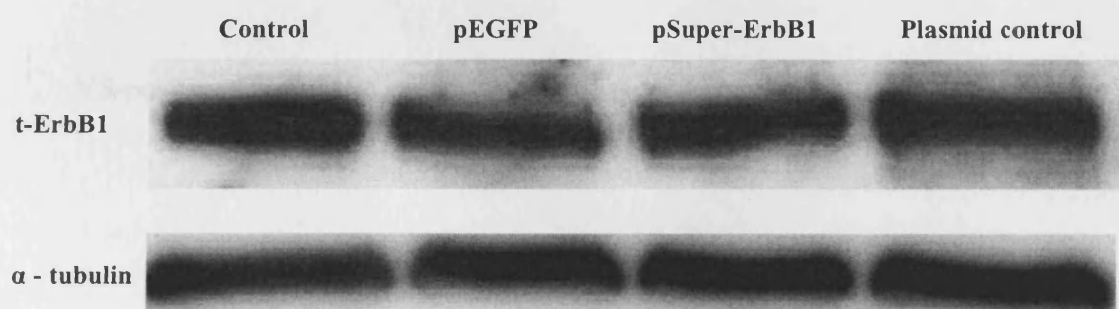
Figure 3.21b – J82 cells

Figure 3.21

Western blots to investigate the downregulation of ErbB1 expression by pSuper-ErbB1. RT112 (a) and

J82 (b) cells were transfected with plasmids, control and pSuper-ErbB1, and grown until around 80 –

90% confluence. Lysates were made, and total amount of the proteins were quantified by protein assay.

25 μg protein of each lysate was resolved by SDS-PAGE and Western blot analysis was performed.

Detection of α-tubulin was used as a loading control.

3.4.2   Dominant-negative approach to suppression of ErbB1 function

3.4.2.1 Immunocytostaining of stable clones

RT112 and J82 cells were transfected with the dominant-negative CD533 plasmid, stable clones were selected, and these were grown and stained for expression of the V5-epitope by immunocytostaining as described in Materials and Methods.

Cells that expressed the V5-epitope stained brown, and those negative for V5 did not show any staining when analysed under the microscope (figure 3.22).

V5-positive clones of each cell line were chosen for further analysis.
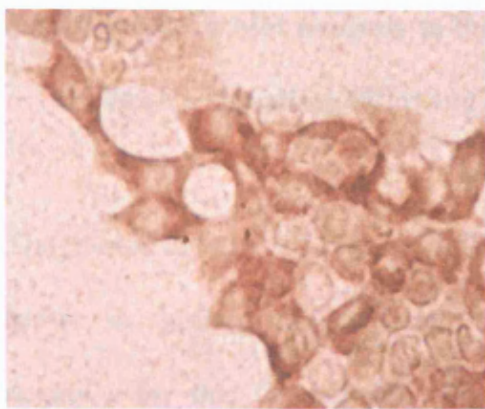
Figure 3.22a – RT112 V5 positive   **Figure 3.22b** – RT112 V5 negative
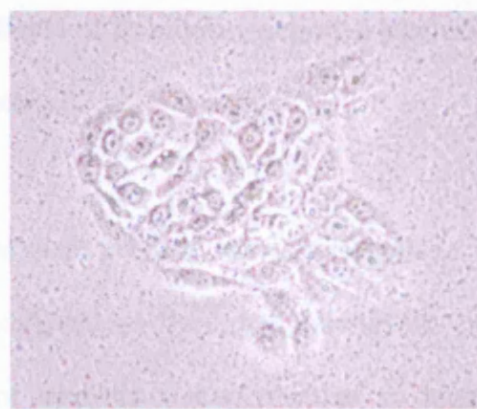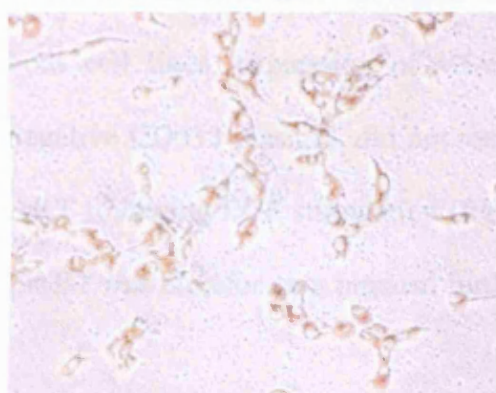
Figure 3.22c – J82 V5 positive   **Figure 3.22d** – J82 V5 negative
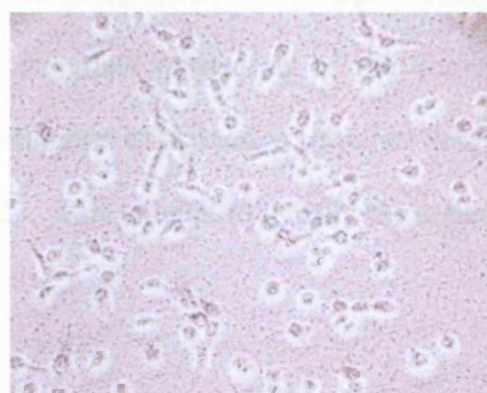
Figure 3.22

Images of cells as visualised under the light microscope after immunocytostaining for the V5-epitope. RT112 and J82 cells were transfected with the dominant-negative CD533 plasmid, and stable clones were isolated. Clones were grown in petri dishes until around 50% confluence and immunocytostaining to look for expression of the V5-epitope was performed. Cells were analysed under the microscope. The images represent the following: a – RT112 cells positive for V5; b –RT112 cells negative for V5; c – J82 cells positive for V5; d – J82 cells negative for V5.

161

3.4.2.2 Western blot analysis to look for effects of dominant-negative plasmid on ErbB1 signalling following transfection

The clones of both RT112 and J82 cells that were positive for the V5-epitope were grown in flasks, stimulated with EGF, and lysed as described, alongside clones negative for the V5-epitope. Western blot analysis was performed to look for expression of the V5-epitope, ErbB1 and AKT, along with p-ErbB1 and p-AKT to assess the effect of EGF on signal transduction in transfected cells (figure 3.23). In both cell lines, expression of V5-epitope, and thus expression of the dominant-negative CD533 plasmid, did not result in inhibition of activation of either ErbB1 or AKT following EGF stimulation (figure 3.23). This attempt to modify the actions of ErbB1 was therefore not pursued further.
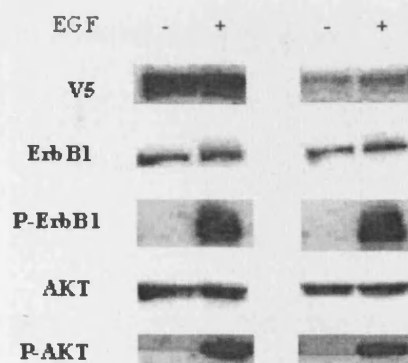
Figure 3.23a – RT112 cells
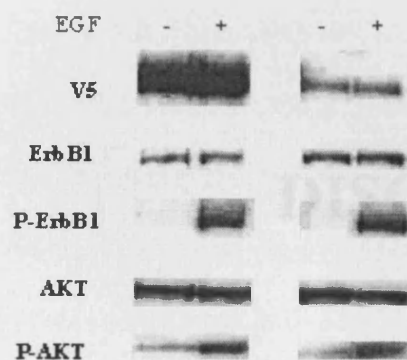
Figure 3.23b – J82 cells

Figure 3.23

Western blots to investigate the effect of expression of the dominant-negative CD533 plasmid on ErbB1 receptor signal transduction. RT112 (a) and J82 (b) cells were transfected with plasmids, and clones expressing the V5-epitope (first lane), and therefore the CD533 plasmid, were grown until around 50% confluence, alongside clones negative for the V5-epitope (second lane). Cells were starved for 24 hours prior to either stimulation with 100 ng/ml EGF for five minutes, or no treatment. Lysates were made, and total amount of the proteins were quantified by protein assay. 25 µg protein of each lysate was resolved by SDS-PAGE and Western blot analysis was performed. Detection of α-tubulin was used as a loading control.

CHAPTER 4

DISCUSSION

4.1 Tyrosine kinase inhibitors as adjuncts to chemotherapy in bladder cancer

Metastatic transitional cell carcinoma (TCC) of the bladder has few treatment options, with systemic chemotherapy being the mainstay of management. The gold standard regimen is a combination of four agents (methotrexate, vinblastine, adriamycin [doxorubicin] and cisplatin, or MVAC), which gives a median survival of just one year [49, 50], and only to those patients who are both eligible for treatment and can tolerate the significant side-effects and comorbidity it produces. More recently, the slightly more tolerable combination of gemcitabine and cisplatin (GC) has been introduced after demonstrating similar efficacy as MVAC [54]. A significant proportion of patients are still unable to receive this regimen however, as patients with metastatic bladder cancer tend to be in the older age group with significant medical problems both related, such as renal impairment, and unrelated to their disease. This group of patients therefore present an important clinical dilemma, and the issues of both poor survival and toxicity with current chemotherapeutic regimens need to be addressed. A large phase III trial is underway, looking at introducing paclitaxel into the GC combination, following promising results from phase II trials where overall survival was improved by up to eight months when compared to standard MVAC [57 - 59]. However, much interest currently centres on developing novel therapies against molecular targets, such as small molecule tyrosine kinase inhibitors (TKIs) against the ErbB group of receptors. The combination of TKIs with current chemotherapeutic regimens has not been studied to date in bladder cancer, although theoretically they could have the potential to either increase survival, decrease chemotherapy dose and therefore toxicity, or both. Results arising from the current *in vitro* study are

promising, and support the need for clinical studies of the dual ErbB1/ErbB2 TKI, lapatinib, in patients with bladder cancer.

4.2 Molecular characteristics of bladder cancer cell lines

Initially, a panel of 6 bladder cancer cell lines was studied using Western blot analyses, to determine their expression of receptors and downstream signalling proteins, and the response of these cell lines to stimulation with ErbB ligands. The bladder cancer cell lines were all from the American Tissue Culture Collection, and represented a range of invasive capacities [197]. Two of the cell lines, RT112 and RT4 cells, were known to be low or intermediate grade (G1/2), whereas the other four – T24, UMUC3, J82 and HT1376 cells – were documented as high grade (G3), poorly differentiated cell lines. From initial experiments investigating the expression of specific molecular targets including ErbB receptors, it was possible to clearly split the cell lines into two separate groups. These groups were also morphologically distinct. The first group consisted of RT112, RT4 and HT1376 cells, and were epithelial in morphology. The second group, J82, UMUC3 and T24 cells, were mesenchymal in morphology. Supporting this division, it was found that the epithelial cells expressed E-cadherin, whereas the mesenchymal cells did not. E-cadherin is an epithelial transmembrane glycoprotein involved in cell-cell adhesion, and is lost in epithelial-mesenchymal transition, a phenomenon that occurs in the malignant progression of carcinoma [198].

Beyond these morphological differences, it was also apparent that there was a clear distinction in levels of expression of ErbB receptors and their downstream signalling proteins. The epithelial cells expressed higher levels of ErbB1 and ErbB2 receptors, although both were expressed throughout, and ErbB3 expression appeared uniform across all cell lines. All three receptors have been implicated as poor prognostic factors in bladder cancer, though contradictory reports exist regarding the importance of ErbB2 and ErbB3 expression [94, 97 - 101, 103]. The other distinction of interest between the two groups is the level of AKT expression, which was higher in the mesenchymal cells. This is of interest as data suggests that the PI3K/AKT pathway is important in bladder cancer cell lines. However, of greater interest than expression of total levels of proteins, is the expression of phosphorylated, or activated, levels of the receptors and signalling proteins. Here it is important to know both levels of constitutively activated proteins, and their ability to be activated by ligands of the ErbB receptors, in order to assess their effect on cell behaviour.

Therefore, the next experiment looked at the effect of stimulating cells using the ErbB1 ligand, epidermal growth factor (EGF). As expected, ErbB1 tyrosine residues were activated, apparently in proportion to the total levels of the receptor. A similar trend was seen in activation of ErbB2, but with only very low levels of activation detectable in the mesenchymal cell lines. There was some variation of activation of ErbB3 receptors however. There were easily detectable levels of constitutive activation of ErbB3 in all cell lines, but p-ErbB3 levels actually decreased after stimulation with EGF in all of the mesenchymal cells, and also in HT1376 cells. This could possibly be explained by displacement of ErbB3 from heterodimers with ErbB2,

which may preferentially form heterodimers with ErbB1 in these cell lines in the presence of such high levels of EGF. In contrast, p-ErbB3 levels were increased in RT112 cells after exposure to EGF. In this cell line, there was a very strong p-ErbB1 signal after stimulation and so more activated ErbB1 may be available to heterodimerise with ErbB3 as well as with its preferred partner, ErbB2. This represents evidence that there is cross-talk between ErbB1, ErbB2 and ErbB3, probably via heterodimerisation, as EGF is able to modulate phosphorylation levels not only in ErbB1, but also in the other two receptors.

The downstream signalling proteins AKT and MAPK behaved in similar ways after EGF stimulation of the cells. Stimulation led to increases in phosphorylated forms of the proteins in all mesenchymal cell lines, and also in RT112 cells, showing that these pathways are driven by the ErbB receptors. There may however also be other driving forces for these pathways, as there was significant constitutive activation of MAPK throughout all cell lines, and of AKT in J82 and UMUC3 cells. This latter observation is most likely explained by the reduced levels of the tumour suppressor gene product PTEN in these two cell lines, and is potentially of importance for two main reasons. Firstly, mutation of *PTEN* is seen in up to 30% of bladder cancer cells [107, 108], and secondly, constitutive activation of AKT has been linked to chemoresistance in other cancers, including prostate and NSCLC cell lines [199, 200]. The STAT proteins were constitutively active, and unaffected by EGF stimulation. This shows that they are clearly not driven by the ErbB receptors in these bladder cancer cell lines. Overall, EGF treatment induced receptor phosphorylation in all cell lines analysed. However, while two epithelial cell lines, RT4 and HT1376 appeared to

be incompetent in transducing signals to the downstream targets, in other cells, p42/44MAPK and AKT pathways were activated in response to EGF.

It was decided that further experiments investigating the ErbB receptors and signalling pathways should be performed on cell lines representative of each group. J82 was chosen to represent the mesenchymal cells, especially in view of it being one of the cell lines with constitutive activation of AKT. RT112 cells represented the epithelial cells, as the ErbB receptors in this cell line appear to drive the downstream pathways more dominantly than in the other epithelial cell lines.

The effect of the ErbB3 ligand heregulin-1β (HRG1β) on the receptors and signalling pathways in the two cell lines was studied. The reasons for this were two-fold. Firstly, ErbB3 was expressed in all bladder cancer cell lines analysed and it was felt important to analyse further its role in cell signalling, especially in view of the fact that ErbB2 is the preferential partner for ErbB3 heterodimerisation, and ErbB3 is only activated in the context of heterodimers due to its lack of intrinsic tyrosine kinase activity [77]. Secondly, the expression of HRG1β is associated with poor survival in patients with bladder cancer [103].

HRG1β stimulated phosphorylation of ErbB1, ErbB2 and ErbB3 in RT112 cells, along with both AKT and p42/44 MAPK. This again represents evidence of cross-talk between the three receptors in response to stimulation by different ligands. In J82 cells, only activation of ErbB3 by its ligand could be detected, with no activation of ErbB1 and ErbB2 found, however it again induced an increase in activation of the two

downstream signalling proteins, showing further the importance of ErbB3 in cell signalling pathways.

4.3 Effect of lapatinib on cell signalling pathways

Next, experiments were undertaken to investigate the ability of lapatinib to inhibit the EGF- and HRG1β-induced activation of the ErbB receptors and downstream signalling pathways. For this it was necessary to calculate the IC_{50} concentration of lapatinib in both RT112 and J82 cells, using the MTT assay. The IC_{50} values of the three chemotherapeutic agents, cisplatin, gemcitabine and paclitaxel, were also calculated in a similar way, for use in later experiments. The resultant IC_{50} values were consistent with those for all the agents throughout the literature. Both this fact, and the tight error bars obtained for all of these experiments, indicate the effectiveness and reproducibility of the MTT assay when used with both cell lines throughout this study. Also, the ability of lapatinib to inhibit cell growth with IC_{50} values around 1 μmol is consistent with ErbB-dependent cell proliferation in bladder cancer cells, even though there are marked differences in levels of ErbB1 and ErbB2 expression between the two cell lines used here. Thus it is possible that co-expression of ErbB3 is important in predicting response to lapatinib in bladder cancer cell lines, as ErbB3 levels were similar in the two cell lines. However, previous observations in two EGFR-overexpressing breast cancer cell lines are noted which failed to show any correlation between total ErbB3 expression and response to lapatinib [201].

Incubation of cells with lapatinib at its IC_{50} dose prior to addition of either ligand caused inhibition of ligand-induced activation of the ErbB receptors, AKT and p42/44 MAPK. It was clear that lapatinib acts at numerous tyrosine residues on ErbB1, as all five p-Tyrosine residues activated with EGF were inhibited by lapatinib. In both sets of experiments, phosphorylated levels of all proteins were reduced down towards basal levels only by lapatinib, and were not completely inhibited, an effect that was particularly evident for AKT and p42/44 MAPK. This again suggests that there are alternative signals feeding into these pathways, the significance of which is unclear at this stage. The effect of negating ligand-induced activation of signalling pathways is important however, particularly in the PI3K/AKT pathway, where its inhibition has been shown to drastically reduce the invasive capacity of bladder cancer cell lines [106].

The similarity in results between the experiments using EGF as the ligand, and those using HRG1β, demonstrate the importance of the use of a dual tyrosine kinase inhibitor of ErbB1 and ErbB2. Whilst inhibitors of ErbB1 would be able to affect all heterodimers involving ErbB1, the important heterodimer of ErbB2-ErbB3 would not be affected. Not only is ErbB2 apparently the preferential partner for ErbB3 [80], but also the ErbB2-ErbB3 heterodimer has been shown to be a potent activator of the AKT pathway [202], and it is potentially the most potent heterodimer in terms of cell growth and transformation [81]. A previous study confirms the ability of lapatinib to inhibit the ErbB2-ErbB3 heterodimer [145]. A truncated ErbB2 receptor ($p95^{ErbB2}$), overexpressed in some advanced breast cancers, was stimulated by HRG but not EGF. $p95^{ErbB2}$ formed heterodimers with ErbB3 only (unlike full-length ErbB2, which

heterodimerises with both ErbB1 and ErbB3), and was inhibited by lapatinib, but not by the ErbB2 monoclonal antibody, trastuzumab. This evidence is backed up by the present study, and the ability of lapatinib to inhibit HRG1β-induced activation of signalling pathways in both cell lines, even in J82 cells where little receptor activation could be detected on Western blotting, is an important finding. Perhaps mutated, or truncated, receptors that are not detected by conventional antibodies also drive downstream signalling pathways. If this is the case, it is important that inhibitors are effective on these receptors. This appears to be true of lapatinib, as suggested by the results in this study, and also of gefitinib, reports of which showed responsiveness of specific ErbB1 mutations to the ErbB1 TKI [135, 136].

The next step with this body of work was to investigate the effect of chemotherapeutic agents on the signalling pathways, to elucidate whether such effects may have a bearing on the clinical effectiveness of chemotherapy. As previously discussed, all three chemotherapy agents in this study have individually shown stimulatory effects on the ErbB signalling pathways [172 - 174]. These studies looked only at the late effects of chemotherapy on cell lines, four or more hours after addition of the agents. In the present study, both early (10 minutes of incubation) and late (20 hours of incubation) timepoints after addition of a combination of gemcitabine, paclitaxel and cisplatin (GTC) were studied, along with the effect of inhibition by lapatinib. Mild early (10 minutes) activation of ErbB1 by GTC was demonstrated using immunoprecipitation in both cell lines, along with a similar activation of ErbB3 in J82 cells. This was translated to a corresponding activation of AKT (Ser478 residue), along with late activation of AKT at 20 hours in both cell lines. Prior treatment with lapatinib showed its ability to inhibit the activation of ErbB1 along with the early

activation of AKT in both cell lines, and the late activation of AKT in RT112 cells. However, late activation of AKT in J82 cells was not inhibited, suggesting a mode of activation other than via the ErbB receptors at this timepoint. In view of the previous reports linking constitutive activation of AKT to chemoresistance, it was of interest whether later experiments would show a differential effect of lapatinib and chemotherapy on cell viability between the two cell lines.

The immunoprecipitation experiments showed a further important finding. It was clear that lapatinib completely inhibited p-ErbB1 in both cell lines, and p-ErbB2 in RT112 cells (p-ErbB2 could not be detected in J82 cells), to undetectable levels. This was evident in both unstimulated and stimulated cells. The effect was not seen using Western blotting alone, presumably due to non-specific staining of these membranes. This provides evidence of the specificity of lapatinib for both receptors, and its ability to inhibit all causes of their phosphorylation.

Thus a number of conclusions have been drawn from this group of experiments. It is apparent that lapatinib is a specific TKI against both ErbB1 and ErbB2, and that via heterodimerisation it is also effective at inhibiting ErbB3. It also inhibits ligand- and chemotherapy-induced activation of the important PI3K/AKT downstream signalling pathway. The potential clinical impact of these findings, particularly the combination of lapatinib and chemotherapy, was investigated further using the MTT cellular proliferation assay.

4.4 Effect of lapatinib and chemotherapy on cell viability

The initial experiments investigating the behaviour of all cell lines during the MTT assay were in preparation for those looking at the effect of lapatinib and chemotherapy on cell viability. As well as assisting in decision making about cell numbers to be seeded and optimal growing conditions, it was shown that the MTT assay was reliable and highly reproducible, with narrow error bars throughout. Of interest, the levels of mitochondrial dehydrogenase activity were widely variable between cell lines, and this was not related to morphological group. It was decided to seed 1000 cells/well, and to grow them in medium with 1% serum over a period of 96 hours for subsequent experiments. This was based on data that showed that these conditions should result in adequate numbers of cells to produce sufficient absorbance levels without leading to cell death through excessive numbers of cells. The ideal would have been to use serum-free medium for all assays in order to minimise the presence of exogenous growth factors, but in these experiments such conditions led to very little cell growth. RT112 and J82 cells were taken forward for further experiments as previously, as representatives of the two morphologically distinct groups of cells.

As previously stated, the IC_{50} values for lapatinib and the three chemotherapeutic agents as calculated from the MTT assay were consistent with those in the literature. This, and once again the narrow error bars in the assays, confirms that the MTT assay is reliable for evaluating the effect of chemotherapeutic agents on cell viability. Of interest from this group of assays, increasing the dose of the drug led to cell viability levels falling towards zero, except with gemcitabine in both cell lines. Here cell

viability levels reached a plateau at 40% cell viability in RT112 cells, and at 20% cell viability in J82 cells, and increasing the dose of gemcitabine above those shown in the graphs did not alter this. The reasons for this are not clear, and cannot be explained by its proposed mechanism of action as a pyrimidine analogue.

The assays to assess the optimal sequences of application of lapatinib and chemotherapeutic agents showed a general trend in both cell lines of addition of lapatinib decreasing cell viability when compared to chemotherapy alone, either single-agent or in combination. The chemotherapy combinations of GC and GTC were chosen for these assays, as opposed to any other combinations, as GC represents the combination currently favoured for clinical use in the UK [54], and the combination currently being studied in a phase III trial [60]. Overall, the optimal sequence of application of the drugs was lapatinib before and during chemotherapy, and lapatinib concomitant with chemotherapy was generally better that lapatinib after chemotherapy, with only a few minor exceptions to these rules. Statistical significance was proven, with highly significant p-values throughout. There was a clear effect of lapatinib even when the initial response to chemotherapy was marked. In J82 cells, GTC reduced cell viability to 30% even at 1/8 IC_{50} of GTC, but lapatinib was able to reduce this cell viability further to 20% when added prior to chemotherapy (p<0.001).

Interactions plots were performed to see whether the effect of lapatinib added before and during chemotherapy was additive or synergistic. In these plots, parallel lines show an additive interaction, whereas converging lines show a synergistic interaction. Lapatinib showed synergistic interactions with all single-agent and combinations of

chemotherapy agents in both cell lines when added before and during, apart from when combined with single-agent cisplatin in J82 cells, where an additive interaction was found.

However what is the mode of interaction leading to this sequence dependent synergy? Clearly it is not related to the mode of action of the chemotherapeutic agent, as adding lapatinib before and during chemotherapy was consistently the optimal sequence across all combinations in both cell lines. Data from other tumour types have shown differing conclusions as to the optimal sequencing of chemotherapy and TKIs. In head and neck squamous cell carcinoma cell lines, gefitinib was optimal before and during cisplatin/5FU [153], and in breast cancer cell lines gefitinib was optimal before paclitaxel [203]. In contrast, gefitinib after chemotherapy was the optimal sequence in colon cancer cell lines [154, 155]. This may suggest that sequencing is actually dependent on tumour type, rather than drug-dependent. Therefore there is an argument for suggesting the need to test scheduling in pre-clinical models prior to performing clinical trials in each tumour system. This need is evident when considering the lack of benefit of gefitinib or erlotinib combined with chemotherapy, over chemotherapy alone, in terms of overall survival in advanced NSCLC in the INTACT, TALENT and TRIBUTE phase III trials [157 - 160].

Some clues as to the reason why lapatinib before and during chemotherapy is the best sequence come from the Western blot and immunoprecipitation data in this study. Although there has previously been a link between constitutive activation of AKT and chemoresistance, J82 cells, which have easily detectable levels of constitutive activation of AKT, were very sensitive to the GTC combination. However, even in

this combination, lapatinib before and during chemotherapy enhanced the effects of chemotherapy. Lapatinib inhibited the early peak of AKT activation caused by chemotherapy in both cell lines, and the early peak of ErbB1 activation. Thus it may be that it is this early inhibition that is important in bladder cancer cell lines, especially in view of the fact that lapatinib before and during chemotherapy shows a synergistic interaction.

A further important finding from this group of experiments is the apparent dose-sparing effect of lapatinib. Lapatinib was able to reduce the dose of chemotherapy to 1/8 IC_{50} whilst achieving the same or lower levels of cell viability as with chemotherapy alone at its full IC_{50} dose. This finding was true for all sequences in some chemotherapy combinations, but was consistently true with lapatinib before and during chemotherapy. The only exception was with paclitaxel in RT112 cells, where the dose could only be reduced to 1/2 IC_{50}. This ability to dose-spare chemotherapy when combined with lapatinib has important clinical implications. This would lead to a decrease in the toxicity caused by chemotherapy, as lapatinib has a relatively minor side effects profile [149, 150]. Therefore, hopefully more patients would be eligible for treatment that could prolong their survival time, and improve the quality of life of those already able to receive chemotherapy.

Having shown the sequence-dependent synergy and dose-sparing effects of lapatinib in combination with chemotherapy, the next step was to assess whether this effect was cystostatic or cytotoxic.

4.5 Effects of lapatinib and chemotherapy on cell survival and cell cycle

Two different apoptosis assays were used to assess the effects of lapatinib and chemotherapeutic agents on the two cell lines. Initially, the Mitocapture™ apoptosis assay kit was used, which relies upon the changes in mitochondrial membrane potential seen in early apoptosis. Apoptotic cells fluoresce green, and viable cells red. However, in spite of modifying the assay after communication with the manufacturers, both treated and untreated cells exhibited both green and red fluorescence, rendering the results uninterpretable. The reasons for this apparent failure of the assay were unclear, with a possible explanation being alterations in the mitochondrial membrane during the fixing or other stages of the assay. Another explanation may be that the bladder cancer cell lines in this study were unsuitable for this assay. It is unclear as to whether bladder cancer cell lines have been used in this assay previously, though no such data could be found in the published literature. Therefore after discussion with local experts, a decision was made to change to the Annexin V assay.

The Annexin V assay is a widely used assay in which flow cytometry detects the fluorescence emitted by treated cells. This assay again relies upon changes seen in early apoptosis, namely the externalisation of phosphatidyl serine (PS) on the surface membrane of the cell. This then binds the anticoagulant protein Annexin V, conjugated with FITC, in the presence of calcium and emits a fluorescent signal that is detected at a wavelength 518 nm [184]. The assay also involves propidium iodide (PI) that is taken up by late apoptotic and necrotic cells that have permeable

membranes, but is excluded from viable and early apoptotic cells. It emits a signal at 620 nm. Such necrotic cells also bind Annexin V on internal PS. Therefore, four groups of cells are sorted by the flow cytometer: viable cells with no fluorescence, early apoptotic cells with fluorescence at 518 nm only, late apoptotic and necrotic cells with fluorescence at both 518 nm and 620 nm, and cells which fluoresce at only 620 nm [204]. In theory, there should be no cells in the last group, as any cells that are permeable to PI should also be permeable to Annexin V. Low numbers of cells in this group is an indication of a successful assay, as the common limiting factor is poor uptake of Annexin V that would lead to larger numbers of cells in the latter group. All assays had a proportion of cells in this group of less than 4%.

Results from the Annexin V assay in this study were surprising in view of the synergistic interaction witnessed between lapatinib and chemotherapeutic agents in the MTT assays. The chemotherapy combinations, GC and GTC, on the whole caused small increases in apoptosis, except for GC with RT112 cells. Lapatinib, however, showed a trend of causing a decrease in the levels of apoptosis, when compared to cells with no treatment and cells treated with chemotherapy alone. This was more evident in J82 cells than RT112 cells, where very small increases in apoptosis were seen when lapatinib was added prior to GC or to cells alone. Therefore, overall lapatinib had only minor effects on the levels of apoptosis, but was more likely to reduce the number of cells entering into apoptosis. This would either suggest that lapatinib has a cytostatic effect on these two bladder cancer cell lines, or apoptosis in these cell lines in not reliably detected by the Annexin V assay. One of the failings of the Annexin V assay is that it can't distinguish late apoptotic cells from necrotic cells as both take up Annexin V and PI, and so if cells have passed beyond early apoptosis,

the proportion of cells undergoing apoptosis may be underestimated [205]. However, on further analysis of the results in this study, numbers of cells in the early apoptotic/necrotic group were generally also decreased by addition of lapatinib with or without chemotherapy. Also, although there are a couple of reports of lapatinib causing a 23 x increase in apoptosis in a couple of cell lines, this finding has not been consistent across all cell lines investigated [138, 206].

When considering results from one type of apoptosis assay, it should be remembered that "the lack of evidence of apoptosis, detected by a particular method, is not evidence of the lack of apoptosis" [205], and that ideally other methods should be used to check results. Evidence for a cytostatic effect of lapatinib, and also chemotherapeutic agents, was backed up by FACS analysis on cell samples treated with lapatinib and chemotherapy, as discussed below.

FACS analysis was carried out on cells treated in the same way as those studied in the Annexin V assay. Lapatinib showed an overall trend of shifting cells into the G_0/G_1 phase of the cell cycle. This was seen in both cell lines, both with lapatinib alone, and when lapatinib was added prior to GC and GTC. GC and GTC alone in RT112 cells also produced a similar shift in the cell cycle, an effect that was increased by lapatinib. In J82 cells, however, GC and GTC alone actually caused a marked shift of cells into S phase. When lapatinib was added to these combinations, some shift of cells into both G_0/G_1 and G_2/M was seen. Therefore, the effects of chemotherapy on the cell lines is variable, and thus difficult to explain by their modes of action. Lapatinib was however consistent in its effects throughout, and appears to exert its effects by arresting cells in the early stages of the cell cycle.

Apoptosis can also be analysed by FACS. When preparing cells for the analysis, ethanol is added which fixes the DNA in the cells. The degraded DNA in apoptotic cells is not fully preserved, and this fraction leaks out during subsequent cell rinsing and staining. Thus apoptotic cells have a reduced DNA content, producing a group of cells with lower DNA stainability than G_1 cells, causing a "sub-G_1" peak [205]. The sub-G_1 peak has a low specificity however, as this population can also contain mechanically damaged cells, cells with lower DNA content, or cells with a different chromatin structure [205]. It was found that there were only small sub-G_1 peaks throughout all analyses, confirming the findings from the Annexin V assays. Therefore it can be concluded that lapatinib is cytostatic in the two bladder cancer cell lines in this study. Despite no evident cytotoxic actions, the effect of lapatinib on cell viability when added prior to chemotherapy was clearly very marked.

4.6 Genetic approaches to down-regulation of ErbB1 expression and signal transduction

The final part of this study was to attempt to genetically modify J82 and RT112 cells, in order to alter ErbB1 expression and signal transduction. The reason for this was to allow further study into its role in downstream signalling and the role of lapatinib in the pathway.

The initial approach to altering expression of ErbB1 was using a pSuper RNAi system. The pSuper-ErbB1 vector had been successfully used previously to

downregulate ErbB1 expression in telomerase-immortalised fibroblast cells [207], and so work began to transfect them into J82 and RT112 cells, both of which have previously been successfully transfected with siRNA constructs [208, 209]. Transformation and isolation of both the control and ErbB1 vectors was successful, as shown by the minigel after digestion of the vectors, and so transfection was performed. Transfection efficiencies were very different between the cell lines. With both methods of transfection, electrical and chemical, J82 cells showed high efficiencies of around 50% or greater. RT112 cells were more difficult to transfect, with efficiencies of less than 20% with both methods, although this was slightly higher with electroporation than chemical transfection. However, even in J82 cells, no downregulation of ErbB1 was seen after transfection of the pSuper-ErbB1. The reasons for this failure to affect the ErbB1 expression in the two cell lines were unclear. It is true that efficiency of transfection is dependent on both the efficiency of vector delivery and the efficiency of expression of the vector [191]. Therefore, in RT112 cells it is possible that the failure was related to the poor delivery of the vector into the cells, with low transfection efficiencies seen with pEGFP. This is unlikely to be true in J82 cells, and so the problem must lie in the part of the process after expression of the plasmid DNA in cells. Thus possible areas to consider are inability of the pSuper-ErbB1 to integrate with the dsRNA, or simply the failure of the vector to suppress ErbB1 in these cell lines.

The second method used to attempt to genetically modify the function of ErbB1 in RT112 and J82 cell lines was using a dominant-negative mutant of ErbB1, CD533. The CD533 vector has been successfully used in a number of cell lines, and has been shown to form inactive homodimers with wild-type ErbB1 [210]. It has also been

shown to generate an inhibitory influence on the kinase activity of ErbB2 via heterodimerisation [192]. However, in one study expression of the dominant-negative CD533 vector by rat fibroblasts did not have any inhibitory effects on ErbB1 phosphorylation [211]. This conflicting data would suggest that the effect of CD533 expression is cell-dependent. This observation could perhaps either be due to varying levels of CD533 expression, or differences in levels of homodimerisation versus heterodimerisation of wild-type ErbB1 between cell lines. In this study, transfection of the CD533 vector was successful and clones were selected using Zeocin^{TM}, followed by confirmation of CD533 expression using immunocytostaining to identify the V5-epitope in positive clones. The effect of expression of the mutant ErbB1 receptor on cellular function was then investigated by stimulation of cells using the ErbB1 ligand, EGF. Stimulated and unstimulated V5 positive clones were studied alongside V5 negative clones using Western blot analysis to assess phosphorylated levels of ErbB1 and AKT. Expression of the dominant-negative CD533 vector by the positive clones did not have any inhibitory effect on ErbB1 phosphorylation or on activation of its downstream signalling pathway, AKT, in either cell line. The reasons for the failure of the dominant-negative CD533 vector to affect ErbB1 signalling in either cell line is unclear, especially as RT112 and J82 cells are morphologically distinct and have widely varying levels of ErbB1 expression. No further investigations into the effects of the CD533 vector on the two cell lines were undertaken in this study.

Further work to suppress ErbB1 expression and signal transduction was not pursued after the failure to achieve results with the p-Super RNAi and dominant-negative ErbB1 systems. However, future investigations in this area would be of benefit, to

gain more information about the mechanisms behind the intracellular effects of lapatinib. This work would ideally also involve inhibiting expression of ErbB2, so that the effects of lapatinib on the powerful heterodimer of ErbB2-ErbB3 could be studied.

CHAPTER 5

CONCLUSIONS

Early clinical trials combining small molecule TKIs with chemotherapy in advanced NSCLC failed to show any benefit of the addition of the TKI over chemotherapy alone in terms of survival. There are a number of theories as to why no benefit was seen, including problems with the sequencing of the drugs. Another feature that has not been considered is the use of ErbB1 specific TKIs in these trials, rather than newer TKIs, such as the dual ErbB1/ErbB2 inhibitor, lapatinib. To date, there have been no pre-clinical or clinical studies combining TKIs with chemotherapy in bladder cancer, a disease in which improving survival, or availability of chemotherapy to patients with metastatic disease is a priority.

In this study lapatinib has been shown to inhibit activation of ErbB1, ErbB2 and ErbB3 and the PI3K/AKT signalling pathway. Importantly, this dual inhibitor is able to act upon ErbB3, presumably via the potent ErbB2-ErbB3 heterodimer, even in the presence of an ErbB3 ligand. This is clearly a benefit over the more widely studied ErbB1-specific TKIs. A further important finding was its ability to inhibit the chemotherapy-induced early activation of receptors and AKT, the constitutive activation of which has been linked to chemoresistance. This is possibly an explanation for the sequence-dependent synergy shown between lapatinib and both single-agent and clinically relevant combinations of gemcitabine, paclitaxel and cisplatin. The synergistic interaction found when lapatinib was added before and during chemotherapy was evident in spite of this being due to cytostatic, rather than cytotoxic, effects of the drugs. A final promising feature of this work was the apparent ability of lapatinib to produce a dose-sparing effect with chemotherapy, a finding that could have important clinical implications.

The results of this *in vitro* study together with data already published on the safety of lapatinib in normal patients [149 -151], its efficacy in patients with chemo-refractory TCC bladder [212], and its efficacy in animal models of other tumours, should provide the impetus for further clinical trials of lapatinib in bladder cancer, without first testing on animal models of bladder cancer. Firstly, it would be interesting to consider a trial of neoadjuvant lapatinib in patients with muscle-invasive bladder cancer who are planned for radical cystectomy. Endpoints would include assessment of biomarkers in the cystectomy specimen and determination of toxicity issues such as delay in cystectomy. Secondly, to investigate whether lapatinib would increase survival when combined with current chemotherapy regimens in patients with metastatic bladder cancer. From the results shown here, a program with lapatinib prior to and between chemotherapy cycles is recommended. Thirdly, to investigate lapatinib combined with reduced-dose chemotherapy. In this setting results should show whether such a combination produces similar survival to full-dose chemotherapy alone, and also whether toxicity is reduced. The latter would both improve the quality of life of those receiving chemotherapy, and also potentially allow more patients to receive this treatment, and thus prolong their survival.

REFERENCES

1. Office for National Statistics, Cancer Statistics registrations: Registrations of cancer diagnosed in 2002, England. Series MB1 no.33. 2005, National Statistics: London.

2. Welsh Cancer Intelligence and Surveillance Unit, 2005.

3. ISD Online. 2005, Information and Statistics Division, NHS Scotland.

4. Northern Ireland Cancer Registry, Cancer Incidence and Mortality. 2005.

5. Office for National Statistics, http://www.statistics.gov.uk.

6. Registrar General for Scotland. Annual report 2003. GRO For Scotland (2004).

7. Registrar General for Northern Ireland. Annual report 2003. GRO for Northern Ireland (2003).

8. Amling CL. Diagnosis and management of superficial bladder cancer. Curr Probl Cancer 2001; 25: 224-78

9. Sobin DH, Whitteking CH. Classification of malignant tumours, 5th edition; Wiley-Liss: New York, 1997.

10. Mostofi FK, Sobin LH, *et al.* Histological typing of urinary bladder tumours. International classification of tumours 19. Geneva: World Health Organization, 1973.

11. Epstein J, Amin M, *et al.* The World Health Organization/International Society of Urological Pathology consensus classification of urothelial (transitional cell) neoplasms of the urinary bladder. Am J Surg Pathol 1998; 22: 1435-48.

12. Mostofi FK, Davis CJ, *et al.* Histological typing of urinary bladder tumours. World Health Organisation, international histological classification of tumours, 2nd ed. Berlin: Springer Verlag, 1999.

13. Epstein JI. The new World Health Organization/International Society of Urological Pathology (WHO/ISUP) classification for TA, T1 bladder tumors: is it an improvement? Crit Rev Oncol Hematol 2003; 47: 83-9.

14. Montironi R, Lopez-Beltran A, *et al.* Classification and grading of the non-invasive urothelial neoplasms: recent advances and controversies. J Clin Pathol 2003; 56: 91-5.

15. Hoover R, Cole P. Population trends in cigarette smoking and bladder cancer. Am J Epidemiol 1991; 94: 409-18.

16. Wynder EL, Goldsmith R. The epidemiology of bladder cancer: a second look. Cancer 1977; 40: 1246-68.

17. Morrison AS, Cole P. Epidemiology of bladder cancer. Urol Clin North Am 1976; 3: 13-29.

18. Steineck G, Plato N *et al.* Urothelial cancer and some industry-related chemicals: an evaluation of the epidemiologic literature. Am J Ind Med 1990; 17: 371-91.

19. Silverman DT, Levin LI *et al.* Occupational risks of bladder cancer in the United States: I White men. J Natl Cancer Inst 1989; 81: 1472-80.

20. Silverman DT, Levin LI *et al.* Occupational risks of bladder cancer in the United States: II Nonwhite men. J Natl Cancer Inst 1989; 81: 1480-3.

21. Chiou HY, Chiou ST, *et al.* Incidence of transitional cell carcinoma and arsenic in drinking water: a follow-up study of 8,102 residents in an

arseniasis-endemic area in northeastern Taiwan. Am J Epidemiol 2001; 153: 411-8.

22. Lamm SH, Engel A, *et al.* Arsenic in drinking water and bladder cancer mortality in the United States: an analysis based on 133 U.S. counties and 30 years of observation. J Occup Environ Med 2004; 46: 298-306.

23. Morales S-VM, Llopis GA, *et al.* Concentration of nitrates in drinking water and its relationship with bladder cancer. J Environ Pathol Toxicol Oncol 1993; 12: 229-36.

24. Gulis G, Czompolyova M, *et al.* An ecologic study of nitrate in municipal drinking water and cancer incidence in Trnava District, Slovakia. Environ Res 2002; 88: 182–7.

25. Kurth KH, Denis L, *et al.* Factors affecting recurrence and progression in superficial bladder tumours. Eur J Cancer 1995; 31A: 1840-6.

26. Parmar MKB, Freedman LS, *et al.* Prognostic factors for the recurrence and follow-up policies in the treatment of superficial bladder cancer: report from the British Medical Research Council subgroup on Superficial Bladder Cancer (Urological Cancer Working Party). J Urol 1989; 142: 284-8.

27. Reading J, Hall RR, *et al.* The application of a prognostic factor analysis for Ta.T1 bladder cancer in routine urological practice. BJU 1995; 75: 604-7.

28. Witjes JA, Kiemenig La LM, *et al.* Prognostic factors in superficial bladder cancer. Eur Urol 1992; 21: 81-97.

29. Kurth KH, Ten Kate FJW, *et al.* Prognostic factors in superficial bladder tumours. Problems in Urology 1992; 6: 471-83.

30. Allard P, Bernard P, *et al.* The early clinical course of primary Ta and T1 bladder cancer: a proposed prognostic index. Br J Urol 1998; 81: 692-8.

31. Witjes JA. Bladder carcinoma in situ in 2003: state of the art. Eur Urol 2004; 45: 142-6.

32. H. Wolf, F. Melsen, *et al.* Natural history of carcinoma in situ of the urinary bladder. Scand J Urol Nephrol Suppl 1994; 157: 147–51.

33. Oosterlinck W, Lobel B, *et al.* Guidelines on bladder cancer. European Association of Urologists, 2001. www.uroweb.org.

34. Guilliford MC, Petruckevitch A, *et al.* Survival with bladder cancer, evaluation of delay in treatment, type of surgeon, and modality of treatment. BMJ 1991; 303: 437-40.

35. Mansson A, Anderson H, *et al.* Time lag to diagnosis of bladder cancer – influence of psychosocial parameters and level of health-care provision. Scand J Urol Nephrol 1993; 27: 363-5.

36. Cookson MS, Herr HW, *et al.* The treated natural history of high risk superficial bladder cancer: 15 year outcome. J Urol 1997; 158: 62-7.

37. Tolley DA, Parmar MK, *et al.* The effect of intravesical mitomycin C on recurrence of newly diagnosed superficial bladder cancer: a further report with 7 years of follow up. J Urol 1996; 155: 1233-8.

38. Oosterlinck W, Kurth KH, *et al.* A prospective European Organisation for Research and Treament of Cancer Genitourinary Group randomised trial comparing transurethral resection followed by a single intravesical installation of epirubicin or water in single Ta, T1 papillary carcinoma of the bladder. J Urol 1993; 149: 749-52.

39. Malmstrom PU, Wijkstrom H, *et al.* 5 year followup of a randomised prospective study comparing mitomycin C and bacillus Calmette-Guerin in patients with superficial bladder carcinoma. J Urol 1999; 161: 1124-7.

40. Lamm LD, Blumenstein BA, *et al.* Maintenance Bacillus Calmette-Guerin immunotherapy for recurrent Ta, T1 and carcinoma in situ transitional cell carcinoma of the bladder: a randomized southwest oncology subgroup study. J Urol 2000; 163: 1124-9.

41. Sylvester RJ, van der Meijden AP, *et al.* Intravesical bacillus Calmette-Guerin reduces the risk of progression in patients with superficial bladder cancer: a meta-analysis of the published results of randomized clinical trial. J Urol 2002; 168: 1964-70.

42. Sylvester RJ, van der Meijden AP, *et al.* Bacillus Calmette-Guerin versus chemotherapy for the intravesical treatment of patients with carcinoma in situ of the bladder: a meta-analysis of the published results of randomized clinical trials. J Urol 2005; 174: 86-91.

43. Griffiths TRL, Charlton M, *et al.* Treatment of carcinoma in situ with intravesical bacillus Calmette-Guerin without maintenance. J Urol 2002; 167: 2408-12.

44. Herr HW. The value of second transurethral resection in evaluating patients with bladder tumors. J Urol 1999; 162: 74-6.

45. Stein JP, Lieskovsky G, *et al.* Radical cystectomy in the treatment of invasive bladder cancer: long term results in 1,054 patients. J Clin Oncol 2001; 19: 666-75.

46. Duncan W, and Quilty PM. The results of a series of 963 patients with transitional cell carcinoma of the urinary bladder primarily treated by radical megavoltage X-ray therapy. Radiother Oncol 1986; 7: 299-310.

47. Mills RD, Turner WH, *et al.* Pelvic lymph node metastases from bladder cancer: outcome in 83 patients after radical cystectomy and pelvic lymphadenectomy. J Urol 2001; 166: 19-23.

48. Sternberg CN, Yagoda A, *et al.* Preliminary results of M-VAC (methotrexate, vinblastine, doxorubicin and cisplatin) for transitional cell carcinoma of the urothelium. J Urol 1985; 133: 403-7.

49. Loehrer PJ Sr, Einhorn LH, *et al.* A randomised comparison of cisplatin alone or in combination with methotrexate, vinblastine, and doxorubicin in patients with metastatic urothelial carcinoma: a cooperative group study. J Clin Oncol 1992; 10: 1066-73.

50. Logothetis CJ, Dexeus FH, *et al.* A prospective randomised trial comparing MVAC and CISCA chemotherapy for patients with metastatic urothelial tumours. J Clin Oncol 1990; 8: 1050-5.

51. Mead GM, Russell M, *et al.* A randomized trial comparing methotrexate and vinblastine (MV) with cisplatin, methotrexate and vinblastine (CMV) in advanced transitional cell carcinoma: results and a report on prognostic factors in a Medical Research Council study. MRC Advanced Bladder Cancer Working Party. Br J Cancer 1998; 78; 1067–75.

52. Saxman SB, Propert KJ, *et al.* Long-term follow-up of a phase III intergroup study of cisplatin alone or in combination with methotrexate, vinblastine, and doxorubicin in patients with metastatic urothelial carcinoma: a cooperative group study. J Clin Oncol 1997; 15: 2564-9.

53. Sternberg CN, de Mulder PH, *et al.* Randomized phase III trial of high-dose-intensity methotrexate, vinblastine, doxorubicin, and cisplatin (MVAC) chemotherapy and recombinant human granulocyte colony-stimulating factor

versus classic MVAC in advanced urothelial tract tumours: European Organization for Research and Treatment of Cancer Protocol No. 30924. J Clin Oncol 2001; 19: 2638-46.

54. Von der Maase H, Hansen SW, *et al.* Gemcitabine and cisplatin versus methotrexate, vinblastine, doxorubicin, and cisplatin in advanced or metastatic bladder cancer: results of a large, randomised, multinational, multicentre, phase III study. J Clin Oncol 2000; 18: 3068-77.

55. Burch PA, Richardson RL, *et al.* Phase II study of paclitaxel and cisplatin for advanced urothelial cancer. J Urol 2000; 164: 1538-42.

56. Pycha A, Grbovic M, *et al.* Paclitaxel and carboplatin in patients with metastatic transitional cell cancer of the urinary tract. Urology 1999; 53: 510-5.

57. Bellmunt J, Guillem V, *et al.* Phase I-II study of paclitaxel, cisplatin, and gemcitabine in advanced transitional-cell carcinoma of the urothelium. Spanish Oncology Genitourinary Group. J Clin Oncol 2000; 18: 3247-55.

58. Hussain M, Vaishampayan U, *et al.* Combination paclitaxel, carboplatin, and gemcitabine is an active treatment for advanced urothelial cancer. J Clin Oncol 2001; 19: 2527-33.

59. Bajorin DF, McCaffrey JA, *et al.* Ifosfamide, paclitaxel, and cisplatin for patients with advanced transitional cell carcinoma of the urothelial tract: final report of a phase II trial evaluating two dosing schedules. Cancer 2000; 88: 1671-8.

60. de Wit R, and Bellmunt J. Overview of gemcitabine triplets in metastatic bladder cancer. Crit Rev Oncol Hematol 2003; 45: 191-7.

61. Sternberg CN, Calabro F, *et al.* Chemotherapy with an every-2-week regimen of gemcitabine and paclitaxel in patients with transitional cell carcinoma who have received prior cisplatin-based therapy. Cancer 2001; 92: 2993-8.

62. Bajorin DF, Dodd PM, *et al.* Long-term survival in metastatic transitional-cell carcinoma and prognostic factors predicting outcome of therapy. J Clin Oncol 199; 17: 3173-81.

63. Stadler WM, Hayden A, *et al.* Long-term survival in phase II trials of gemcitabine plus cisplatin for advanced transitional cell cancer. Urol Oncol 2002; 7: 153-7.

64. Chester JD, Hall GD, *et al.* Systemic chemotherapy for patients with bladder cancer - current controversies and future directions. Cancer Treatment Reviews 2004; 30: 343-8.

65. International collaboration of trialists. Neoadjuvant cisplatin, methotrexate, and vinblastine chemotherapy for muscle-invasive bladder cancer: A randomised controlled trial. Lancet 1999; 354: 533-40.

66. Advanced Bladder Cancer (ABC) Meta-analysis Collaboration. Neoadjuvant chemotherapy in invasive bladder cancer: update of a systematic review and meta-analysis of individual patient data. Eur Urol 2005; 48: 202-6.

67. Sylvester R, and Sternberg C. The role of adjuvant combination chemotherapy after cystectomy in locally advanced bladder cancer. What we do not know and why. Ann Oncol 2000; 11: 851-6.

68. Advanced Bladder Cancer (ABC) Meta-analysis Collaboration. Adjuvant chemotherapy in invasive bladder cancer: a systematic review and meta-analysis of individual patient data. Eur Urol 2005; 48: 189-99.

69. Sternberg CN. Current perspectives in muscle invasive bladder cancer. Eur J Cancer 2002; 38: 460-7.

70. Juffs HG, Moore MJ, et al. The role of systemic chemotherapy in the management of muscle-invasive bladder cancer. The Lancet Oncology 2002; 3: 738-47.

71. Green JA, Kirwan JM, et al. Survival and recurrence after concomitant chemotherapy and radiotherapy for cancer of the uterine cervix: a systematic review and meta-analysis. The Lancet 2001; 358: 781-6.

72. Coppin CM, Gospodarowicz MK, et al. Improved local control of invasive bladder cancer by concurrent cisplatin and preoperative or definitive radiation. The National Cancer Institute of Canada Clinical Trials Group. J Clin Oncol 1996; 14: 2901-7.

73. Danesi DT, Arcangeli G, et al. Conservative treatment of invasive bladder carcinoma by transurethral resection, protracted intravenous infusion chemotherapy, and hyperfractionated radiotherapy: long term results. Cancer 2004; 101: 2540-8.

74. M.A. Knowles. The genetics of transitional cell carcinoma: progress and potential clinical application. BJU Int 1999; 84: 412–27.

75. Mellon K, Wright C, et al: Long-term outcome related to epidermal growth factor receptor status in bladder cancer. J Urol 1995; 153: 919-25.

76. Yarden Y. The EGFR family and its ligands in human cancer: signalling mechanisms and therapeutic opportunities. Eur J Cancer 2001; 37: S3-S8.

77. Guy PM, Platko JV, et al. Insect cell-expressed p180erbB3 possesses an impaired tyrosine kinase activity. Proc Natl Acad Sci USA 1994; 91: 8132-6.

78. Klapper LN, Glathe S, *et al.* The ErbB-2/HER2 oncoprotein of human carcinomas may function solely as a shared coreceptor for multiple stroma-derived growth factors. Proc Natl Acad Sci USA 1999; 96: 4995-5000.

79. Prenzel N, Fischer OM, *et al.* The epidermal growth factor receptor family as a central element for cellular signal transduction and diversification. Endocr Relat Cancer 2001; 8: 11-31.

80. Riese DJ, Stern DF. Specificity within the EGF family/ErbB receptor family signalling network. BioEssays 1998; 20: 41-8.

81. Pinkas-Kramarski R, Soussan L, *et al.* Diversification of Neu differentiation factor and epidermal growth factor signalling by combinatorial receptor interactions. EMBO J 1996; 15: 2452-67.

82. Marmor MD, Skaria KB, *et al.* Signal transduction and oncogenesis by ErbB/HER receptors. Int J Radiat Oncol Biol Phys 2004; 58: 903-13.

83. Rodriguez-Viciana P, Sabatier C, *et al.* Signaling specificity by Ras family GTPases is determined by the full spectrum of effectors they regulate. Mol Cell Biol 2004; 24: 4943-54.

84. Schlessinger J. Cell signalling by receptor tyrosine kinases. Cell 2000; 103: 211-25.

85. Cantley LC, Neel BG. New insights into tumour suppression: PTEN suppresses tumor formation by restraining the phosphoinositide 3-kinase/AKT pathway. Proc Natl Acad Sci USA 1999; 96: 4240-5.

86. Bromberg JF. Activation of STAT proteins and growth control. Bioessays 2001; 23: 161-9.

87. Bowman T, Garcia R, *et al.* STATs in oncogenesis. Oncogene 2000; 19: 2474-88.

88. Busse D, Yakes FM, *et al.* Tyrosine kinase inhibitors: rationale, mechanisms of action and implications for drug resistance. Semin Oncol 2001; 28: 47-55.

89. Wells A. EGF receptor. Int J Biochem Cell Biol 1999; 31: 637-43.

90. Neal DE, Marsh C, *et al.* Epidermal-growth-factor receptors in human bladder cancer: comparison of invasive and superficial tumours. Lancet 1985; 1: 366-8.

91. Lipponen P, Eskelinen M. Expression of epidermal growth factor receptor in bladder cancer as related to established prognostic factors, oncoprotein (c-erbB-2, p53) expression and long-term prognosis. Br J Cancer 1994; 69: 1120-5.

92. Turkeri LN, Erton ML, *et al.* Impact of the expression of epidermal growth factor, transforming growth factor α, and epidermal growth factor receptor on the prognosis of superficial bladder cancer. Urology 1998; 51: 645-9.

93. Neal DE, Mellon K. Epidermal growth factor receptor and bladder cancer: a review. Urol Int 1992; 48: 365-71.

94. Chow N-H, Chan S-H, *et al.* Expression profiles of ErbB family receptors and prognosis in primary transitional cell carcinoma of the urinary bladder. Clin Cancer Res 2001; 7: 1957-62.

95. Chow N-H, Liu H-S, *et al.* Expression patterns of erbB receptor family in normal urothelium and transitional cell carcinoma. An immunohistochemical study. Virchows Arch 1997; 430: 461-6.

96. McCann A, Dervan PA, *et al.* C-erbB-2 oncoprotein expression in primary human tumours. Cancer (Phila) 1990; 65: 88-92.

97. Zhau HE, Zhang X, *et al.* Amplification and expression of the c-erbB-2/neu proto-oncogene in human bladder cancer. Mol Carcinog 1990; 3: 254-7.

98. Kruger S, Weitsch G, *et al*. HER2 overexpression in muscle-invasive urothelial carcinoma of the bladder: prognostic implications. Int J Cancer 2002; 102: 514-8.

99. Sato K, Moriyama AM, *et al*. An immunohistologic evaluation of C-erbB2 gene product in patients with urinary bladder carcinoma. Cancer (Phila) 1992; 70: 2493-8.

100. Lipponen P. Expression of c-erbB-2 oncoprotein in transitional cell bladder cancer. Eur J Cancer 1993; 29: 749-53.

101. Gandour-Edwards R, Lara PN, *et al*. Does *HER2/neu* expression provide prognostic information in patients with advanced urothelial carcinoma? Cancer 2002; 95: 1009-15.

102. Rajkumar T, Stamp GW, *et al*. Expression of the type 1 tyrosine kinase growth factor receptors EGF receptor, c-erbB2 and c-erbB3 in bladder cancer. J Pathol 1996; 179: 381-5.

103. Memon AA, Sorenson BS, *et al*. Expression of HER3, HER4 and their ligand heregulin-4 is associated with better survival in bladder cancer patients. Br J Cancer 2004; 91: 2034-41.

104. Itoh M, Murata T, *et al*. Requirement of STAT3 activation for maximal collagenase-1 (MMP-1) induction by epidermal growth factor and malignant characteristics in T24 bladder cancer cells. Oncogene 2006; 25: 1195-204.

105. Friedrich MG, Chandrasoma S, *et al*. Prognostic relevance of methylation markers in patients with non-muscle invasive bladder carcinoma. Eur J Cancer 2005; 41: 2769-78.

106. Wu X, Obata T, *et al*. The phosphatidylinositol-3 kinase pathway regulates bladder cancer cell invasion. BJU Int 2004; 93: 143-50.

107.Wang DS, Rieger-Christ K, *et al.* Molecular analysis of PTEN and MXI1 in primary bladder carcinoma. Int J Cancer 2000; 88: 620-5.

108.Aveyard JS, Skilleter A, *et al.* Somatic mutation of PTEN in bladder cancer. Br J Cancer 1999; 80; 904-8.

109.Swiatkowski S, Seifert HH, *et al.* Activities of MAP-kinase pathways in normal uroepithelial cells and urothelial carcinoma cell lines. Exp Cell Res 2003; 282: 48-57.

110.Slichenmyer WJ, Fry DW. Anticancer therapy targeting the ErbB family of receptor tyrosine kinases. Semin Oncol 2001; 28: 67-79.

111.Pai-Scherf LH, Villa J, *et al.* Hepatotoxicity in cancer patients receiving erb-38, a recombinant immunotoxin that targets the erbB2 receptor. Clin Cancer Res 1999; 5: 2311-5.

112.Yang SP, Song ST, *et al.* Advancements of antisense oligonucleotides in treatment of breast cancer. Acta Pharmacol Sin 2003; 24: 289-95.

113.Cunningham CC. New modalities in oncology: antisense oligonucleotides. Proc (Bayl Univ Med Cen) 2002; 15: 125-8.

114.Perrotte P, Matsumoto T, *et al.* Anti-epidermal growth factor receptor antibody C225 inhibits angiogenesis in human transitional cell carcinoma growing orthotopically in nude mice. Clin Cancer Res 1999; 5: 257-65.

115.Inoue K, Slaton JW, *et al.* Paclitaxel enhances the effects of the anti-epidermal growth factor receptor monoclonal antibody ImClone C225 in mice with metastatic human bladder transitional cell carcinoma. Clin Cancer Res 2000; 6: 4874-84.

116.Carter P, Presta L, *et al.* Humanization of an anti-p185HER2 antibody for human cancer therapy. Proc Natl Acad Sci USA 1992; 89: 4285-9.

117.Slamon DJ, Leyland-Jones B, *et al.* Use of chemotherapy plus a monoclonal antibody against HER2 for metastatic breast cancer that overexpresses HER2. N Engl J Med 2001; 344: 783-92.

118.Harari PM. Epidermal growth factor receptor inhibition strategies in oncology. Endocr Relat Cancer 2004; 11: 689-708.

119.Sion-Vardy N, Vardy D, *et al.* Antiproliferative effects of tyrosine kinase inhibitors (tyrphostins) on human bladder and renal carcinoma cells. J Surg Res 1995; 59: 675-80.

120.Ciardiello F, Caputo R, *et al.* Inhibition of growth factor production and angiogenesis in human cancer cells by ZD1839 (Iressa) a selective epidermal growth factor receptor tyrosine kinase inhibitor. Clin Cancer Res 2001; 7: 1459-65.

121.Hambek M, Baghi M, *et al.* Iressa (ZD 1839) inhibits phosphorylation of three different downstream signal transducers in head and neck cancer (SCCHN). Anticancer Res 2005; 25: 1871-5.

122.Sirotnak FM, Zakowski MF, *et al.* Efficacy of cytotoxic agents against human tumor xenografts is markedly enhanced by coadministration of ZD 1839 (Iressa), an inhibitor of EGFR tyrosine kinase. Clin Cancer Res 2000; 6: 4885-92.

123.Ranson M, Hammond LA, *et al.* ZD1839, a selective oral epidermal growth factor receptor-tyrosine kinase inhibitor, is well tolerated and active in patients with solid malignant tumours: results of a phase I trial. J Clin Oncol 2002; 20: 2240-50.

124.Hidalgo M, Siu LL, *et al.* Phase I and pharmacologic study of OSI-774, an epidermal growth factor receptor tyrosine kinase inhibitor, in patients with advanced solid malignancies. J Clin Oncol 2001; 19: 3267-79.

125.Nemunaitis J, Eiseman I, *et al.* Phase I clinical and pharmacokinetics evaluation of oral CI-1033 in patients with refractory cancer. Clin Cancer Res 2005; 11: 3846-53.

126.Smith J. Erlotinib: small-molecule targeted therapy in the treatment of non-small-cell lung cancer. Clin Ther 2005; 27: 1513-34.

127.Kris M, Natale RB, *et al.* A phase II trial of ZD 1839 ("Iressa") in advanced non-small cell lung cancer (NSCLC) patients who had failed platinum and docetaxel-based regimens (IDEAL-2) [abstract]. Proc Am Soc Clin Oncol 2002; 21: 292a.

128.Thatcher N, Chang A. Gefitinib plus best supportive care in previously treated patients with refractory advanced non-small-cell lung cancer: results from a randomised, placebo-controlled, multicentre study (Iressa Survival Evaluation in Lung Cancer). Lancet 2005; 366: 1527-37.

129.Shepherd FA, Rodrigues Pereira J, *et al.* for the National Cancer Institute of Canada Clinical Trials Group. Erlotinib in previously treated non-small cell lung cancer. N Engl J Med 2005; 353: 123-32.

130.Arteaga CL. Epidermal growth factor receptor dependence in human tumours: more than just expression? Oncologist 2002; 7: 31-9.

131.Meye A, Fiedler U, *et al.* Growth inhibitory effects of ZD1839 ('Iressa') on human bladder cancer cell lines. Proc Am Assoc Cancer Res 2001; 42: 805.

132.Ciardiello F, Caputo R, *et al.* Antitumour effect and potentiation of cytotoxic drugs activity in human cancer cells by ZD1839 (Iressa), an epidermal growth factor inhibitor. Clin Cancer Res 2000; 6: 2053-63.

133.Bishop PC, Myers T, *et al.* Differential sensitivity of cancer cells to inhibitors of the epidermal growth factor receptor family. Oncogene 2002; 21: 119-27.

134.Nishikawa R, Ji XD, *et al.* A mutant epidermal growth factor receptor common in human glioma confers enhanced tumorigenicity. Proc Natl Acad Sci USA 1994; 91: 7727-31.

135.Learn CA, Archer GE, *et al.* Oral administration of the specific epidermal growth factor receptor tyrosine kinase inhibitor (EGFR-TKI) ZD1839 (Iressa) is efficacious against EGFR-overexpressing intracranial tumors. Proc Natl Assoc Cancer Res 2002; 43: A3890.

136.Lynch TJ, Bell DW. Activating mutations in the epidermal growth factor receptor underlying responsiveness of non-small-cell lung cancer to gefitinib. N Engl J Med 2004; 350: 2129-39.

137.Jackman DM, Yeap BY, *et al.* Exon 19 deletion mutations of epidermal growth factor receptor are associated with prolonged survival in non-small cell lung cancer patients treated with gefitinib or erlotinib. Clin Cancer Res 2006; 12: 3908-14.

138.Xia W, Mullin RJ, *et al.* Anti-tumor activity of GW572016: a dual tyrosine kinase inhibitor blocks EGF activation of EGFR/erbB2 and downstream Erk1/2 and AKT pathways. Oncogene 2002; 21: 6255-63.

139.Zhou Y, Li S, *et al.* Blockade of EGFR and ErbB2 by the novel dual EGFR and ErbB2 tyrosine kinase inhibitor GW572016 sensitizes human colon carcinoma GEO cells to apoptosis. Cancer Res 2006; 66: 404-11.

140. Liu Y, Majumder S, et al. Inhibition of HER-2/neu kinase impairs androgen receptor recruitment to the androgen responsive enhancer. Cancer Res 2005; 65: 3404-9.

141. Xia W, Gerard CM, et al. Combining lapatinib (GW572016), a small molecule inhibitor of ErbB1 and ErbB2 tyrosine kinases, with therapeutic anti-ErbB2 antibodies enhances apoptosis of ErbB2-overexpressing breast cancer cells. Oncogene 2005; 24: 6213-21.

142. Chu I, Blackwell K, et al. The dual ErbB1/ErbB2 inhibitor, lapatinib (GW572016), cooperates with tamoxifen to inhibit both cell proliferation- and estrogen-dependent gene expression in antiestrogen-resistant breast cancer. Cancer Res 2005; 65: 18-25.

143. Konecny GE, Pegram MD, et al. Activity of the dual kinase inhibitor lapatinib (GW572016) against HER-2-overexpressing and trastuzumab-treated breast cancer cells. Cancer Res 2006; 66: 1630-9.

144. Xia W, Bisi J, et al. Regulation of survivin by ErbB2 signaling: therapeutic implications for ErbB2-overexpressing breast cancers. Cancer Res 2006; 66: 1640-7.

145. Xia W, Liu LH, et al. Truncated ErbB2 receptor ($p95^{ErbB2}$) is regulated by heregulin through heterodimer formation with ErbB3 yet remains sensitive to the dual EGFR/ErbB2 kinase inhibitor GW572016. Oncogene 2004; 23: 646-53.

146. Gregory CW, Whang YE, et al. Heregulin-induced activation of HER2 and HER3 increases androgen receptor transactivation and CWR-R1 human recurrent prostate cancer cell growth. Clin Cancer Res 2005; 11: 1704-12.

147. Grana TM, Sartor CI, *et al.* Epidermal growth factor receptor autocrine signalling in RIE-1 cells transformed by the Ras oncogene enhances radiation resistance. Cancer Res 2003; 63: 7807-14.

148. Zhou H, Kim YS, *et al.* Effects of the EGFR/HER2 kinase inhibitor GW572016 on EGFR- and HER2-overexpressing breast cancer cell line proliferation, radiosensitization, and resistance. Int J Radiat Oncol Biol Phys 2004; 58: 344-52.

149. Burris HA, Hurwitz HI, *et al.* Phase I safety, pharmacokinetics, and clinical activity study of lapatinib (GW572016), a reversible dual inhibitor of epidermal growth factor receptor tyrosine kinases, in heavily pretreated patients with metastatic carcinomas. J Clin Oncol 2005; 23: 5305-13.

150. Bence AK, Anderson EB, *et al.* Phase I pharmacokinetic studies evaluating single and multiple doses of oral GW572016, a dual EGFR-ErbB2 inhibitor, in healthy subjects. Invest New Drugs 2005; 23: 39-49.

151. Spector NL, Xia W, *et al.* Study of the biologic effects of lapatinib, a reversible inhibitor of ErbB1 and ErbB2 tyrosine kinases, on tumor growth and survival pathways in patients with advanced malignancies. J Clin Oncol 2005; 23: 2502-12.

152. Brognard J, Clark AS, *et al.* Akt/protein kinase B is constitutively active in non-small cell lung cancer cells and promotes cellular survival and resistance to chemotherapy and radiation. Cancer Res 2001; 61: 3986-97.

153. Magné N, Fischel JL, *et al.* Sequence-dependent effects of ZD1839 ('Iressa') in combination with cytotoxic treatment in human head and neck cancer. Br J Cancer 2002; 86: 819-27.

154. Azzariti A, Xu JM, et al. The schedule-dependent enhanced cytotoxic activity of 7-ethyl-10-hydroxy-camptothecin (SN-38) in combination with gefitinib (Iressa™, ZD1839). Biochem Pharmacol 2004; 68: 135-44.

155. Xu JM, Azzariti A, et al. Characterization of sequence-dependent synergy between ZD1839 ('Iressa') and oxaliplatin. Biochem Pharmacol 2003; 66: 551-63.

156. Pollack VA, Savage DM, et al. Inhibition of epidermal growth factor receptor-associated tyrosine phosphorylation in human carcinomas with CP-358,774: dynamics of receptor inhibition in situ and antitumour effects in athymic mice. J Pharmacol Exp Ther 1999; 291: 739-48.

157. Giaccone G, Herbst RS, et al. Gefitinib in combination with gemcitabine and cisplatin in advanced non-small-cell lung cancer: a phase III trial – INTACT 1. J Clin Oncol 2004; 22: 777-84.

158. Herbst RS, Giaccone G, et al. Gefitinib in combination with paclitaxel and carboplatin in advanced non-small-cell lung cancer: a phase III trial – INTACT 2. J Clin Oncol 2004; 2004: 785-94.

159. Gatzemeier U, Pluzanska A, et al. Results of a phase III trial of erlotinib (OSI-774) combined with cisplatin and gemcitabine (GC) chemotherapy in advanced non-small cell lung cancer (NSCLC). Proceedings from the 40th annual meeting of the American Society of Clinical Oncology 2004; 23: 617.

160. Herbst RS, Prager D, et al. TRIBUTE: a phase III trial of erlotinib hydrochloride (OSI-774) combined with carboplatin and paclitaxel chemotherapy in advanced non-small-cell lung cancer. J Clin Oncol 2005; 23: 5856-8.

161.Hama R, Sakaguchi K. The gefitinib story. International Society of Drug Bulletins (ISDB) newsletter 2003; 17: 6-9.

162.Inoue A, Saijo Y, et al. Severe acute interstitial pneumonia and gefitinib. Lancet 2003; 361: 137-9.

163.Bell DW, Lynch TJ, et al. Epidermal growth factor receptor mutations and gene amplification in non-small-cell lung cancer: molecular analysis of the IDEAL/INTACT gefitinib trials. J Clin Oncol 2005; 23: 8081-92.

164.Moore MJ, Goldstein D, et al. Erlotinib plus gemcitabine compared to gemcitabine alone in patients with advanced pancreatic cancer. A phase III trial of the National Cancer Institute of Canada Clinical Trials Group [NCIC-CTG]. Proceedings from the 41st annual meeting of the American Society of Clinical Oncology 2005; abstract no: 1.

165.Highshaw RA, McConkey DJ, et al. Integrating basic science and clinical research in bladder cancer: update from the first bladder Specialized Program of Research Excellence (SPORE). Curr Opin Urol 2004; 14: 295-300.

166.Small EJ, Halabi S, et al. Overview of bladder cancer trials in the Cancer and Leukaemia Group B. Cancer 2003; 97: 2090-8.

167.Fuertesa MA, Castillab J, et al. Cisplatin biochemical mechanism of action: from cytotoxicity to induction of cell death through interconnections between apoptotic and necrotic pathways. Curr Med Chem 2003; 10: 257-66.

168.Gemcitabine. USP DI. Volume 1. Drug information for the health care professional. Update monographs. Englewood, Colorado: Micromedex, Inc.; 18 October, 1999.

169.Horwitz SB. Taxol (paclitaxel): mechanisms of action. Ann Oncol 1994; 5: S3-6.

170.Vogel C, Hager C, *et al.* Mechanisms of mitotic cell death induced by chemotherapy-mediated G2 checkpoint abrogation. Cancer Res 2007; 67: 339-45.

171.Kastan MB, Bartek J. Cell-cycle checkpoints and cancer. Nature 2004; 432: 316-23.

172.Benhar M, Engelberg D, *et al.* Cisplatin-induced activation of the EGF receptor. Oncogene 2002; 21: 8723-31.

173.Sumitomo M, Asano T, *et al.* ZD1839 modulates paclitaxel response in renal cancer by blocking paclitaxel-induced activation of the epidermal growth factor receptor-extracellular signal-regulated kinase pathway. Clin Cancer Res 2004; 10: 794-801.

174.Nelson JM, Fry DW. Akt, MAPK (Erk1/2), and p38 act in concert to promote apoptosis in response to ErbB receptor family inhibition. J Biol Chem 2001; 276: 14842-7.

175.Hu L, Hofmann J, *et al.* Inhibition of phosphatidylinositol 3'-kinase increases efficacy in *in vitro* and *in vivo* ovarian cancer models. Cancer Res 2002; 62: 1087-92.

176.Laemmli UK. Cleavage of structural proteins during the assembly of the head of bacteriophage T4. Nature 1970; 227: 680-5.

177.Smith PK, Krohn RI, *et al.* Measurement of protein using bicinchoninic acid. Anal Biochem 1985; 150: 76-85.

178.Burnette WN. "Western blotting": electrophoretic transfer of proteins from sodium dodecyl sulfate-polyacrylamide gels to unmodified nitrocellulose and radiographic detection with antibody and radioiodinated protein A. Anal Biochem 1981; 112: 195-203.

179.Price P, McMillan J. Use of the tetrazolium assay in measuring the response of human tumor cells to ionising radiation. Cancer Res 1990; 50: 1392-6.

180.Carmichael J, DeGraff WG, *et al.* Evaluation of a tetrazolium-based semiautomated colorimetric assay: assessment of chemosensitivity testing. Cancer Res 1987; 47: 936-42.

181.Kerr JFR, Wyllie AH, *et al.* Apoptosis: a basic biological phenomenon with wide ranging implications in tissue kinetics. Br J Cancer 1972; 26: 239-57.

182.Calbiochem. Mitocapture apoptosis detection kit, user protocol 475866. http://www.merckbiosciences.co.uk/docs/docs/PROT/475866.pdf .

183.Boersma AW, Nooter K, *et al.* Quantification of apoptotic cells with fluorescein isothiocyanate-labeled annexin V in Chinese hamster ovary cell cultures treated with cisplatin. Cytometry 1996; 24: 123-30.

184.Martin SJ, Reutelingsperger CP, *et al.* Early redistribution of plasma membrane phosphatidylserine is a general feature of apoptosis regardless of the initiating stimulus: inhibition by overexpression of Bcl-2 and Abl. J Exp Med 1995; 182: 1545-56.

185.Ibrahim SF, van den Engh G. High-speed cell sorting: fundamentals and recent advances. Curr Opin Biotechnol 2003; 14: 5-12.

186.Zhang L, Fogg DK, *et al.* RNA interference-mediated silencing of the S100A10 gene attenuates plasmin generation and invasiveness of Colo 222 colorectal cancer cells. J Biol Chem 2004; 279: 2053-62.

187.Elbashir SM, Harborth J, *et al.* Duplexes of 21-nucleotide RNAs mediate RNA interference in cultured mammalian cells. Nature 2001; 411: 494-8.

188.Brummelkamp TR, Bernards R. A system for stable expression of short interfering RNAs in mammalian cells. Science 2002; 296: 550-3.

189.Bergmans HE, van Die IM, *et al.* Transformation in Escherichia coli: stages in the process. J Bacteriol 1981; 146: 564-70.

190.Mehier-Humbert S, Guy RH. Physical methods for gene transfer: improving the kinetics of gene delivery into cells. Adv Drug Deliv Rev 2005; 57: 733-53.

191.Luo D, Saltzman WM. Synthetic DNA delivery systems. Nat Biotechnol 2000; 18: 33-7.

192.Spivak-Kroizman T, Rotin D, *et al.* Heterodimerization of c-erbB2 with different epidermal growth factor receptor mutants elicits stimulatory or inhibitory responses. J Biol Chem1992; 267: 8056-63.

193.Livneh E, Prywes R, *et al.* Reconstitution of human epidermal growth factor receptors and its deletion mutants in cultured hamster cells. J Biol Chem 1986; 261: 12490-7.

194.http://www.cayla.com/support/datasheets/zeotech.pdf

195.Haj FG, Markova B, *et al.* Regulation of receptor tyrosine kinase signalling by protein tyrosine phosphatase-1B. J Biol Chem 2003; 278: 739-44.

196.Slater TF, Sawyer B, *et al.* Studies on succinate-tetrazolium reductase systems. III. Points of coupling of four different tetrazolium salts. Biochim Biophys Acta 1963; 77: 383-93.

197.American Tissue Culture Collection. www.atcc.org

198.Andersen H, Mejlvang J, *et al.* Immediate and delayed effects of E-cadherin inhibition on gene regulation and cell motility in human epidermoid carcinoma cells. Mol Cell Biol 2005; 25: 9138-50.

199. Thakkar H, Chen X, *et al.* Pro-survival function of Akt/protein kinase B in prostate cancer cells. Relationship with TRAIL resistance. J Biol Chem 2001; 276: 38361-9.

200. Brognard J, Clark AS, *et al.* Akt/protein kinase B is constitutively active in non-small cell lung cancer cells and promotes cellular survival and resistance to chemotherapy and radiation. Cancer Res 2001; 61: 3986-97.

201. Zhou H, Kim Y-S, *et al.* Effects of the EGFR/HER2 kinase inhibitor GW572016 on EGFR- and HER2-overexpressing breast cancer cell line proliferation, radiosensitization, and resistance. Int J Radiat Oncol Biol Phys 2004; 58: 344-52.

202. Tari AM, Lopez-Berestein G. Serum predominantly activates MAPK and akt kinases in EGFR- and ErbB2-over-expressing cells, respectively. Int J Cancer 2000; 86: 295-7.

203. Solit DB, She Y, *et al.* Pulsatile administration of the epidermal growth factor receptor inhibitor gefitinib is significantly more effective than continuous dosing for sensitizing tumours to paclitaxel. Clin Cancer Res 2005; 11: 1983-9.

204. Koopman G, Reutelingsperger CPM, *et al.* Annexin V for flow cytometric detection of phosphatidylserine expression of B cells undergoing apoptosis. Blood 1994; 84: 1415-20.

205. Darzynkiewicz Z, Gloria J, *et al.* Cytometry in cell necrobiology: analysis of apoptosis and accidental cell death (necrosis). Cytometry 1997; 27: 1-20.

206. Rusnak DW, Lackey K, *et al.* The effects of the novel, reversible epidermal growth factor receptor/ErbB-2 tyrosine kinase inhibitor, GW2016, on the

growth of human normal and tumor-derived cell lines in vitro and vivo. Mol

Cancer Ther 2001; 1: 85-94.

207.Scott LA, Vass JK, *et al.* Invasion of normal human fibroblasts induced by v-

Fos is independent of proliferation, immortalization, and the tumor

suppressors p16INK4a and p53. Mol Cell Biol 2004; 24: 1540-59.

208.Robertson N, Potter C, *et al.* Role of carbonic anhydrase IX in human tumor

cell growth, survival and invasion. Cancer Res 2004; 64: 6160-5.

209.Ning S, Fuessel S, *et al.* siRNA-mediated down-regulation of survivin

inhibits bladder cancer cell growth. Int J Oncol 2004; 25: 1065-71.

210.Kasles O, Yarden Y, *et al.* A dominant negative mutation suppresses the

function of normal epidermal growth factor receptors by heterodimerization.

Mol Cell Biol 1991; 11: 1454-63.

211.Daub H, Weiss FU, *et al.* Role of transactivation of the EGF receptor in

signalling by G-protein-coupled receptors. Nature 1996; 379: 557-60.

212.Wülfing C, Machiels J, *et al.* A single arm, multicenter, open label, ph II

study of lapatinib as a 2L treatment of pts with locally advanced/metastatic

transitional cell carcinoma (TCC) of the urothelial tract. J Clin Oncol 2005

ASCO Annual Meeting Proceedings; 23: 4594.

ABBREVIATIONS

5FU	5-fluorouracil
ABC	Advanced bladder cancer
AEC	3-Amino-9-ethylcarbazole
AKT	Protein serine-threonine kinase
ANOVA	Analysis of variance
AP	Alkaline phosphatase
ATP	Adenosine triphosphate
BCA	bicinichoninic acid
BCG	Bacillus Calmette-Guerin
βGP	β-Glycerophosphate
BSA	Bovine serum albumin
CALGB	Cancer and Leukaemia Group B
Cdk	Cyclin dependent kinase
CI	Confidence interval
CO_2	Carbon dioxide
CT	Computed tomography
CMV	Cisplatin, methotrexate and vinblastine
DMEM	Dulbecco's Modified Eagle Media
DMSO	Diethyl sulfoxide
DNA	Deoxyribonucleic acid
dsRNA	Double-stranded RNA
DTE	Dithioerythritiol

DTT	Dithiothreitol
EAU	European Association of Urology
EDTA	Ethylenediaminetetraacetic acid
E-Coli	Escherichia Coli
EGF	Epidermal growth factor
EGFP	Enhanced green fluorescent protein
EGFR	Epidermal growth factor receptor
EORTC	European Organisation for Research and Treatment of Cancer
EtBr	Ethidium bromide
ETOH	Ethanol
FACS	Fluorescence-activated cell sorting
FBS	Fetal bovine serum
FDA	Food and Drug Administration
FITC	Fluorescein isothiocyanate
G1	GAP-1
G2	GAP-2
GC	Gemcitabine and cisplatin
GDP	Guanine diphosphate
GFP	Green fluorescent protein
GTC	Gemcitabine, paclitaxel and cisplatin
GTP	Guanine triphosphate
HD-MVAC	High-dose MVAC
HR	Hazards ratio
HRG	Heregulin
HRP	Horseradish peroxidase

IC_{50}	Half maximal inhibitory concentration
IDEAL	Iressa Dose Evaluation in Advanced Lung Cancer
INTACT	Iressa NSCLC Trial Assessing Combination Treatment
ISEL	Iressa Survival Evaluation in Lung Cancer
ISUP	International Society of Urological Pathologists
IVP	Intravenous pyelography
LB	Lysogeny Broth
mRNA	Messenger RNA
M	Mitosis
MAb	Monoclonal antibody
MAPK	Mitogen-activated protein kinase
$MgCl_2$	Magnesium chloride
MRC	Medical Research Council
MTT	3-[4,5-dimethyl(thiazol-2-yl)-3,5-diphery]tetradium bromide
MV	Methotrexate and vinblastine
MVAC	Methotrexate, vinblastine, adriamycin (doxorubicin) and cisplatin
Na_3VO_4	Sodium orthovanadate
NaCl	Sodium chloride
NaF	Sodium fluoride
NCIC-CTG	National Cancer Institute of Canada Clinical Trials Group
NEAA	Non-essential amino acids
NP40	Nonidet P40
NSCLC	Non-small cell lung cancer
PBS	Phosphate-buffered saline
PI	Propidium iodide

PI3K	Phosphatidylinositol 3-kinase
PMSF	Phenylmethysulphonyl fluoride
PS	Phosphatidyl serine
P-S	Penicillin-streptomycin
PTEN	Phosphatase and tensin homologue deleted on chromosome ten
PTP1B	Protein tyrosine phosphatase 1B
PUNLMP	Papillary neoplasm of low malignant potential
PVDF	Polyvinylidene fluoride
Rb	Retinoblastoma
RNA	Ribonucleic acid
RNAi	RNA interference
RNase A	Ribonuclease A
S	Synthesis
SDS	Sodium dodecyl sulphate
SDS-PAGE	SDS-Polyacrylamide Gel Electrophoresis
SF	Serum free
SiRNA	Small interfering RNA
SPORE	Specialized Program of Research Excellence
STAT	Signal Transducer and Activator of Transcription
TALENT	Erlotinib with cisplatin and gemcitabine in NSCLC trial
TBE	Tris/Borate/EDTA
TBS-T	Tris-buffered saline with TWEEN
TCC	Transitional cell carcinoma
TEMED	N,N,N',N'-Tetramethylethylenediamine
TGF	Transforming growth factor

Tis	Tumour *in situ*
TK	Tyrosine kinase
TKI	Tyrosine kinase inhibitor
TNM	Tumour Node Metastasis
TRIBUTE	Erlotinib with paclitaxel and carboplatin in NSCLC trial
TUR	Transurethral resection
UICC	Union International Contre le Cancer
US	United States
UTI	Urinary tract infection
UV	Ultraviolet
WHO	World Health Organisation
Y	Tyrosine residues

RELATED PUBLICATIONS AND RESEARCH

ABSTRACTS

Publications

Tyrosine kinase inhibitors of the epidermal growth factor receptor as adjuncts to systemic chemotherapy for muscle-invasive bladder cancer.

Lynsey A. McHugh, T.R. Leyshon Griffiths, Marina Kriajevska, R. Paul Symonds and J. Kilian Mellon

Urology 2004; 63: 619-24.

Combined treatment of bladder cancer cell lines with lapatinib and varying chemotherapy regimens – evidence of schedule-dependent synergy.

Lynsey A. McHugh, Marina Kriajevska, John K. Mellon and Thomas R. Griffiths

Urology 2007; 69: 390-4.

Research abstracts

GW572016, a dual tyrosine kinase inhibitor, blocks activation of ErbB1 and ErbB2 in a bladder cancer cell line

Lynsey A. McHugh, Thomas R.L. Griffiths, Alexandra J. Colquhoun, Marina Kriajevska, J. Kilian Mellon

Poster presentation

Presented at Urological Research Society meeting, Royal College of Surgeons of England, London, UK, January 2004.

GW572016, a dual tyrosine kinase inhibitor, blocks activation of ErbB1 and ErbB2 in bladder cancer cell lines

Lynsey A. McHugh, Thomas R.L. Griffiths, Alexandra J. Colquhoun, Marina Kriajevska, J. Kilian Mellon

Poster presentation

American Association of Cancer Research annual meeting, Orlando, Florida, USA, March 2004.

Gefitinib ('Iressa', ZD1839) inhibits ionizing radiation mediated activation of epidermal growth factor receptor in the invasive bladder cancer cell line RT112

A. Colquhoun, L. McHugh, E. Tulchinsky, M. Kriajevska, J. Mellon

Poster presentation

American Association of Cancer Research annual meeting, Orlando, Florida, USA, March 2004.

GW572016, a dual tyrosine kinase inhibitor, blocks activation of ErbB1 and ErbB2 in bladder cancer cell lines

Lynsey A. McHugh, Thomas R.L. Griffiths, Alexandra J. Colquhoun, Marina Kriajevska, J. Kilian Mellon

Poster presentation

American Urological Association annual meeting, San Francisco, California, USA, May 2004.

Dual ErbB1/ErbB2 tyrosine kinase inhibition by GW572016 – a potential adjunct to systemic chemotherapy in bladder cancer

Lynsey A. McHugh, Thomas R.L. Griffiths, Marina Kriajevska, J. Kilian Mellon

Poster presentation

Urological Research Society meeting, Royal College of Surgeons of England, London, UK, January 2005.

Dual ErbB1/ErbB2 tyrosine kinase inhibition by GW572016 – a potential adjunct to systemic chemotherapy in bladder cancer

Lynsey A. McHugh, Thomas R.L. Griffiths, Marina Kriajevska, J. Kilian Mellon

Poster presentation

American Association of Cancer Research annual meeting, Annaheim, California, USA, April 2005.

Dual ErbB1/ErbB2 tyrosine kinase inhibition – a potential adjunct to systemic chemotherapy in bladder cancer

Lynsey A. McHugh, Thomas R.L. Griffiths, Marina Kriajevska, J. Kilian Mellon

Poster presentation

British Association of Urological Surgeons annual meeting, Glasgow, UK, June 2005.

Dual ErbB1/ErbB2 tyrosine kinase inhibition – a potential adjunct to chemotherapy in bladder cancer

Lynsey A. McHugh, Thomas R.L. Griffiths, Marina Kriajevska, J. Kilian Mellon

Oral presentation

LNR 'Delivering the Best' Conference, Loughborough, UK, July 2005.

Combined treatment of bladder cancer cell lines with lapatinib (GW572016) and chemotherapy – evidence of schedule-dependent synergy

Lynsey A. McHugh, Marina Kriajevska, J. Kilian Mellon, T.R. Leyshon Griffiths

Poster presentation

Urological Research Society meeting, Royal College of Surgeons of England, London, UK, January 2006.

Combined treatment of bladder cancer cell lines with lapatinib (GW572016) and chemotherapy – evidence of schedule-dependent synergy

Lynsey A. McHugh, Marina Kriajevska, J. Kilian Mellon, T.R. Leyshon Griffiths

Poster presentation

American Association of Cancer Research annual meeting, Washington DC, USA, April 2006.

Combined treatment of bladder cancer cell lines with lapatinib (GW572016) and chemotherapy – evidence of schedule-dependent synergy

Lynsey A. McHugh, Marina Kriajevska, J. Kilian Mellon, T.R. Leyshon Griffiths

Poster presentation

British Association of Urological Surgeons annual meeting, Manchester, UK, June 2006.